COHESIVE BEHAVIORS OF COOPERATIVE MULTIAGENT SYSTEMS WITH INFORMATION FLOW CONSTRAINTS

DISSERTATION

Presented in Partial Fulfillment of the Requirements for

the Degree Doctor of Philosophy in the

Graduate School of The Ohio State University

By

Yanfei Liu, B.S., M.E, M.S.

* * * * *

The Ohio State University

2004

Dissertation Committee:

Kevin M. Passino, Adviser

Jose B. Cruz, Jr.

Andrea Serrani

Paul A.G. Sivilotti

Approved by

Adviser

Department of Electrical Engineering

ABSTRACT

Bacteria, bees and birds often work together in groups to find food. A group of robots can be designed to coordinate their activities. Networked cooperative UAVs are being developed for commercial and military applications. In order for such multiagent systems to succeed it is often critical that they can both maintain cohesive behaviors and appropriately respond to environmental stimuli. Stimulated by the growing interest in biomimicry of the mechanisms of foraging and swarming for use in engineering applications, this dissertation focuses on mathematical modeling and analysis of stability properties of swarms.

We construct a generic swarm model which considers the interagent attractions and repulsions and the effect of resource profiles. Based on this model, we study its cohesion properties in a stability-theoretic framework. First, we consider the effects of sensor noise and error on sensing resource profiles on stability of continuous-time swarms and give the conditions for the swarm to achieve uniformly ultimate boundedness (UUB). Next, we analyze the stability properties of the swarm model in discrete time and obtain stability properties similar to the continuous-time case. Then, we extend the results by adding an interagent sensing network topology, asynchronism and time delays into the model and studying their effects on stability. The conditions under which the system trajectories are uniformly ultimately bounded and exponential stability can be achieved are given. Such stability analysis is of fundamental

importance if one wants to understand the coordination mechanisms for groups of autonomous vehicles or robots where inter-member communication channels are less than perfect.

To my family.

ACKNOWLEDGMENTS

I would like to express my sincere gratitude to my adviser, Professor Kevin M. Passino, for his excellent guidance and continuous support during my graduate studies. Thanks for broadening my scope and helping me achieving my goals. I could not have reached this far without his help.

I would like to thank Professor Jose B. Cruz Jr., Professor Andrea Serrani, and Professor Paul A.G. Sivilotti for serving in my dissertation committee. I would also like to thank my colleagues and friends at OSU for their help in my academic and daily life.

I want to thank the financial support from the DARPA MICA program via AFRL, and AFRL/VA and AFOSR CCCS at different stages of my studies.

Finally, I would like to thank my family for their unconditional love and support throughout my life.

VITA

September 13, 1973 ..... Born - Jinzhou, China

July 1994 ..... B.S. in Design & Manufacturing
College of Automotive Engineering
Jilin University of Technology
Changchun, China

September 1994 - May 1997 ..... Graduate Research Associate
Automotive Engineering
College of Mechanical Engineering
Huazhong Univ. of Sci. and Tech.
Wuhan, China

May 1997 ..... M.E. in Automotive Engineering
College of Mechanical Engineering
Huazhong Univ. of Sci. and Tech.
Wuhan, China

June 1997 - July 1998 ..... Associate Lecturer
Automotive Engineering
College of Mechanical Engineering
Tianjin University
Tianjin, China

September 1998 - June 2001 ..... Graduate Fellow,
Graduate Research Associate,
Graduate Teaching Associate
Department of Mechanical Engineering
The Ohio State University
Columbus, OH

June 2001 ..... M.S. in Mechanical Engineering
The Ohio State University
Columbus, OH

July 2001 - present ..... Graduate Research Associate
Dept. of Elec. & Computer Eng.
The Ohio State University
Columbus, OH

PUBLICATIONS

Research Publications

Y. Liu and K. M. Passino, "Stable Social Foraging Swarms in a Noisy Environment," in *IEEE Transactions of Automatic Control*, Vol. 49, No. 1, 2004.

Y. Liu and K. M. Passino, "Cohesive Behaviors of Multiagent Systems with Information Flow Constraints," Submitted to *IEEE Transaction on Automatic Control*, 2004.

Y. Liu and K. M. Passino, "Stability Analysis of Swarms in a Noisy Environment," in *Proceedings of the 42th IEEE Conference on Decision and Control*, Maui, Hawaii, pp. 3573-3578, Dec., 2003.

Y. Liu and K. M. Passino, "Cohesive Behaviors of Multiple Cooperative Mobile Discrete-Time Agents in a Noisy Environment," in *the 4th International Conference on Cooperative Control and Optimization*, FL, Nov., 2003.

Y. Liu and K. M. Passino, "Biomimicry of Social Foraging Behavior for Distributed Optimization: Models, Principles, and Emergent Behaviors," in *Journal of Optimization Theory and Applications*, Vol. 115, No. 3, 2002.

F. Bi and Y. Liu, "Simulation of Clutch Engagement on Vehicle Start-up Stage," in *Machine Design* (in Chinese), No. 2, 1998.

Y. Liu, "Modeling for Electric Vehicle Performance Simulation and Its Application," in *Mechanical and Electrical Engineering* (in Chinese), Vol. 15, No. 3, 1998.

Y. Liu, X. Guo, and G. Jin "A Comparative Analysis of Hydrodynamic Split Torque Converter and Its Quasi-Equivalent Torque Converter," in *Machine Design and Research* (in Chinese), No. 3, 1997.

FIELDS OF STUDY

Major Field: Electrical Engineering

TABLE OF CONTENTS

Page

LIST OF FIGURES

Figure **Page**

CHAPTER 1

INTRODUCTION

This dissertation studies mathematical modeling and stability analysis of asynchronous swarms. The background of the dissertation research is introduced by reviewing some of the most relevant areas to our research in this chapter. Afterwards, the relevant progress in the literature that focuses on swarm stability is summarized. At last, the dissertation organization is described.

1.1 Literature Review

"Swarming," or aggregation and coordinated motion of organisms in group, is frequently observed in nature. Examples include schools of fish, flocks of birds, herds of animals and colonies of bacteria. Evolution of swarming behaviors indicates that such collective and coordinated behaviors have certain advantages such as avoiding dangers (e.g., noxious substances, predators, etc.), minimizing energy consumption, increasing nutrient intake, or reducing the variance on energy intake. Swarms have been studied extensively not only in biology, but also in physics and engineering. Below we will overview the work in each of these fields. By studying the operational principles of such biological systems including swarm modeling, coordination strategies, and grouping dynamics, we may get better ideas for developing distributed

cooperative control, coordination, and learning strategies for autonomous multi-agent systems such as multi-robot teams and uninhabited air vehicles (UAVs).

1.1.1 Literature in Biology

Almost everywhere in nature, we could find swarming of organisms, including bacteria, insects, fish, birds, and mammals. Swarming behaviors have been studied by biologists for a long time and currently of significant interest [1, 2, 3, 4, 5, 6, 7].

The paper by Breder [1] is one of the earliest that studies swarming behaviors mathematically. The author proposed that within fish schools and other animal aggregations there exist attraction-repulsion effects related to distance such that the repulsion dominates when the fish-to-fish distance is small and the attraction dominates otherwise. A simple model was given to represent such effects and the resultant balance position was determined. The author also investigated the "masking" (or "shadowing") effects on swarming, that is, when a large amount of agents (fish) present, an agent cannot see all the other agents since some of them are "hidden" behind other agents and out of its sight. The impact of heterogenous agents on schooling size was also discussed briefly in the paper. The data from four species of fish were collected and compared to validate the model.

In [2], the author introduced a simple random walk model first and showed that it can be expressed as a diffusion-advection equation. Then applying Newton's law of motion, he constructed ordinary differential equations to represent the dynamics of individual animal. Based on this, model for animal grouping dynamics was developed with random components. He investigated various aspects in animal grouping, including group formation processes, grouping around multiple centers, and group

size distribution by studying the statistical properties of the stochastic model. At the last section of the paper, the author made comparisons with various mathematical models when reviewing examples of animal grouping, including insect swarms, zooplankton swarms, fish schools, bird flocks, and mammalian herds.

In [3], the author constructed a model to simulate the self-organizing behaviors of fish schooling. Similar to Okubo [2], the agent dynamics in this paper include a deterministic force and a stochastic part. While the work by [2] is in a regular coordinate framework, Niwa studied the behaviors of the error system through a coordination transformation. A statistical mechanical treatment of the formation process of fish schooling was proposed and a nonlinear Langevin equation was obtained after some simplification. Based on these, the author showed that the systems composed of many fish dramatically change their structure when certain parameters are varied, that is, those fish switching from swarming to schooling, or vice versa.

Grunbaum presented evidence in [4] that even the simplest of interactions between social and tactic behaviors (i.e. a superposition of these two types of behavior) confers enhanced capacity for taxis. His strategy involved assuming each swarming agent performs a biased random walk in a periodic domain, with its dynamics affected by the behaviors and positions of its neighbors. Then it was shown that in a noisy environment schooling behavior can improve the ability of animals to perform taxis to climb gradients, while asocial taxis would possibly be ineffective. This provides a sound mathematical reason why schooling and swarming is so frequently observed in nature. In terms of the theory of the evolution of cooperation [8] it is a type of "mutualism."

Mogilner and Edelstein-Keshet [5] used continuum models to describe swarming behavior when non-local interactions exist. The model consisted of integro-differential advection-diffusion equations, with convolution terms that describe long range attraction and repulsion. The paper focused on the case that the swarm profile has sharp edges and the interior density of the swarm is constant, that is, independent of the total swarm size. The authors concluded that such swarm profiles may be achieved if density dependence in the repulsion term is of a higher order than in the attraction term. It is also indicated that within this framework, true locally stable traveling band solutions occur only when density dependence is put into the diffusion term, otherwise disintegration of the swarm, or instability, would happen.

In her paper [6], Stevens studied the behaviors of myxobacteria which are ubiquitous soil bacteria which aggregate under starvation conditions and build fruiting bodies to survive. She first constructed a stochastic cellular automaton to model gliding and aggregation of myxobacteria, assuming periodic boundary conditions. The simulation based on this showed the interdependence of the different mechanisms which finally cause aggregation. Then a simplified version of this model is formally approximated by a system of partial differential equations. In another paper [9] the author dealt with a rigorous derivation of these types of equations from an interacting stochastic many-particle system.

Couzin et al. [7] presented a self-organizing model of group formation in three-dimensional space and used it to investigate the spatial dynamics of animal groups such as fish schools and bird flocks. It was revealed that minor changes in individual-level interactions may lead to major group-level behavioral transitions. Simulation results showed that when certain parameters are subjected to some minor changes, the

group may exhibit different formations, including aggregates, torus, dynamic parallel group, and highly parallel group, as often observed in fish schooling. The authors also showed the first evidence that "collective memory" exists in such animal groups during the transition of a group from one type of collective behavior to another. The paper indicated that individuals can change their spatial position accurately within a group by employing simple local rules.

Finally, some general references on animal grouping and mathematical models in biology include the books by Parrish and Hamner [10], Edelshtein-Keshet [11], and Murray [12]. Note that for many organisms, swarming often occurs during social foraging, and a good reference for foraging theory is in [13].

1.1.2 Literature in Physics

Besides the work done by mathematical biologists, there is significant relevant literature in physics where collective behavior of "self-propelled particles" is studied [14, 15, 16, 17, 18, 19].

Rauch et al. [14] used a Langevin type equation to model a kind of stochastic particle-field system in which the motion of the particles both changes the field and is affected by the field. The authors did not intend to consider the continuous limit of the system behaviors but rather the case where internal fluctuations are significant. The location of the boundary separating totally random behavior from ordered behavior in the physiological phase space was found by using mean-field theory. The authors postulated that such a transition boundary may locate a region where ordered patterns of flow can form, but also the swarms could better respond to a changing

environment if the dynamics are such that there can be significant fluctuations in the patterns of mass action.

In the paper [15], a model with very simple dynamics was introduced in order to investigate the emergence of self-ordered motion in systems of particles with biologically motivated interaction. In this model particles are driven with a constant absolute velocity and at each time step assume the average direction of motion of the particles in their neighborhood with some random perturbation. A kinetic phase transition is observed in some of the simulations. Large-scale Monte Carlo simulations were performed in [20] based on the same model as in [15], except that the "neighborhood" of each agent is defined in a slightly different way. In that paper, the authors showed that a long-range ordered phase emerges in this system in a phase-space domain which is a function of two parameters, the amplitude of noise and the average density of the particles. The relationship between these two parameters along the border line is also given.

Shimoyama et al. [16] used a heading vector and an "anisotropic" interaction term in their model. They concentrated on the viscous regime and neglected the higher order dynamics in the system. By carrying out numerical simulations for various control parameters and observing the collective motions, the authors showed that the deterministic kinetic model may be used to describe several kinds of cluster motion seen in nature, including marching, wavy and circling oscillation, wandering and swarming, some of which may demonstrate chaotic behaviors. To characterize their transitions, the collective motions are analyzed numerically with respect to a disorder parameter and Lyapunov spectra in the paper.

In [17], Toner and Tu presented a quantitative continuum theory of "flocking." They used a model similar to [15], but with a continuum "hydrodynamic" description of the flock. In fact, the model is similar in many ways to the Navier-Stokes equations for a simple compressible fluid. With this model, some short-ranged details are ignored, but detailed, quantitative predictions for the long-distance, long-time behavior of the "broken symmetry state" can be made. The authors mainly focused on the isotropic model, that is, a model where no specific moving direction is preferred by any agent. They also argued that the best boundary conditions for simulating such a model are "torus" conditions (that is, reflecting walls in $n-1$ directions, and periodic boundary conditions in the remaining direction) since with these conditions one knows a priori that, if the clock does spontaneously order, its mean velocity will necessarily be in the periodic direction.

Levine and Rappel [18] investigated a discrete model consisting of self-propelled particles that obey simple interaction rules. They did not follow the approach adopted by most earlier work which have in common that the flocks have infinite extent and fill the entire computational box in simulations. Instead, flocks with finite size were assumed in the paper. Also, when calculating the average velocity in the neighborhood of each agent, the authors did not specify a circle to represent the neighborhood, instead, they used a factor which is exponentially weighted with respect to the distance between agents to obtain the localized average velocity. It was shown that this model can self-organize and exhibit coherent localized solutions in one and two-dimensions. A continuum version of the discrete model was obtained by coarse-grain averaging the discrete equations and proven to provide the same results as the discrete equations.

Finally, Grégoire et al. [19] introduced a microscopic, stochastic, minimal model for collective and cohesive motion of identical self-propelled particles. It is interesting that the authors interpreted different collective motion status as phases gas, liquid and solid and the transition of these status were illustrated by the form of phase diagram. With intensive numerical simulation, they showed that even though the particles interact strictly locally in a very noisy manner, it is possible to maintain the cohesion, even in the zero-density limit of an arbitrarily large flock in a infinite space. It turned out this is achieved mainly by increasing the magnitude of the attraction term. The effects of changing population and box size were also discussed.

1.1.3 Literature in Engineering

In recent years, swarms have also been studied in various aspects of engineering, mainly due to the emergence of relevant problems related to computer graphics, optimization algorithms, formation control for robots and aircraft, cooperative control for uninhabited autonomous (air) vehicles, and intelligent vehicle highway systems.

To present in computer animation the aggregate motion of a flock of organisms, Renolds [21] explored an approach as an alternative to scripting the paths of each bird individually. The simulated flock is regarded as an elaboration of a particle system, with the simulated birds being the particles. The aggregate motion of the simulated flock is created by a distributed behavioral model where each bird chooses its own course. Three rules were given to prescribe the behaviors of the flock, which are, in order of decreasing precedence, collision avoidance, velocity matching, and flock centering. The resultant computer animation resembled an observer's intuitive notion of what constitutes "flock-like motion."

The search algorithm of particle swarm optimization (PSO) [22, 23] is based on evolutionary computation techniques and motivated from the social behavior of organisms in nature. PSO searches a space by adjusting the trajectories of individual vectors, called "particles" as they are conceptualized as moving points in multidimensional space. Each particle is defined within the context of a topological neighborhood and is drawn stochastically toward the positions of its own previous best performance and the best previous performance of their neighbors. In [22], the authors analyzed the impact of certain parameters on the performance of the algorithm. In [23], the properties (pro and con) of PSO were investigated and a generalized model of the algorithm was presented.

Intelligent vehicle highway systems (IVHS) may be regarded as a special type of swarm. In IVHS, communication, vehicle control and traffic management techniques are incorporated to provide safe, fast and more efficient surface transportation. For the scenario where cars move along the highway in a tightly spaced platoon, which is often the case, the swarming behaviors are observed in a one-dimensional domain. Swaroop et al. [24, 25] investigated spacing and headway control laws for automatically controlled vehicles. For constant spacing control, the authors introduced a measure of string stability and presented a systematic method for spacing controllers design. For autonomous headway control laws, it was shown that the desired control torques are inversely proportional to the headway time to avoid collision. In [26], the authors presented control schemes for the leader vehicle in a platoon so that issues like maintaining safe spacing, tracking a optimal velocity, and performing various maneuvers (including merging, splitting, and changing lange) could be handled. Spooner and Passino [27] developed a robust longitudinal sliding-mode control algorithm and

proved that this algorithm is stable for various vehicle and AHS faults. It was also shown that the inter-vehicle spacing error will not be amplified in the event of a loss of lead vehicle information.

Significant swarms-related work is done on multi-robot teams that are tasked for path planning, searching or collecting objects. The paper [28] proposed a distributed control method, which the authors called "social potential fields method." Simple artificial force laws, which incorporated both attraction and repulsion, were defined between pairs of robots or robot groups and each individual robot's motion is controlled by the resultant artificial force imposed by other robots and other components of the system. In [29], the author presented a feedback control law to coordinate the motion of multiple mobile robots to capture/enclose a target which implicitly is stationary or has a prescribed motion trajectory. To achieve this cooperative behavior without making collisions, it is assumed that each robot has its own coordinate system and can sense the target/invader, other robots and obstacles. Fujimori et al. [30] proposed a collision avoidance technique called "cooperative collision avoidance" for multiple mobile robots. The idea involved first detecting the danger of collision by considering the geometric aspects of the paths of those robots, then implementing the direction control and speed control for each robot. Simulation showed that the technique is successful when only two robots present, but when the number of robots is over two, collision avoidance is not guaranteed.

Formation control is an active research topic for both military and commercial projects. In [31], reactive behaviors for four formations and three formation reference types were presented by assuming global information is available to all the robots. The behaviors were demonstrated successfully in both laboratory experiments and

field tests. Suzuki and Yamashita [32] considered in their paper a multi-robot system where there exists no global x-y coordinate system and the robots may move either synchronously or asynchronously. Algorithms for converging the robots to a single point and moving the robots to a single point in a finite number of steps were presented. Also the class of geometric patterns that the robots can form, given their initial configuration, was characterized. Desai et al. [33] addressed the control of a team of nonholonomic mobile robots navigating through obstacles while maintaining certain formations. Similar to [31], a leader-follower scheme was adopted. But instead of using potential field theory, the authors used a digraph, which is based on graph theory, to prescribe the desired formation. The paper by Egerstedt and Hu [34] uses the idea of "virtual leader" on formation control. In this framework, the problems of formation and tracking are decoupled. Specifically, the virtual leaders are constructed first with a certain formation and trajectories, then those real agents are to track the virtual agents to achieve desired performance. Similar to [34], Leonard et al. [35, 36] used virtual leaders and artificial potentials and presented a coordination strategy for formation missions involving group translation, rotation, expansion and contraction. In their work, the direction of motion of the virtual leaders is designed to satisfy the mission while the speed of the virtual leaders is designed to ensure stability and convergence properties of the formation.

Early work on swarm stability is in [37, 38]. The authors [37] investigated the stability of synchronized distributed control of a one-dimensional swarm structure and a two-dimensional one. Assuming all the swarm agents have fixed topology and have certain local sensing capability, the authors obtained some stability properties of the system by using a Lyapunov approach. The paper in [38] is among one of the earliest

work on stability with asynchronism (but without time delay). It showed the sufficient conditions under which the swarm system, prescribed by a distributed asynchronous and bounded iterative algorithm, converges. Later work where there is asynchronism and time delays appears in [39, 40, 41, 42]. Liu et al. [39, 40] studied a discrete-time one-dimensional asynchronous swarm with finite-size swarm members that have proximity sensors and neighbor position sensors that only provide delayed position information. Stability properties of the swarm were investigated and conditions under with collision-free convergence were provided. Gazi and Passino [42] used the same single swarm member as defined in [40] but a different mathematical model for the inter-member interactions and motions in a swarm. Stability results were obtained for this system with total asynchronism and time delays. In [41] the authors extended their study in [40] to M-dimensional case. Specifically, the authors showed that even in the presence of sensing delays and asynchronism, an M-dimensional asynchronous swarm with a fixed communication topology following an edge-leader can maintain cohesion under certain conditions.

There is also some work on the stability of swarm systems which focuses on some aspects other than asynchronism and time delays. In [43, 44], the authors specified an individual-based continuous-time model for swarm aggregation and studied its stability properties. The cohesiveness property of individual agent and the bound of the swarm size were also obtained. In [45] the authors generalized the model in [43, 44] and provided a class of attraction/repulsion functions. Then conditions for swarm stability (ultimate swarm size and ultimate behavior) with this generalized model were provided. Similar ideas are seen in [35] where the authors constructed artificial

potentials to define interaction between agents and used a Lyapunov approach to prove the system stability.

The paper in [46] represented progress in the direction of combining the study of aggregating swarms and how during this process decisions about foraging or threat avoidance can affect the collective/individual motion of the swarm/swarm members. Additional work on gradient climbing by swarms, including work on climbing noisy gradients, is in [47]. There, similar to [46], the authors studied climbing gradients, but also considered the case when local gradient information is not readily available.

Recently some work has been done to deal with swarm models with swarming agents having a fixed topology [48, 49, 50]. Based on the ideas from graph theory, Jadbabaie and Morse [48] provided a theoretical explanation for the observed behaviors from the model proposed in [15]. They also derived convergence results for several other similarly inspired models. Tanner et al. [49] further extended the study of switching networks to a system where the behaviors of each agent are dominated by a second order equation. It is shown that the stability of such a system is directly associated with the connectivity properties of the interconnection network "on the fly." Similar to [48] and [49], the authors in [50] used graph theory to study the performance of a network with mobile nodes and switching topology. They proposed a group disagreement function, which is based on balanced graphs, to perform convergence analysis for the above network.

1.2 Organization of the Dissertation

The dissertation is organized as follows. In Chapter 2, we characterize swarm cohesiveness as a stability property and use a Lyapunov approach to develop conditions

under which local agent actions will lead to cohesive foraging even in the presence of sensing "noise." The results quantify earlier claims that social foraging is in a certain sense superior to individual foraging when noise is present, and provide clear connections between local agent-agent interactions and emergent group behavior. Moreover, the simulations show that very complicated but orderly group behaviors, reminiscent of those seen in biology, emerge in the presence of noise.

Chapter 3 is a discrete-time version of Chapter 2. Specifically, it focuses on discrete-time case and use of a Lyapunov approach to develop conditions under which local agent actions will lead to cohesive foraging even in the presence of "noise" characterized by uncertainty on sensing other agent's position and velocity, and in sensing nutrients that each agent is foraging for. Similar to Chapter 2, the results quantify earlier claims that social foraging is in a certain sense superior to individual foraging when noise is present.

Chapter 4 characterizes cohesiveness of discrete-time multiagent systems as a boundedness or stability property of the agents' position trajectories and uses a Lyapunov approach to develop conditions under which local agent actions will lead to cohesive group behaviors even in the presence of (i) an interagent "sensing topology" that constrains information flow, where by "information flow," we mean the sensing of positions and velocities of agents of our interest, (ii) a random but bounded delay and "noise" in sensing other agents' positions and velocities, and (iii) noise in sensing a resource profile that represents an environmental stimulus and quantifies the goal of the multiagent system.

Chapter 5 gives a summary of the major contributions of this dissertation and provides an outline of future research directions.

CHAPTER 2

STABLE SOCIAL FORAGING SWARMS IN A NOISY ENVIRONMENT

2.1 Introduction

In this chapter, we continue some earlier work on stability properties of foraging swarms [44, 45, 46]. The main difference with those previous work is that the effect of sensor errors ("noise") and errors in sensing the gradient of a "resource profile" (e.g., a nutrient profile) is considered. We are able to show that even with noisy measurements the swarm can achieve cohesion and follow a nutrient profile in the proper direction. We illustrate that the agents can forage in noisy environments more efficiently as a group than individually, a principle that has been identified for some organisms [4, 51]. The work here builds on the work in (i) [44, 45] where the authors provide a class of attraction/repulsion functions and provide conditions for swarm stability (ultimate swarm size and ultimate behavior), and (ii) [46] that represents progress in the direction of combining the study of aggregating swarms and how during this process decisions about foraging or threat avoidance can affect the collective/individual motion of the swarm/swarm members (i.e., typical characteristics

influencing social foraging). Additional work on gradient climbing by swarms, including work on climbing noisy gradients, is in [47]. There, similar to [46], the authors study climbing gradients, but also consider noise effects and coordination strategies for climbing, something that we do not consider here.

The remainder of this chapter is organized as follows: In Section 2.2 we introduce a generic model for agents, interactions, and the foraging environment. Section 2.3 holds the main results on stability analysis of swarm cohesion. Stability analysis of swarm trajectory following is done in Section 2.4. Section 2.5 holds the simulation results and some concluding remarks are provided in Section 2.6.

2.2 Swarm and Environment Models

2.2.1 Agents and Interactions

Here, rather than focusing on the particular characteristics of one type of animal or autonomous vehicle we consider a swarm composed of an interconnection of N "agents," each of which has point mass dynamics given by

$$\begin{aligned} \dot{x}^i &= v^i \\ \dot{v}^i &= \frac{1}{M_i} u^i \end{aligned} \tag{2.1}$$

where $x^i \in \Re^n$ is the position, $v^i \in \Re^n$ is the velocity, M_i is the mass, and $u^i \in \Re^n$ is the (force) control input for the i^{th} agent. It is assumed that all agents know their own dynamics. For some organisms like bacteria that move in highly viscous environments you can assume that $M_i = 0$ and if you use a velocity damping term in u^i for this you get the model studied in [44, 45, 46]. There, the authors view the choice of u^i as one that seeks to perform "energy minimization" which is consistent with other energy

formalisms in mathematical biology. Here, we do not assume $M_i = 0$. Moreover, we will assume that each agent can sense information about the position and velocity of other agents, but possibly with some errors (what we will call "noise"), something not considered in [44, 45, 46].

Agent to agent interactions considered here are of the "attract-repel" type where each agent seeks to be in a position that is "comfortable" relative to its neighbors (and for us all other agents are its neighbors). Attraction indicates that each agent wants to be close to every other agent and it provides the mechanism for achieving grouping and cohesion of the group of agents. Repulsion provides the mechanism where each agent does not want to be too close to any other agent (e.g., for animals to avoid collisions and excessive competition for resources). There are many ways to define attraction and repulsion, each of which can be represented by characteristics of how we define u^i for each agent. Attraction here will be represented by a term in u^i like $-k_p^i (x^i - x^j)$ where $k_p^i > 0$ is a scalar that represents the strength of attraction. If the agents are far apart, then there is a large attraction between them, and if they are close there is a small attraction. For repulsion, we let the 2-norm $\|z\| = \sqrt{z^\top z}$ and use a repulsion term in u^i of the form

$$k_r^i \exp\left(\frac{-\frac{1}{2}\|x^i - x^j\|^2}{{r_s^i}^2}\right)\left(x^i - x^j\right) \tag{2.2}$$

where $k_r^i > 0$ is the magnitude of the repulsion, and $r_s^i > 0$ quantifies the region size around the agent from which it will repel its neighbors. When $\|x^i - x^j\|$ is big relative to r_s^i the whole term approaches zero. The combined effect of repulsion and attraction terms influence the so-called "equilibrium of attraction and repulsion" that represents that two agents are at a "comfortable" distance from one another. Many

other types of attraction and repulsion terms are possible; see the references cited earlier.

2.2.2 Environment Model

Next, we will define the environment that the agents move in. While there are many possibilities, here we will simply consider the case where they move (forage) over a "resource profile" (e.g., nutrient profile) $J(x)$, where $x \in \Re^n$. For this, positions x such that $J(x) = 0$ represent a "neutral" environment that does not influence the motion of agents, $J(x) > 0$ are locations where the agents do not want to be (e.g., locations where there are noxious substances), and $J(x) < 0$ are regions where agents want to be (e.g., locations where there are nutrients). We will assume that $J(x)$ is differentiable and has bounded slope at all points. Agents move in the direction of the negative gradient of $J(x)$ (i.e., in the direction of $-\nabla J(x) = -\frac{\partial J}{\partial x}$) in order to move away from "bad" areas and into "good" areas of the environment (e.g., to avoid noxious substances and find nutrients). That is, they will use a term in their u^i that holds the negative gradient of $J(x)$.

Clearly there are many possible shapes for $J(x)$, including ones with many peaks and valleys. Here, we simply list two simple forms for $J(x)$ as follows:

- *Plane:* In this case we have $J(x) = J_p(x)$ where

$$J_p(x) = R^\top x + r_p$$

  where $R \in \Re^n$ and r_p is a scalar. Here, $\nabla J_p(x) = R$.

- *Gaussian:* In this case we have $J(x) = J_g(x)$ where

$$J_g(x) = r_{m_1} \exp\left(-r_{m_2} \|x - R_c\|^2\right) + r_e$$

where r_{m_1}, r_{m_2} and r_e are scalars, $r_{m_2} > 0$ and $R_c \in \Re^n$. Here, $\nabla J_e(x) = -2r_{m_1}r_{m_2}\exp\left(-r_{m_2}\|x - R_c\|^2\right)(x - R_c)$.

Below, we will assume that each agent can sense the gradient, but only with some errors, which we will refer to as "noise." When we want to refer to agent i as following a possibly different profile than agent j, $j \neq i$, we will use, for example, J_p^i, R^i, and r_p^i for the plane profiles. Throughout this chapter, we will in fact study this case where agents follow different plane profiles, since these are simple yet representative. Moreover, locally, typical profiles will have a constant slope.

2.3 Stability Analysis of Swarm Cohesion Properties

Cohesion and swarm dynamics will be quantified and analyzed using stability analysis of the swarm error dynamics that we define next.

2.3.1 Controls and Error Dynamics

First, assume there are N agents in the environment and let

$$\bar{x} = \frac{1}{N}\sum_{i=1}^{N} x^i$$
$$\bar{v} = \frac{1}{N}\sum_{i=1}^{N} v^i$$

be the average position and velocity of the swarm, respectively. The objective of each agent is to move so as to end up at $\bar{x}$ and $\bar{v}$; in this way an emergent behavior of the group is produced where they aggregate dynamically and end up near each other and ultimately move in the same direction at nearly the same velocity (i.e., cohesion). The problem is that since all the agents are moving at the same time, $\bar{x}$ and $\bar{v}$ are time-varying; hence, in order to study the stability of swarm cohesion we study the

dynamics of an error system with

$$e_p^i = x^i - \bar{x}$$

$$e_v^i = v^i - \bar{v}$$

Other choices for error systems are also possible and have been used in some studies of swarm stability. For instance, you could use $\tilde{e}_p^i = \sum_{j=1}^{N} (x^i - x^j)$. This corresponds to computing the errors to each other agent and then trying to get all those errors to go to zero. Note, however, that

$$\tilde{e}_p^i = N \left(x^i - \frac{1}{N} \sum_{j=1}^{N} x^j \right) = N \left(x^i - \bar{x} \right) = N e_p^i.$$

So this error definition is a scaled version of what we use.

The error dynamics are given by

$$\begin{aligned} \dot{e}_p^i &= e_v^i \\ \dot{e}_v^i &= \frac{1}{M_i} u^i - \frac{1}{N} \sum_{j=1}^{N} \frac{1}{M_j} u^j. \end{aligned} \tag{2.3}$$

We assume that each agent can sense its own position and velocity relative to $\bar{x}$ and $\bar{v}$, but with some errors. In particular, let $d_p^i \in \Re^n$ and $d_v^i \in \Re^n$ be these sensing errors for agent i, respectively. We assume that $d_p^i(t)$ and $d_v^i(t)$ are any trajectories that are sufficiently smooth and fixed a priori for all the time (but below we will study the stability for the case when the d_p^i and d_v^i trajectories can be any of a certain class). We will refer to these terms somewhat colloquially as "noise" but clearly our framework is entirely deterministic. Thus, each agent actually senses

$$\hat{e}_p^i = e_p^i - d_p^i$$

$$\hat{e}_v^i = e_v^i - d_v^i$$

and below we will also assume that it can sense its own velocity. It is important to highlight here our motivation for studying the addition of noise. On the one hand it adds another element of realism to have a sensor for e_p^i and e_v^i might operate and the results below will help quantify the effects of the noise on cohesion. We also view our approach as progress in the direction of not requiring that each agent can sense the variables of all the other agents or even the accurate values of $\bar{x}$ and $\bar{v}$.

The i^{th} agent will also try to follow a plane nutrient profile J_p^i defined earlier. We assume that it senses the gradient of J_p^i, but with some sufficiently smooth error $d_f^i(t)$ that is fixed a priori for all the time (as with d_p^i and d_v^i we will allow below d_f^i to be any in a certain class of trajectories) so each agent actually senses $\nabla J_p^i\left(x^i\right) - d_f^i$. In fact this can be viewed as either sensing error or "noise" (variations, ripples) on the resource profile.

Suppose the general form of the control input for each agent is

$$\begin{aligned} u^i &= -M_i k_p^i \hat{e}_p^i - M_i k_v^i \hat{e}_v^i - M_i k v^i \\ &\quad + M_i k_r^i \sum_{j=1, j\neq i}^{N} \exp\left(\frac{-\frac{1}{2}\left\|\hat{e}_p^i - \hat{e}_p^j\right\|^2}{{r_s^i}^2}\right)\left(\hat{e}_p^i - \hat{e}_p^j\right) \\ &\quad - M_i k_f^i\left(R^i - d_f^i\right). \end{aligned} \tag{2.4}$$

Here, we think of the scalars $k_p^i > 0$ and $k_v^i > 0$ as the "attraction gains" which indicate how aggressive each agent is in aggregating. The gain $k_r^i > 0$ is a "repulsion gain" which sets how much that agent wants to be away from others and r_s^i represents its repulsion range. The gain $k > 0$ works as a "velocity damping gain"(note that we use the same such gain for all agents). The last term in (2.4) indicates that each agent wants to move along the negative gradient of the i^{th} resource profile with the gain $k_f^i > 0$ proportional to that agent's desire to follow its profile. Obviously if

$d_p^i = 0$ for all i, there is no sensing error on repulsion, and a repulsion term of the form explained in (2.2) is obtained. The sensing errors create the possibility that agents will try to move away from each other when they may not really need to, and they may move toward each other when they should not. Similarly, the attractions gains k_p^i and k_v^i dictate how the attraction forces operate but the presence of the noise results in additive noise terms to u^i that are multiplied by k_p^i and k_v^i. Hence, raising the attraction gains also has a negative influence on u^i in that it results in more noise entering the control and hence poor aggregating decisions by individuals (e.g., if $\|x^i - x^j\|$ is small but d_p^i is relatively large, noise will set the control value). Clearly, this complicates the situation for the whole swarm to achieve cohesiveness.

Note that by writing the repulsion term as in (2.4), we are assuming each agent can also sense the positions of all other agents relative to $\bar{x}$; however, the sensed values for other agents are only needed in the repulsion term and any term corresponding to a distant agent will be close to zero due to the exponential term. Alternatively, we may construct this term by replacing $\hat{e}_p^i - \hat{e}_p^j$ with $\hat{x}^i - \hat{x}^j$, with $\hat{x}^i$ and $\hat{x}^j$ defined as the noise-contaminated positions of agent i and j, respectively. Then we have $\hat{x}^i - \hat{x}^j = x^i - x^j + d_p^{ij}$, d_p^{ij} being the measurement noise. In physical sense, these two options of constructing the repulsion term are significantly different from each other since different variables are required to be measured. But note that

$$\begin{aligned} \hat{e}_p^i - \hat{e}_p^j &= \left(\left(x^i - \bar{x}\right) - d_p^i\right) - \left(\left(x^j - \bar{x}\right) - d_p^j\right) \\ &= \left(\hat{x}^i - \hat{x}^j\right) - \left[d_p^{ij} + \left(d_p^i - d_p^j\right)\right]. \end{aligned}$$

It turns out that in our proof, we will obtain the same stability properties with either option. A quick explanation is that the repulsion term is bounded by the same constants (in both directions), whether we adopt $\hat{e}_p^i - \hat{e}_p^j$ or $\hat{x}^i - \hat{x}^j$. This will become

more clear by inspecting the proof in the later sections. From now on, we will use the one in (2.4) throughout the chapter.

To study stability properties, we will substitute the above choice for u^i into the error dynamics in Equation (2.3). First, consider the $\dot{v}^i$ term of $\dot{e}_v^i = \dot{v}^i - \dot{\bar{v}}$ and note that

$$\begin{aligned}\dot{v}^i = \frac{1}{M_i}u^i &= -k_p^i e_p^i + k_p^i d_p^i - k_v^i e_v^i + k_v^i d_v^i - kv^i \\ &\quad + k_r^i \sum_{j=1, j\neq i}^{N} \exp\left(\frac{-\frac{1}{2}\left\|\hat{e}_p^i - \hat{e}_p^j\right\|^2}{{r_s^i}^2}\right)\left(\hat{e}_p^i - \hat{e}_p^j\right) \\ &\quad - k_f^i\left(R^i - d_f^i\right). \end{aligned} \tag{2.5}$$

Define $\bar{k}_p = \frac{1}{N}\sum_{j=1}^{N} k_p^j$ and $\Delta k_p^j = k_p^j - \bar{k}_p$. Since

$$\sum_{j=1}^{N} e_p^j = \sum_{j=1}^{N}\left(x^j - \bar{x}\right) = N\bar{x} - \sum_{j=1}^{N}\bar{x} = 0$$

we have

$$\sum_{j=1}^{N} k_p^j e_p^j = \sum_{j=1}^{N} \Delta k_p^j e_p^j + \sum_{j=1}^{N} \bar{k}_p e_p^j = \sum_{j=1}^{N} \Delta k_p^j e_p^j.$$

Similarly, define $\bar{k}_v$ and Δk_v^j, so we have $\sum_{j=1}^{N} k_v^j e_v^j = \sum_{j=1}^{N} \Delta k_v^j e_v^j$. Then, substituting u^i into $\dot{\bar{v}}$ and we have

$$\begin{aligned}\dot{\bar{v}} &= -\frac{1}{N}\sum_{j=1}^{N} \Delta k_p^j e_p^j + \frac{1}{N}\sum_{j=1}^{N} k_p^j d_p^j - \frac{1}{N}\sum_{j=1}^{N} \Delta k_v^j e_v^j \\ &\quad + \frac{1}{N}\sum_{j=1}^{N} k_v^j d_v^j - \frac{1}{N}\sum_{j=1}^{N} kv^j \\ &\quad + \frac{1}{N}\sum_{l=1}^{N} k_r^l \sum_{j=1, j\neq l}^{N} \exp\left(\frac{-\frac{1}{2}\left\|\hat{e}_p^l - \hat{e}_p^j\right\|^2}{{r_s^l}^2}\right)\left(\hat{e}_p^l - \hat{e}_p^j\right) \\ &\quad - \frac{1}{N}\sum_{j=1}^{N} k_f^j\left(R^j - d_f^j\right). \end{aligned} \tag{2.6}$$

Define $E^i = [{e_p^i}^\top,\ {e_v^i}^\top]^\top$ and $E = [{E^1}^\top, {E^2}^\top, \ldots, {E^N}^\top]^\top$. Since

$$kv^i - \frac{1}{N}\sum_{j=1}^{N} kv^j = kv^i - k\bar{v} = ke_v^i$$

from (2.5) and (2.6) we have

$$\dot{e}_v^i = \dot{v}^i - \dot{\bar{v}} = -k_p^i e_p^i - \left(k_v^i + k\right) e_v^i + g^i + \phi(E) + \delta^i(E). \tag{2.7}$$

where

$$\begin{aligned}
g^i &= k_p^i d_p^i + k_v^i d_v^i + k_f^i d_f^i - k_f^i R^i && (2.8)\\
\phi(E) &= \frac{1}{N}\sum_{j=1}^{N} \Delta k_p^j e_p^j + \frac{1}{N}\sum_{j=1}^{N} \Delta k_v^j e_v^j - \frac{1}{N}\sum_{j=1}^{N} k_p^j d_p^j \\
&\quad -\frac{1}{N}\sum_{j=1}^{N} k_v^j d_v^j + \frac{1}{N}\sum_{j=1}^{N} k_f^j \left(R^j - d_f^j\right) && (2.9)\\
\delta^i(E) &= k_r^i \sum_{j=1, j\neq i}^{N} \exp\left(\frac{-\frac{1}{2}\left\|\hat{e}_p^i - \hat{e}_p^j\right\|^2}{{r_s^i}^2}\right)\left(\hat{e}_p^i - \hat{e}_p^j\right) \\
&\quad -\frac{1}{N}\sum_{l=1}^{N} k_r^l \sum_{j=1, j\neq l}^{N} \exp\left(\frac{-\frac{1}{2}\left\|\hat{e}_p^l - \hat{e}_p^j\right\|^2}{{r_s^l}^2}\right)\left(\hat{e}_p^l - \hat{e}_p^j\right) && (2.10)
\end{aligned}$$

which is a nonlinear non-autonomous system. With I an $n \times n$ identity matrix, the error dynamics of the i^{th} agent may be written as

$$\begin{aligned}
\dot{E}^i &= \overbrace{\begin{bmatrix} 0 & I \\ -k_p^i I & -\left(k_v^i + k\right) I \end{bmatrix}}^{A_i} E^i \\
&\quad + \overbrace{\begin{bmatrix} 0 \\ I \end{bmatrix}}^{B} \left(g^i + \phi(E) + \delta^i(E)\right). && (2.11)
\end{aligned}$$

Note that any matrix

$$\begin{bmatrix} 0 & I \\ -k_1 I & -k_2 I \end{bmatrix}$$

with $k_1 > 0$, $k_2 > 0$ has eigenvalues given by the roots of $\left(s^2 + k_2 s + k_1\right)^n$, which are in the strict left half plane. Thus, the matrix A_i above is Hurwitz with $k_p^i > 0$, $k_v^i > 0$ and $k > 0$.

2.3.2 Cohesive Social Foraging with Noise

Our analysis methodology involves viewing the error system in (2.11) as generating $E^i(t)$ trajectories for a given $E^i(0)$ and the fixed sensing error trajectories $d_p^i(t)$, $d_v^i(t)$, and $d_f^i(t)$, $t \geq 0$. We do not consider, however, all possible sensing error trajectories. We only consider a class of ones that satisfy for all $t \geq 0$

$$\begin{aligned} \|d_f^i(t)\| &\leq D_f^i \\ \|d_p^i(t)\| &\leq D_{p_1}^i \left\|E^i(t)\right\| + D_{p_2}^i \\ \|d_v^i(t)\| &\leq D_{v_1}^i \left\|E^i(t)\right\| + D_{v_2}^i \end{aligned} \tag{2.12}$$

where $D_{p_1}^i$, $D_{p_2}^i$, $D_{v_1}^i$, $D_{v_2}^i$ and D_f^i are known non-negative constants for $i = 1, \ldots, N$. So we assume for position and velocity the sensing errors have linear relationship with the magnitude of the state of the error system. Basically the assumption means that when two agents are far away from each other, the sensing errors can increase. The noise d_f^i on the nutrient profile is unaffected by the position of an agent. By considering only this class of fixed sensing error trajectories we prune the set of possibilities for E^i trajectories and it is only for that pruned set that our analysis holds.

Uniform Ultimate Boundedness of Inter-Agent Trajectories

Theorem 1: *Consider the swarm described by the model in (2.3) with control input u^i given in (2.4). Assume that the nutrient profile for each agent is a plane*

defined by $\nabla J_p^i(x) = R^i$ *and the noise satisfies (2.12). Let*

$$\begin{aligned}\beta_1^i &= \frac{\left(k_p^i+1\right)^2+\left(k_v^i+k\right)^2}{2k_p^i\left(k_v^i+k\right)} \\ &\quad +\sqrt{\left(\frac{{k_p^i}^2+\left(k_v^i+k\right)^2-1}{2k_p^i\left(k_v^i+k\right)}\right)^2+\frac{1}{{k_p^i}^2}}\end{aligned} \tag{2.13}$$

for $i = 1, \ldots, N$*. If for all* i *we have*

$$k_p^i D_{p_1}^i + k_v^i D_{v_1}^i < \frac{1}{\beta_1^i} \tag{2.14}$$

and the parameters are such that

$$\sum_{i=1}^{N} \frac{\beta_1^{i^*}\left(k_p^i D_{p_1}^i + k_v^i D_{v_1}^i + \sqrt{{\Delta k_p^i}^2+{\Delta k_v^i}^2}\right)}{N\left(1-\theta^i\right)\left(1-\beta_1^i\left(k_p^i D_{p_1}^i + k_v^i D_{v_1}^i\right)\right)} < 1 \tag{2.15}$$

for some constants $0 < \theta^i < 1$*, where*

$$i^* = \arg\max_i \beta_1^i,\ i = 1, \ldots, N$$

then the trajectories of (2.11) are uniformly ultimately bounded.

Proof: To study the stability of the error dynamics, it is convenient to choose Lyapunov function for each agent

$$V_i\left(E^i\right) = {E^i}^\top P_i E^i \tag{2.16}$$

with $P_i = P_i^\top$ a $2n \times 2n$ matrix and $P_i > 0$ (a positive definite matrix). Then we have

$$\begin{aligned}\dot{V}_i &= {E^i}^\top P_i \dot{E}^i + {\dot{E}^i}^\top P_i E^i \\ &= {E^i}^\top \overbrace{\left(P_i A_i + A_i^\top P_i\right)}^{-Q_i} E^i \\ &\quad +2{E^i}^\top P_i B\left(g^i + \phi^i(E) + \delta^i(E)\right).\end{aligned} \tag{2.17}$$

Note that when $Q_i = Q_i^\top$ and $Q_i > 0$, the unique solution P_i of $P_i A_i + A_i^\top P_i = -Q_i$ has $P_i = P_i^\top$ and $P_i > 0$ as needed.

Choose for the composite system

$$V(E) = \sum_{i=1}^{N} V_i(E^i)$$

where $V_i(E^i)$ is given in (2.16). Since for any matrix $M = M^\top > 0$ and vector X

$$\lambda_{min}(M) X^\top X \leq X^\top M X \leq \lambda_{max}(M) X^\top X$$

where $\lambda_{min}(M)$ and $\lambda_{max}(M)$ denote the minimum and maximum eigenvalue of M, respectively, from (2.16) we have

$$\sum_{i=1}^{N} \left(\lambda_{min}(P_i) \left\| E^i \right\|^2 \right) \leq V(E) \leq \sum_{i=1}^{N} \left(\lambda_{max}(P_i) \left\| E^i \right\|^2 \right).$$

It is easy to show that the function $F(\psi) = \exp\left(\frac{-\frac{1}{2}\|\psi\|^2}{{r_s^i}^2} \right) \|\psi\|$, with ψ any real vector, has a unique maximum value of $\exp(-\frac{1}{2}) r_s^i$ which is achieved when $\|\psi\| = r_s^i$ [44]. Defining

$$\begin{aligned} \Delta^i &= k_r^i \exp\left(-\frac{1}{2}\right) \sum_{j=1, j\neq i}^{N} r_s^j \\ &\quad + \frac{1}{N} \exp\left(-\frac{1}{2}\right) \sum_{l=1}^{N} k_r^l \sum_{j=1, j\neq l}^{N} r_s^j \end{aligned} \tag{2.18}$$

we have $\|\delta^i(E)\| \leq \Delta^i$ for $i = 1, \ldots, N$. Define

$$\tilde{R} = \frac{1}{N} \sum_{i=1}^{N} k_f^i R^i.$$

Then substituting (2.11) into (2.17), and using (2.18) and the fact that $\|B\| = 1$ we have

$$\begin{aligned}
\dot{V}(E) &= \sum_{i=1}^{N} \dot{V}_i(E^i) \\
&= \sum_{i=1}^{N} \left[-{E^i}^\top Q_i E^i + 2{E^i}^\top P_i B \left(g^i + \phi^i(E) + \delta^i(E) \right) \right] \\
&\leq \sum_{i=1}^{N} \left[-c_1^i \left\| E^i \right\|^2 + c_2^i \left\| E^i \right\| + \left\| E^i \right\| \sum_{j=1}^{N} \left(a^{ij} \left\| E^j \right\| \right) \right]
\end{aligned} \tag{2.19}$$

with c_1^i, c_2^i and a^{ij} constants and

$$\begin{aligned}
c_1^i &= \lambda_{min}(Q_i) \left(1 - \frac{2\lambda_{max}(P_i)}{\lambda_{min}(Q_i)} \left(k_p^i D_{p_1}^i + k_v^i D_{v_1}^i \right) \right) \\
c_2^i &= 2\lambda_{max}(P_i) \left(k_p^i D_{p_2}^i + k_v^i D_{v_2}^i + k_f^i D_f^i + \left\| k_f^i R^i - \tilde{R} \right\| \right. \\
&\quad \left. + \frac{1}{N} \sum_{j=1}^{N} k_p^j D_{p_2}^j + \frac{1}{N} \sum_{j=1}^{N} k_v^j D_{v_2}^j + \frac{1}{N} \sum_{j=1}^{N} k_f^j D_f^j + \Delta^i \right) \\
a^{ij} &= \frac{2}{N} \lambda_{max}(P_i) \left(k_p^j D_{p_1}^j + k_v^j D_{v_1}^j + \sqrt{{\Delta k_p^j}^2 + {\Delta k_v^j}^2} \right).
\end{aligned}$$

Obviously $c_2^i > 0$, $a^{ij} > 0$, and if we have

$$k_p^i D_{p_1}^i + k_v^i D_{v_1}^i < \frac{1}{\beta_0^i} \tag{2.20}$$

where

$$\beta_0^i = \frac{2\lambda_{max}(P_i)}{\lambda_{min}(Q_i)}$$

then $c_1^i > 0$.

Before we proceed, note that in (2.20), we want β_0^i to be as small as possible so that the system may tolerate noise with the largest possible bounds ($D_{p_1}^i$ and $D_{v_1}^i$) while keeping stability. Notice that we can influence the size of the β_0^i by the choice of $Q_i > 0$. In fact, we can show that $\min_{Q_i} \beta_0^i = \beta_1^i$. To see this, note that from

[52], β_0^i is minimized by letting $Q_i = k_q^i I$ with $k_q^i > 0$ a free parameter, and it can be proven that

$$\min_{Q_i} \beta_0^i = \left. \frac{2\lambda_{max}(P_i)}{\lambda_{min}(Q_i)} \right|_{Q_i = k_q^i I} = \frac{k_q^i \beta_1^i}{k_q^i} = \beta_1^i. \tag{2.21}$$

Thus, from (2.20) and (2.21), if (2.14) holds, then by choosing $Q_i = k_q^i I$, the corresponding constant c_1^i for (2.19) is positive.

Now for simplicity, we choose $Q_i = I$ for all i (so $k_q^i = 1$) and use (2.21), so c_1^i, c_2^i and a^{ij} of (2.19) are simplified to become

$$\begin{aligned}
c_1^i &= 1 - \beta_1^i \left(k_p^i D_{p_1}^i + k_v^i D_{v_1}^i \right) && (2.22) \\
c_2^i &= \beta_1^i \Bigg(k_p^i D_{p_2}^i + k_v^i D_{v_2}^i + k_f^i D_f^i + \left\| k_f^i R^i - \tilde{R} \right\| + \\
&\quad \frac{1}{N} \sum_{j=1}^{N} k_p^j D_{p_2}^j + \frac{1}{N} \sum_{j=1}^{N} k_v^j D_{v_2}^j + \\
&\quad \frac{1}{N} \sum_{j=1}^{N} k_f^j D_f^j + \Delta^i \Bigg) && (2.23) \\
a^{ij} &= \frac{\beta_1^i}{N} \left(k_p^j D_{p_1}^j + k_v^j D_{v_1}^j + \sqrt{\Delta {k_p^j}^2 + \Delta {k_v^j}^2} \right). && (2.24)
\end{aligned}$$

Now, return to (2.19) and note that for any θ^i, $0 < \theta^i < 1$,

$$\begin{aligned}
& -c_1^i \left\| E^i \right\|^2 + c_2^i \left\| E^i \right\| \\
= \; & -(1-\theta^i) c_1^i \left\| E^i \right\|^2 - \theta^i c_1^i \left\| E^i \right\|^2 + c_2^i \left\| E^i \right\| \\
\leq \; & -(1-\theta^i) c_1^i \left\| E^i \right\|^2, \; \forall \; \left\| E^i \right\| \geq r^i \\
= \; & \sigma^i \left\| E^i \right\|^2 && (2.25)
\end{aligned}$$

where $r^i = \frac{c_2^i}{\theta^i c_1^i}$ and $\sigma^i = -(1-\theta^i) c_1^i < 0$. This implies that as long as $\|E^i\| \geq r^i$, the first two terms in (2.19) combined will give a negative contribution to $\dot{V}(E)$.

Next, we seek conditions under which $\dot{V}(E) < 0$. To do this, we consider the third term in (2.19) and combine it with the above results. First, note that the third term

in (2.19) can be over-bounded by replacing a^{ij} by a^{i^*j} where

$$a^{i^*j} = \max_{1 \leq i \leq N} a^{ij} \tag{2.26}$$

which were defined in the statement of the theorem via (2.24). Next, we consider the general situation where some of the E^i are such that $\|E^i\| < r^i$ and others are not. Accordingly, define sets

$$\Pi_O = \left\{ i : \left\|E^i\right\| \geq r^i,\ i \in 1, \ldots, N \right\} = \left\{ i_O^1,\ i_O^2, \ldots,\ i_O^{N_O} \right\}$$

and

$$\Pi_I = \left\{ i : \left\|E^i\right\| < r^i,\ i \in 1, \ldots, N \right\} = \left\{ i_I^1,\ i_I^2, \ldots,\ i_I^{N_I} \right\}$$

where N_O and N_I are the size of Π_O and Π_I, respectively, and $N_O + N_I = N$. Also, $\Pi_O \bigcup \Pi_I = \{1, \ldots, N\}$ and $\Pi_O \bigcap \Pi_I = \phi$. Of course, we do not know the explicit sets Π_O and Π_I; all we know is that they exist. The explicit values in the sets clearly depend on time but we will allow that time to be arbitrary so the analysis below will be for all t. For now, we assume $N_O > 0$, that is, the set Π_O is non-empty. We will later discuss the $N_O = 0$ case. Then using analysis ideas from the theory of stability of interconnected systems [53] and using (2.19), (2.25) and (2.26), we have

$$\begin{aligned} \dot{V}(E) \ \leq \ & \sum_{i \in \Pi_O} \sigma^i \left\|E^i\right\|^2 + \sum_{i \in \Pi_O} \left(\left\|E^i\right\| \sum_{j \in \Pi_O} a^{i^*j} \left\|E^j\right\| \right) \\ & + \sum_{i \in \Pi_O} \left(K_1 + K_3 a^{i^*i} \right) \left\|E^i\right\| + K_2 + K_4 \end{aligned}$$

where we use the fact that for each fixed N_O, there exist positive constants $K_1(N_O)$, $K_2(N_O)$, $K_3(N_O)$ and $K_4(N_O)$ such that,

$$\begin{aligned} K_1(N_O) &\geq \sum_{j\in\Pi_I} a^{i^*j} \left\|E^j\right\| \\ K_2(N_O) &\geq \sum_{i\in\Pi_I} \left(-c_1^i \left\|E^i\right\|^2 + c_2^i \left\|E^i\right\|\right) \\ K_3(N_O) &\geq \sum_{i\in\Pi_I} \left\|E^i\right\| \\ K_4(N_O) &\geq \sum_{i\in\Pi_I} \left(\left\|E^i\right\| \sum_{j\in\Pi_I} a^{i^*j} \left\|E^j\right\|\right). \end{aligned} \tag{2.27}$$

Let $w^\top = \left[\|E^{i_O^1}\|, \|E^{i_O^2}\|, \ldots, \|E^{i_O^{N_O}}\|\right]$ (the composition of this vector can be different at different times) and the $N_O \times N_O$ matrix $S = [s_{jn}]$ be specified by

$$s_{jn} = \begin{cases} -(\sigma^{i_O^j} + a^{i^* i_O^j}), & j = n \\ -a^{i^* i_O^j}, & j \neq n \end{cases} \tag{2.28}$$

so we have

$$\dot{V}(E) \leq -w^\top S w + \sum_{i\in\Pi_O} \left(K_1 + K_3 a^{i^*i}\right) \left\|E^i\right\| + K_2 + K_4.$$

For now, assume that $S > 0$ in the above equation and thus, $\lambda_{min}(S) > 0$, then we have

$$\begin{aligned} \dot{V}(E) \;\leq\; & -\lambda_{min}(S) \sum_{i\in\Pi_O} \left\|E^i\right\|^2 \\ & + \sum_{i\in\Pi_O} \left(K_1 + K_3 a^{i^*i}\right) \left\|E^i\right\| + K_2 + K_4. \end{aligned} \tag{2.29}$$

So when the $\|E^i\|$ for $i \in \Pi_O$ are sufficiently large, the sign of $\dot{V}(E)$ is determined by $-\lambda_{min}(S) \sum_{i\in\Pi_O} \|E^i\|^2$ and $\dot{V}(E) < 0$. This analysis is valid for any value of N_O, $1 \leq N_O \leq N$; hence for any $N_O \neq 0$ the system is uniformly ultimately bounded if $S > 0$, so we seek to prove that next.

A necessary and sufficient condition for $S > 0$ is that its successive principal minors are all positive. Define $|S_m|$ as the determinants of the principal minors of S, $m = 1, \ldots, N_O$. Then we can show that

$$|S_m| \;=\; \left(1 + \sum_{j=1}^{m} \frac{a^{i^* i_O^j}}{\sigma^{i_O^j}}\right) \prod_{k=1}^{m} \left(-\sigma^{i_O^k}\right).$$

Since $-\sigma^{i_O^k} > 0$ for $k = 1, \ldots, m$, to have all the above determinants positive we need

$$\sum_{j=1}^{m} \frac{a^{i^* i_O^j}}{\sigma^{i_O^j}} > -1$$

that is

$$\sum_{j=1}^{m} \frac{\beta_1^{i^*} \left(k_p^{i_O^j} D_{p_1}^{i_O^j} + k_v^{i_O^j} D_{v_1}^{i_O^j} + \sqrt{\Delta k_p^{i_O^j}{}^2 + \Delta k_v^{i_O^j}{}^2}\right)}{N \left(1 - \theta^{i_O^j}\right) \left(1 - \beta_1^{i_O^j} \left(k_p^{i_O^j} D_{p_1}^{i_O^j} + k_v^{i_O^j} D_{v_1}^{i_O^j}\right)\right)} < 1$$

for all $m = 1, \ldots, N_O$. Since $1 \leq m \leq N_O \leq N$, the equation above is satisfied when (2.15) is satisfied and thus, $S > 0$ for all $N_O \neq 0$. Hence, when $\|E^i\|$ is sufficiently large, $\dot{V}(E) < 0$ and the uniform ultimate boundedness of the trajectories of the error system is achieved.

To complete the proof, we need to consider the case when $N_O = 0$. Note that when $N_O = 0$, $\|E^i\| < r^i$ for all i. If we have $N_O = 0$ persistently, then we could simply take $\max_i r^i$ as the uniform ultimate bound. If otherwise, at certain moment the system changes such that some $\|E^i\| \geq \max_i r^i$, then we have $N_O \geq 1$ immediately, then all the analysis above, which holds for any $1 \leq N_O \leq N$, applies. Thus, in either case we obtain the uniform ultimate boundedness. This concludes the proof. ■

Remark 1 *Uniform ultimate boundedness is obtained when (2.14) and (2.15) are satisfied. Note that these conditions do not depend on k_r^i and r_s^i; these two parameters can affect the size of the ultimate bound but it is the attraction gains k_p^i and k_v^i and*

damping gain k that determine if boundedness can be achieved for given parameters that quantify the size of the noise. The conditions also do not depend on $D^i_{p_2}$ and $D^i_{v_2}$, but these too will affect the size of the ultimate bound. The conditions do not depend on k^i_f, R^i and D^i_f since our error system quantifies swarm cohesiveness, not how well the resource profile is followed.

Remark 2 *From (2.13), if both k^i_p and k^i_v are fixed, when k is sufficiently large, increasing k will increase β^i_1, which means $D^i_{p_1}$ and $D^i_{v_1}$ have to be decreased to satisfy (2.14). This means that although we may expect a large k to dampen the error system faster, it could make the system more vulnerable to noise.*

Remark 3 *Note that when all other parameters are fixed, β^i_1 goes to infinity when k^i_p either goes to infinity or approaches zero. Thus, when k^i_p is the only free parameter, there exists some upper bound for $D^i_{p_1}$ beyond which (2.14) can never hold whatever k^i_p is. This is because when $D^i_{p_1}$ is large enough, k^i_p has to be sufficiently small to decrease the product $k^i_p D^i_{p_1}$ in (2.14), while the β^i_1 corresponding to this sufficiently-small k^i_p will be so large that (2.14) cannot be satisfied. Basically this means that if $D^i_{p_1}$ is too large and leads to potential instability, it cannot be remedied by merely tuning k^i_p. In comparison, if k^i_v is a free parameter with other parameters fixed and $D^i_{p_1}$ sufficiently small, then for any arbitrarily large $D^i_{v_1}$, we can always find some k^i_v such that (2.14) still holds. This is because k^i_v and k always appear together in β^i_1 and thus, for any large $D^i_{v_1}$, we are free to decrease k^i_v such that the product of $k^i_v D^i_{v_1}$ is small.*

Remark 4 *We can see that the smaller $\Delta k_p^{j^2}$ ($\Delta k_v^{j^2}$) is, meaning k^i_p (k^i_v) and k^j_p (k^j_v) are closer to each other for all i and j, the easier it is to meet the condition specified by (2.15). This means better approximations of the agent parameters may*

facilitate the boundedness of the error system. In fact when all agents are identical, the sufficient condition (2.15) can be immediately simplified to

$$\frac{\beta_1 \left(k_p D_{p_1} + k_v D_{v_1}\right)}{(1-\theta)\left(1 - \beta_1 \left(k_p D_{p_1} + k_v D_{v_1}\right)\right)} < 1$$

by letting $k_p^i = k_p$, $k_v^i = k_v$, $\beta_1^i = \beta_1$, $D_{p_1}^i = D_{p_1}$ *and* $D_{v_1}^i = D_{v_1}$ *for all* i. *Note the term* $\sqrt{\Delta {k_p^i}^2 + \Delta {k_v^i}^2}$ *is zero now since* $k_p^i = \bar{k}_p$ *and* $k_v^i = \bar{k}_v$ *for all* i. *Furthermore, when* $D_{p_1}^i = D_{v_1}^i = 0$ *for all* i, *the conditions (2.14) and (2.15) will always hold. This means when agents are identical and noise is constant or with constant bound, the trajectories of the error system are always uniformly ultimately bounded. Also note that since the agents are in general* not *identical and have different parameters, the conditions stated by the theorem are actually quite conservative.*

Remark 5 *Although we start with plane profiles, the nutrient profile can actually be extended to more general cases. In fact any profile that is smooth and has bounded slope at all points, provided the upper bound of its slope is known, can be fit into the framework. To see this, denote the slope upper bound by* ∇J_{max}^i *for agent* i, *and replace all "*R^i*" in the system with "*∇J_{max}^i*," then all the proofs follow.*

Remark 6 *Note that with a repulsion term of the form defined in (2.2), collision avoidance is not guaranteed. Theorem 1 does not say anything about collision avoidance either. But as we have found that larger* k_r^i *and* r_s^i, *meaning stronger repulsion effect, will result in larger swarm size, we expect they may also help reduce collisions between the agents. See additional discussions on this point in Section 2.5.1. Moreover, as in [35, 45] it is possible to extend the results of this chapter to consider a "hard repel" case by using a different form for the repel term.*

Ultimate Bound on Inter-Agent Trajectories

So far we have shown that the swarm error system is uniformly ultimately bounded when certain conditions are satisfied. We have shown that the bound exists but have not specified it. If we define the bound as $R_b > 0$, then the set

$$\Omega_c = \left\{ E : \left\| E^i \right\| \leq R_b, i = 1, \ldots, N \right\}$$

is attractive and compact. One such bound is given by the Corollary below. Before we state the Corollary, some new notation needs to be introduced. Notice that for each given N_O, $1 \leq N_O \leq N$, the set Π_O can have $N_{N_O} = C_N^{N_O}$ types of compositions, where $C_N^{N_O}$ is the number of combinations of choosing N_O members from a set with N members. (Note that the special case of $N_O = 0$ will be considered separately at the end of the proof for the Corollary.) Let $\Pi_O^{(k)}$ be the set Π_O corresponding to the k^{th} composition, $k = 1, \ldots, N_{N_O}$. Let the $N_O \times N_O$ matrix $S^{(k)}$ be specified in the same way as S, defined in (2.28), but corresponding to the k^{th} composition, $k = 1, \ldots, N_{N_O}$. Define for $k = 1, \ldots, N_{N_O}$

$$\begin{aligned} a_d^k(N_O) &= \lambda_{min}(S^{(k)}_{N_O \times N_O}) \\ b_d(N_O) &= K_1(N_O) + K_3(N_O)\hat{a} \\ c_d(N_O) &= K_2(N_O) + K_4(N_O) \end{aligned}$$

where K_1, K_2, K_3 and K_4 are defined in (2.27), and

$$\hat{a} = \max_{1 \leq i \leq N,\, 1 \leq j \leq N} a^{ij} = \max_{1 \leq j \leq N} a^{i^* j}$$

with $a^{i^* j}$ defined in (2.26). Note that in Theorem 1 we do *not* highlight the difference between compositions because it does not matter, while in the proof for the Corollary

below it will make things more clear to do so. Also note that b_d and c_d are not affected by the composition because we may choose K_1, K_2, K_3 and K_4 in such a way that (2.27) always holds for *any* composition with $0 \leq N_I \leq N-1$ (and thus, $1 \leq N_O \leq N$). In the following Corollary and proof, all notation is the same as those in Theorem 1 unless otherwise specified.

Corollary 1 *Define* $r^* = \max_{1 \leq i \leq N} r^i$, *with* r^i *defined in (2.25) via some set of* θ^i *that satisfy (2.15). When the conditions in Theorem 1 are all satisfied, there exists some constant* $0 < \theta_d < 1$ *such that the uniform ultimate bound of the trajectories of the error system is*

$$R_b = \max\{r_b, r^*\}$$

where

$$r_b = \frac{b_d^* + \sqrt{N{b_d^*}^2 + 4a_d^* c_d^*}}{2a_d^* \theta_d} \tag{2.30}$$

with a_d^*, b_d^*, *and* c_d^* *are all constants and*

$$\begin{aligned} a_d^* &= min_{k,N_O} a_d^k(N_O) \\ b_d^* &= max_{N_O} b_d(N_O) \\ c_d^* &= max_{N_O} c_d(N_O) \end{aligned}$$

for $N_O = 1, \ldots, N$ *and* $k = 1, \ldots, N_{N_O}$.

Proof: Note that when the conditions of Theorem 1 are all satisfied, a set of constants θ^i exists and can be found. Also recall that both c_1^i and c_2^i are constants, then $r^i = \frac{c_2^i}{\theta^i c_1^i}$ and $\sigma^i = -(1-\theta^i)c_1^i$, defined in (2.25), are constants for all i and can be found. Thus, numeric values of a_d^*, b_d^*, and c_d^* can be found in terms of known

parameters. Now we will first show that this Corollary applies to a fixed $N_O \neq 0$ with a particular composition k.

With $V(E)$ defined in Theorem 1, for $N_O \neq 0$ and $\Pi_O^{(k)}$, from (2.29) we have

$$\begin{aligned} \dot{V}(E) &\leq -a_d^k \sum_{i\in\Pi_O^{(k)}} \left\|E^i\right\|^2 + b_d \sum_{i\in\Pi_O^{(k)}} \left\|E^i\right\| + c_d \\ &= \sum_{i\in\Pi_O^{(k)}} \underbrace{\left[-a_d^k \left(\left\|E^i\right\| - \frac{b_d}{2a_d^k}\right)^2 + \frac{b_d^2}{4a_d^k}\right]}_{F^i} + c_d \end{aligned} \tag{2.31}$$

with a_d^k, b_d and c_d all positive constants. Notice we want to find a bound r_b' such that $\dot{V}(E) < 0$ so long as there exist some $\|E^i\| > r_b'$, $i \in \Pi_O^{(k)}$. Before we start to solve for this r_b', note that F^i in (2.31) can be visualized by Figure 2.1, where F^i is a parabolic function with respect to $\|E^i\|$ and crosses $\|E^i\|$ axis at two points r_A and r_B, respectively. To have $\dot{V}(E) < 0$, one possibility is such that $\|E^i\| > r_B$ and thus, $F^i < 0$ for all $i \in \Pi_O^{(k)}$. (Note that due to the nature of our problem, we do not consider the case of $\|E^i\| < r_A$, though this also results in $F^i < 0$.) We call this situation the "best situation." While in a more general case, we have some $\|E^i\| > r_B$ while all the other $\|E^i\| \leq r_B$, $i \in \Pi_O^{(k)}$ and we call such a situation the "normal situation." For the best situation case, each $\|E^i\|$ just needs to be *a little* bigger than r_B to achieve $\dot{V}(E) < 0$, which means r_b' is just a little bigger than r_B. In comparison, to get $\dot{V}(E) < 0$ for the normal situation, generally it means those $\|E^i\|$ that satisfy $\|E^i\| > r_B$ have to be further to the right on $\|E^i\|$ axis (i.e., *much* bigger than r_B) to counteract the "positive" effects brought in by those $\|E^i\|$ with $\|E^i\| \leq r_B$, meaning r_b' needs to be much bigger than r_B. With this idea, we can see that the worst r_b' happens when there is only *one* F^i, call it $i = i'$, free to change

while all the other F^i, with $i = i_O^1, \ldots, i_O^{N_O}$ and $i \neq i'$, are fixed at their respective maximum (or most "positive" value). Basically this depicts a situation when there is only one agent having its norm of error $\|E^{i'}\|$ slide along $\|E^i\|$ axis (to the right) to bring $\dot{V}(E)$ down to negative value while all other agents in $\Pi_O^{(k)}$ stay in positions as bad as they can (in the sense of keeping stability).

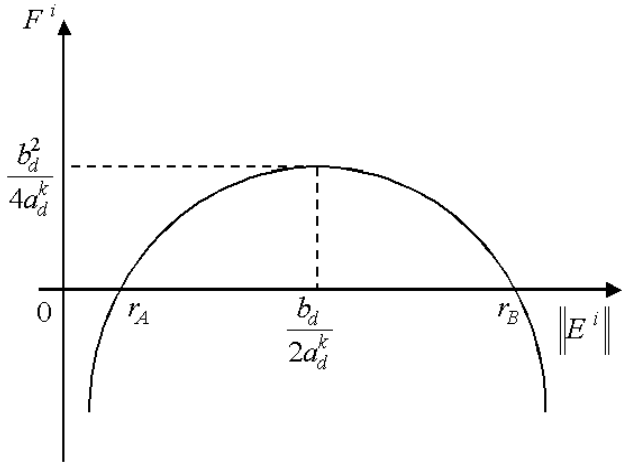

Figure 2.1: F^i vs $\|E^i\|$.

From (2.31) we can see that each F^i achieves its maximum of $\frac{b_d^2}{4a_d^k}$ with $\|E^i\| = \frac{b_d}{2a_d^k}$. Then based on the analysis above, we can solve for the r_b' by letting all $F^i = \frac{b_d^2}{4a_d^k}$ except for $i = i'$. From (2.31), for some constant $0 < \theta_d < 1$ we have

$$\begin{aligned}
\dot{V}(E) &\leq \left[-a_d^k \left(\left\|E^{i'}\right\| - \frac{b_d}{2a_d^k}\right)^2 + \frac{b_d^2}{4a_d^k}\right] \\
&\quad + \sum_{i \in \Pi_O^{(k)}, i \neq i'} \frac{b_d^2}{4a_d^k} + c_d \\
&\leq -a_d^k (1 - \theta_d) \left\|E^{i'}\right\|^2, \forall \left\|E^{i'}\right\| \geq r_b'
\end{aligned}$$

where

$$r_b' = \frac{b_d + \sqrt{N_O b_d^2 + 4a_d^k c_d}}{2a_d^k \theta_d}.$$

Note that in setting $\|E^i\| = \frac{b_d}{2a_d^k}$ to get $F^i = \frac{b_d^2}{4a_d^k}$, we may violate the prerequisite of $i \in \Pi_O^{(k)}$ since it may happen that $r^i > \frac{b_d}{2a_d^k}$ for some $i \in \Pi_O^{(k)}$. But this violation only adds more conservativeness to the resultant r_b' and does not nullify the fact that r_b' is a valid bound. Specifically, when $r^i > \frac{b_d}{2a_d^k}$ for some $i \in \Pi_O^{(k)}$, the corresponding F^i become "less" positive, as seen from Figure 2.1, and thus, the actual bound will be smaller than the r_b' obtained above. Hence, r_b' is still a valid (upper) bound.

Since $r_b \geq r_b'$ with r_b defined in (2.30), and the positive constant $a_d^* \leq a_d^k$, we have $\dot{V}(E) \leq -a_d^*(1-\theta_d)\|E^i\|^2$ when $\|E^i\| \geq r_b$. Now note that the choice of N_O and composition k in the above proof are in fact arbitrary (except that $N_O \neq 0$) and can be time-varying. So we actually have $R_b \geq r_b \geq r_b'$ for any $1 \leq N_O \leq N$ and any composition at any time t. That is, the proof above is actually valid for the general case when N_O ($N_O \neq 0$) and the composition are time-varying.

To complete the proof, we need to show that R_b is also a valid bound for the case of $N_O = 0$, i.e., an empty set Π_O. Notice that $N_O = 0$ means $\|E^i\| < r^i$ for $i = 1, \ldots, N$. Also notice that $r^i \leq \max_{1 \leq i \leq N} r^i \leq R_b$ for all i. Then by definition, as long as $N_O = 0$, the trajectories of the swarm error system stay within the bound R_b. This concludes the proof. ■

Remark 7 *The value of R_b is affected by two components: r_b and r^*. We will discuss r_b first. It is easy to see from (2.30) that increasing a_d^* helps to decrease r_b. Notice a_d^* is a function including many parameters, so it is difficult to provide clear relationships to their effects on r_b. But we may get some ideas based on intuition. Note that*

a_d^* is related to the minimum eigenvalue of matrix S defined in (2.28), where the components $-(\sigma^i + a^{i^*i})$, $i \in 1, \ldots, N$, on the main diagonal reflect the stabilizing effect of the isolated parts of the composite system, while the cross terms $-a^{i^*i}$ reflect the destabilizing effect of the interconnection parts of the composite system. (By abuse of notation, above we use $-(\sigma^i + a^{i^*i})$ instead of $-(\sigma^{i^j_O} + a^{i^*i^j_O})$ as in (2.28). This is because we are discussing the general case and each i^j_O can be any value from 1 to N. Similarly, in this Remark and the next Remark, we do not tell the difference of a^{i^*i} and a^{i^*j}, since both i and j range from 1 to N.) So, the larger magnitude *those main diagonal components have (or relatively, the smaller* magnitude *those cross terms have), the "more stable" the composite system is and thus, we may expect the larger a_d^* is. Based on this analysis and (2.22), since smaller $D^i_{p_1}$ and $D^i_{v_1}$ gives larger c^i_1 and thus, larger σ^i in magnitude (implying "better stability"), it may render larger a_d^* and thus, smaller r_b. When σ^i are relatively big, from (2.24), we may deduce that smaller N and thus, larger a^{i^*i} (implying "worse stability") may lead to smaller a_d^* and thus, larger r_b.*

Remark 8 *Note that b_d^* is affected by a^{i^*j} via $\hat{a}$, $j \in 1, \ldots, N$. Larger a^{i^*j} may lead to larger b_d^* and thus, a larger bound r_b. This is consistent with the analysis in the previous remark. Similar conclusions may be drawn by inspecting c_d^* since it includes K_4, which is affected by a^{i^*j}. It is interesting to note that from (2.30), smaller N means smaller r_b, while in the previous remark we mention that smaller N may lead to larger a^{i^*j} and thus, larger r_b. These seemingly contradictive conclusions in fact make sense intuitively. Too large N does not help reducing r_b because with each agent desiring to keep certain distance from others, large N means large swarm radius. Too small N does not always help reducing r_b because the effect of noise becomes more*

significant when N is small. In the other words, with smaller N, the swarm cannot "average" out the noise and thus, the bound on the trajectories is not reduced. This "noise-averaging" idea will become more clear in the following sections, when we deal with identical agents, and later in other simulations.

Remark 9 *The value of R_b is also affected by r^*. Note that r^* is determined by c_1^i and c_2^i for all i. Specifically, smaller c_2^i and larger c_1^i are helpful in decreasing r^*. Then from (2.22) and (2.23), we can see that all the noise bounds ($D_{p_1}^i$, $D_{v_1}^i$, $D_{p_2}^i$, $D_{v_2}^i$, and D_f^i) affect r^*. Smaller noise bounds help decrease r^* and thus, may decrease R_b. So do smaller k_f^i, k_r^i and r_s^i. All these are consistent with the previous remarks.*

Remark 10 *Similar to Theorem 1, lots of conservativeness is introduced into the deduction of Corollary 1. One example is, K_1, K_2, K_4, and thus, b_d^* and c_d^*, are actually functions of N_O. When N_O increases, b_d^* and c_d^* will generally decrease. This fact is not considered in the above deduction because of the complexity that originated in the use of both heterogeneous swarm agents and resource profiles in the environment.*

2.3.3 Special Case: Identical Agents

Here, we will study the stability of the system when all the agents are identical (i.e., with $k_p^i = k_p$, $k_v^i = k_v$, $k_r^i = k_r$, $r_s^i = r_s$, and $k_f^i = k_f$, for all i), but with different types of noise and nutrient profiles. Equation (2.4) becomes

$$\begin{aligned} u^i &= -M_i k_p \hat{e}_p^i - M_i k_v \hat{e}_v^i - M_i k v^i \\ &\quad + M_i k_r \sum_{j=1, j\neq i}^{N} \exp\left(\frac{-\frac{1}{2}\left\|\hat{e}_p^i - \hat{e}_p^j\right\|^2}{{r_s}^2}\right)\left(\hat{e}_p^i - \hat{e}_p^j\right) \\ &\quad - M_i k_f \left(R^i - d_f^i\right). \end{aligned} \tag{2.32}$$

Also $A_i = A$ in (2.11) for all i. Note that with all agents being identical, we have $\Delta k_p^i = 0$ and $\Delta k_v^i = 0$ for all i. Also,

$$\frac{1}{N}\sum_{l=1}^{N} k_r \sum_{j=1, j\neq l}^{N} \exp\left(\frac{-\frac{1}{2}\left\|\hat{e}_p^l - \hat{e}_p^j\right\|^2}{{r_s^l}^2}\right)\left(\hat{e}_p^l - \hat{e}_p^j\right) = 0.$$

Let $\bar{d}_p = \frac{1}{N}\sum_{i=1}^{N} d_p^i$, $\bar{d}_v = \frac{1}{N}\sum_{i=1}^{N} d_v^i$, $\bar{d}_f = \frac{1}{N}\sum_{i=1}^{N} d_f^i$, and $\bar{R} = \frac{1}{N}\sum_{i=1}^{N} R^i$. Then, (2.6) can be simplified to

$$\dot{\bar{v}} = -k\bar{v} + \underbrace{k_p\bar{d}_p + k_v\bar{d}_v + k_f\bar{d}_f - k_f\bar{R}}_{z(t)} \tag{2.33}$$

and

$$\dot{e}_v^i = -k_p e_p^i - (k_v + k)\, e_v^i + g^i + \phi(E) + \delta^i(E) \tag{2.34}$$

where g^i, $\phi(E)$, and $\delta^i(E)$ are respectively

$$g^i = k_p d_p^i + k_v d_v^i + k_f d_f^i - k_f R^i \tag{2.35}$$

$$\phi(E) = -k_p\bar{d}_p - k_v\bar{d}_v - k_f\bar{d}_f + k_f\bar{R} \tag{2.36}$$

$$\delta^i(E) = k_r \sum_{j=1, j\neq i}^{N} \exp\left(\frac{-\frac{1}{2}\left\|\hat{e}_p^i - \hat{e}_p^j\right\|^2}{{r_s}^2}\right)\left(\hat{e}_p^i - \hat{e}_p^j\right). \tag{2.37}$$

Using the idea of deriving (2.18) we have

$$\left\|\delta^i(E)\right\| \leq k_r r_s (N-1)\exp\left(-\frac{1}{2}\right). \tag{2.38}$$

Noise with Constant Bounds

In this case we assume that $d_p^i(t)$ and $d_v^i(t)$ are sufficiently smooth and bounded by some constants for all i,

$$\begin{aligned} \|d_p^i\| &\leq D_p \\ \|d_v^i\| &\leq D_v \end{aligned} \tag{2.39}$$

where $D_p \geq 0$ and $D_v \geq 0$ are known constants. The sensing error on the gradient of the nutrient profile is assumed to be sufficiently smooth and bounded by known constant $D_f \geq 0$ such that for all i,

$$\|d_f^i\| \leq D_f. \tag{2.40}$$

Theorem 2: *Consider the swarm described by the model in (2.3) with control input u^i given as in (2.32). Assume that the nutrient profile for each agent is a plane defined by $\nabla J_p^i(x) = R^i$. Also assume the noise satisfies (2.39) and (2.40). Let $\|R^*\| = \max_i \left\|R^i - \bar{R}\right\|$. Then, the trajectories of the swarm error system are uniformly ultimately bounded, and E^i for all i will converge to the set Ω_b, where*

$$\Omega_b = \left\{E : \ \left\|E^i\right\| \leq \beta_1\beta_2, \ i = 1, 2, \ldots, N\right\} \tag{2.41}$$

is attractive and compact, with

$$\beta_1 = \frac{(k_p+1)^2 + (k_v+k)^2}{2k_p(k_v+k)} + \sqrt{\left(\frac{k_p^2 + (k_v+k)^2 - 1}{2k_p(k_v+k)}\right)^2 + \frac{1}{k_p^2}}$$

and

$$\begin{aligned} \beta_2 \ &= \ 2k_pD_p + 2k_vD_v + 2k_fD_f \\ &\quad +k_f\|R^*\| + k_r r_s(N-1)\exp\left(-\frac{1}{2}\right). \end{aligned}$$

Moreover, there exists some finite T and constant $0 < \theta < 1$ such that

$$\|\bar{v}(t)\| \leq \exp\left[-(1-\theta)kt\right]\|\bar{v}(0)\|, \ \forall \ 0 \leq t < T$$

and

$$\|\bar{v}(t)\| \leq \frac{\delta}{k\theta}, \ \forall \ t \geq T$$

with $\delta = k_p D_p + k_v D_v + k_f D_f + k_f \|\bar{R}\|$.

Proof: To find the set Ω_b, from (2.17) and (2.34) to (2.38), we have

$$\dot{V}_i \;\leq\; -\lambda_{min}(Q_i) \left\|E^i\right\| \left(\left\|E^i\right\| - 2\frac{\lambda_{max}(P_i)}{\lambda_{min}(Q_i)}\beta_2 \right).$$

Following the idea in Theorem 1, we have by letting $Q_i = I$, β_1 as the counterpart of β_1^i in Theorem 1. So we have

$$\dot{V}_i \leq -\left\|E^i\right\| \left(\left\|E^i\right\| - \beta_1\beta_2 \right). \tag{2.42}$$

That is, $\dot{V}_i < 0$ if $\|E^i\| > \beta_1\beta_2$. So the set

$$\Omega_b = \left\{ E : \; \left\|E^i\right\| \leq \beta_1\beta_2, \; i = 1, 2, \ldots, N \right\}$$

is attractive and compact. Also we know that within a finite amount of time, $E^i \to \Omega_b$. This means that we can guarantee that if the swarm is not cohesive, it will seek to be cohesive, but only if it is a certain distance from cohesiveness as indicated by (2.42).

To study the boundedness of $\bar{v}(t)$, choose a Lyapunov function

$$V_{\bar{v}} = \frac{1}{2}\bar{v}^\top \bar{v}$$

defined on $D = \{\bar{v} \in \Re^n \mid \|\bar{v}\| < r_v\}$ for some $r_v > 0$, and we have

$$\dot{V}_{\bar{v}} = \bar{v}^\top \dot{\bar{v}} = -k\bar{v}^\top \bar{v} + \bar{v}^\top z(t)$$

with $z(t)$ defined in (2.33). Since $\left\|d_p^j\right\| \leq D_p$ for all j, we have $\left\|\bar{d}_p\right\| = \left\|\frac{1}{N}\sum_{j=1}^N d_p^j\right\| \leq D_p$. Similarly, $\left\|\bar{d}_v\right\| \leq D_v$ and $\left\|\bar{d}_f\right\| \leq D_f$. Thus, we have

$$\|z(t)\| \leq \left\|k_p\bar{d}_p\right\| + \left\|k_p\bar{d}_v\right\| + \left\|k_f\bar{d}_f\right\| + \left\|k_f\bar{R}\right\| \leq \delta.$$

If $\delta < k\theta r_v$ for all $t \geq 0$, all $\bar{v} \in D$ and some positive constant $\theta < 1$, then it can be proven that for all $\|\bar{v}(0)\| < r_v$ and some finite T we have

$$\|\bar{v}(t)\| \leq \exp\left[-(1-\theta)kt\right] \|\bar{v}(0)\|, \; \forall \; 0 \leq t < T$$

and

$$\|\bar{v}(t)\| \leq \frac{\delta}{k\theta}, \ \forall \ t \geq T.$$

Since this holds globally we can take $r_v \to \infty$ so these equations hold for all $\bar{v}(0)$. ■

Remark 11 *The size of Ω_b in (2.41), which we denote by $|\Omega_b|$, is directly a function of several known parameters. If there are no sensing errors, i.e., $D_p = D_v = D_f = 0$, then Ω_b reduces to the set representing the no-noise case. For fixed values of N, k_p, k_v, k, and k_r if we increase r_s each agent has a larger region from which it will repel its neighbors so $|\Omega_b|$ is larger. For fixed k_r, k_p, k_v, k, and r_s if we let $N \to \infty$, then $|\Omega_b| \to \infty$ as we expect due to the repulsion.*

Remark 12 *It is interesting to note that in some swarms N is very large and when there is no biasing of sensing errors, we have $\bar{d}_p \approx \bar{d}_v \approx \bar{d}_f \approx 0$. This reduces the bound defined by β_2. Also when $\|R^*\|$ is decreased, implying that R^i is closer to R^j for all i and j, then β_2 is smaller. In the special case when all R^i are the same, we have $\|R^*\| = 0$ and the set $|\Omega_b|$ is minimized with respect to resource profiles. This means when $\|R^*\|$ is large, the agents pursue resource profiles that are far different from each other and the swarm is spread out, while when those profiles are equal to each other, all the agents move along the same profile and smaller swarm size is achieved.*

Remark 13 *If δ and θ are fixed, with increasing k $\|\bar{v}(t)\|$ decreases faster for $0 \leq t < T$ and has smaller bound for $t \geq T$. If δ gets larger with k and θ fixed, $\|\bar{v}(t)\|$ has larger bound for $t \geq T$; hence if the magnitude of the noise becomes larger this increases δ and hence there can be larger magnitude changes in the ultimate average velocity of the swarm (e.g., the average velocity could oscillate). Note that if in (2.33) $z(t) \approx 0$ (e.g., due to noise that destroys the directionality of the resource profile R),*

then the above bound may be reduced but the swarm could be going in the wrong direction.

Remark 14 *Regardless of the size of the bound it is interesting to note that while the noise destroys the ability of an individual agent to follow a gradient accurately, the average sensing errors of the group are what changes the direction of the group's movement relative to the direction of the gradient of* $J_p(x)$*. In some cases when the swarm is large (*N *big) it can be that* $\bar{d}_p \approx \bar{d}_v \approx \bar{d}_f \approx 0$ *since the average sensing error is zero and the group will perfectly follow the proper direction for foraging (this may be a reason why for some organisms, large group size is favorable). In the case when* $N = 1$ *(i.e., single agent), there is no opportunity for a cancellation of the sensor errors; hence an individual may not be able to climb a noisy gradient as easily as a group. This characteristic has been found in biological swarms [4, 51].*

Remark 15 *Note that there is an intimate relationship between sensor noise and observations of biological swarms (e.g., in bee swarms) that there is a type of "inertia" of a swarm. Note that for large swarms (high* N*) there can be regions where the average sensor noise is small so that agents in that region move in the right direction. In other regions there may be alignments of the errors and hence the agents may not be all moving in the right direction so they may get close to each other and impede each other's motion, having the effect of slowing down the whole group. With no noise the group inertia effect is not found since each agent is moving in the right direction. The presence of sensor noise generally can make it more difficult to get the group moving in the right (foraging) direction. Large swarms can help move the group in*

the right direction, but at the expense of possibly slowing their movement initially in a transient period.

Constant Errors

In this case we assume each agent senses the velocity and position of other members and the nutrient profile with some constant errors.

Theorem 3: *Consider the swarm described by the model in (2.3) with control input u^i given as in (2.32). Assume that the nutrient profile for each agent is a plane defined by $\nabla J_p^i(x) = R^i$. Also assume the noise d_p^i, d_v^i, and d_f^i are time-invariant for each agent so that $\bar{d}_p = \frac{1}{N}\sum_{i=1}^N d_p^i$, $\bar{d}_v = \frac{1}{N}\sum_{i=1}^N d_v^i$, $\bar{d}_f = \frac{1}{N}\sum_{i=1}^N d_f^i$, and $\bar{R} = \frac{1}{N}\sum_{i=1}^N R^i$ are constants. Then, the error dynamics of the swarm system are uniformly ultimately bounded and E^i, $i = 1, \ldots, N$, will converge to the attractive and compact set Ω_t defined by*

$$\Omega_t = \left\{E : \ \left\|E^i\right\| \leq \alpha^i \beta_1, \ i = 1, \ldots, N\right\} \tag{2.43}$$

where β_1 is defined in Theorem 2 and

$$\begin{aligned} \alpha^i \ &= \ \left\|k_p\left(d_p^i - \bar{d}_p\right) + k_v\left(d_v^i - \bar{d}_v\right) + k_f\left(d_f^i - \bar{d}_f\right)\right. \\ &\quad \left. - \ k_f\left(R^i - \bar{R}\right)\right\| + k_r r_s (N-1)\exp\left(-\frac{1}{2}\right). \end{aligned}$$

Moreover, $e_v^i \to 0$ and

$$v^i(t) \to \frac{k_p\bar{d}_p + k_v\bar{d}_v + k_f\bar{d}_f - k_f\bar{R}}{k} \tag{2.44}$$

for all i as $t \to \infty$.

Proof: We may obtain the set Ω_t by following the method in Theorem 2, α^i as the counterpart of β_2 in Theorem 2.

To find the ultimate velocity of each agent in the swarm, we consider Ω_t and a Lyapunov function $V^o(E) = \sum_{i=1}^{N} V_i^o(E^i)$ with

$$\begin{aligned} V_i^o\left(E^i\right) &= \frac{1}{2}k_p\left(e_p^i - \frac{\gamma}{k_p}\right)^\top\left(e_p^i - \frac{\gamma}{k_p}\right) + \frac{1}{2}{e_v^i}^\top e_v^i \\ &\quad + k_r r_s^2 \sum_{j=1, j\neq i}^{N} \exp\left(\frac{-\frac{1}{2}\left\|\hat{e}_p^i - \hat{e}_p^j\right\|^2}{r_s^2}\right) \end{aligned} \tag{2.45}$$

where the constant $\gamma = k_p\left(d_p^i - \bar{d}_p\right) + k_v\left(d_v^i - \bar{d}_v\right) + k_f\left(d_f^i - \bar{d}_f\right) - k_f\left(R^i - \bar{R}\right)$. Note that this Lyapunov function is not positive definite, but $V_i^o(E^i) > 0$. Here, we think of the swarm moving so as to *minimize* $V^o(E)$ with the i^{th} agent trying to minimize $V_i^o(E^i)$. Agents try to place themselves at positions to reduce the first term in (2.45), achieve a velocity to reduce the second term, and move to a distance from each other to minimize repulsion quantified in the last term. There is a resulting type of balance that is sought between the conflicting objectives that each of the three terms represent.

Using (2.34), we have

$$\dot{V}_i^o = -\left(k_v + k\right){e_v^i}^\top e_v^i.$$

Hence, $\dot{V}^o = -\left(k_v + k\right)\sum_{i=1}^{N}\left\|e_v^i\right\|^2 \leq 0$ on $E \in \Omega$ for any compact set Ω. Choose Ω so it is positively invariant, which is clearly possible, and so $\Omega_e \in \Omega$ where

$$\Omega_e = \{E:\ \dot{V}^o(E) = 0\} = \{E:\ e_v^i = 0,\ i = 1, 2, \ldots, N\}.$$

From LaSalle's Invariance Principle we know that if $E(0) \in \Omega$ then $E(t)$ will converge to the largest invariant subset of Ω_e. Hence $e_v^i(t) \to 0$ as $t \to \infty$. From (2.33), we have

$$\bar{v}(t) \to \frac{k_p\bar{d}_p + k_v\bar{d}_v + k_f\bar{d}_f - k_f\bar{R}}{k}$$

as $t \to \infty$ since in this case $z(t)$ is a constant with respect to time. Thus, $v^i(t)$ approaches this value also for all i as $t \to \infty$. ■

Remark 16 *From (2.44) we can see that all agents will ultimately be moving at the same velocity despite the existence of constant errors. Contrast this with the earlier more general cases where it is possible that $\bar{v}$ and v^i ultimately, for example, oscillate. Next, note that even if $R^i = R^j$ for all i and j, the presence of $\bar{d}_p$, $\bar{d}_v$, and $\bar{d}_f$ represent the effects of sensor errors and they can result in the swarm not properly following the direction of the profile even when they all intend to go in the same direction. In the case when we have $\bar{d}_p \approx \bar{d}_v \approx \bar{d}_f \approx 0$ with N large enough, then all those agents will be following the "averaged" profile $-\frac{k_f}{k}\bar{R}$. That is, due to the desire to stay together, they each sacrifice following their own profile and compromise to follow the averaged profile. In the special case when $\bar{R} = 0$ or $R^i = 0$ for all i (no resource profile effect), and no sensor errors, both $\bar{v}(t)$ and $v^i(t)$ will go to zero as $t \to \infty$, representing the aggregation of the group independent of the environment. The size of Ω_t in (2.43), which we denote by $|\Omega_t|$, is directly a function of several known parameters. All the remarks for the previous case, i.e., noise with constant bounds, apply here.*

2.4 Stability Analysis of Swarm Trajectory Following

In this section we briefly analyze the stability of the swarm error system when each agent is trying to track their respective trajectories. This is done by applying the same idea as in Section 2.3 to a slightly reformulated system model. Specifically,

redefine the errors as

$$\begin{aligned} e_p^i &= x^i - x_d^i \\ e_v^i &= v^i - v_d^i \end{aligned}$$

where x_d^i is a sufficiently smooth desired position trajectory for agent i, $i = 1, \ldots, N$, and $v_d^i = \dot{x}_d^i$. We assume that there exist known bounds for $\dot{x}_d^i$ and $\dot{v}_d^i$ such that

$$\begin{aligned} \left\|\dot{x}_d^i\right\| &\leq D_{x_d^i} \\ \left\|\dot{v}_d^i\right\| &\leq D_{v_d^i} \end{aligned}$$

where $D_{x_d^i}$ and $D_{v_d^i}$ are known positive constants. Assume the nutrient profile for each agent is a plane defined by $\nabla J_p^i(x) = R^i$. Also let $\dot{e}_p^i$, $\dot{e}_v^i$, $\hat{e}_p^i$, $\hat{e}_v^i$, u^i, and E^i be defined in the same form as in Section 2.3.1. Then the error dynamics of the i^{th} agent is

$$\dot{E}^i = \begin{bmatrix} 0 & I \\ -k_p^i I & -\left(k_v^i + k\right) I \end{bmatrix} E^i + \begin{bmatrix} 0 \\ I \end{bmatrix} \left(g^i + \delta^i(E)\right) \tag{2.46}$$

where

$$g^i = k_p^i d_p^i + k_v^i d_v^i + k_f^i d_f^i - k_f^i R^i \tag{2.47}$$

$$\begin{aligned} \delta^i(E) &= k_r^i \sum_{j=1, j\neq i}^{N} \exp\left(\frac{-\frac{1}{2}\left\|\hat{e}_p^i - \hat{e}_p^j\right\|^2}{{r_s^i}^2}\right)\left(\hat{e}_p^i - \hat{e}_p^j\right) \\ &\quad -k v_d^i - \dot{v}_d^i. \end{aligned} \tag{2.48}$$

Let $d_f^i(t)$, $d_p^i(t)$, and $d_v^i(t)$ be specified in the same way as in Section 2.3.2. Then we have the following theorem.

Theorem 4: *Consider the swarm described by the model in (2.3) with control input u^i given in (2.4). Let β_1^i be defined in Theorem 1. If for all i we have*

$$k_p^i D_{p_1}^i + k_v^i D_{v_1}^i < \frac{1}{\beta_1^i} \tag{2.49}$$

then the trajectories of the error system, specified by (2.46), are uniformly ultimately bounded. Furthermore, E^i for all i will converge to an attractive and compact set Ω_f defined as

$$\Omega_f = \left\{ E : \left\| E^i \right\| \leq \frac{\tilde{c}_2^i}{\tilde{c}_1^i}, i = 1, \ldots, N \right\} \tag{2.50}$$

where

$$\begin{aligned} \tilde{c}_1^i &= 1 - \beta_1^i \left(k_p^i D_{p_1}^i + k_v^i D_{v_1}^i \right) && (2.51) \\ \tilde{c}_2^i &= \beta_1^i \Big(k_p^i D_{p_2}^i + k_v^i D_{v_2}^i + k_f^i D_f^i \\ &\quad + k_f^i \left\| R^i \right\| + k D_{x_d^i} + D_{v_d^i} + \hat{\delta}^i \Big) && (2.52) \end{aligned}$$

with $\hat{\delta}^i = k_r^i r_s^i (N-1) \exp\left(-\frac{1}{2}\right)$. Moreover, if we have for any i and j

$$\left\| x_d^i - x_d^j \right\| \leq D_x \tag{2.53}$$

where D_x is a known constant, then the swarm will stay cohesive and

$$\left\| x^i - \bar{x} \right\| \leq \frac{\tilde{c}_2^i}{\tilde{c}_1^i} + \frac{1}{N} \sum_{j=1}^{N} \frac{\tilde{c}_2^j}{\tilde{c}_1^j} + D_x \tag{2.54}$$

for all i.

Proof: Note that g^i and $\delta^i(E)$, defined in (2.47) and (2.48), are bounded by $k_p^i D_{p_2}^i + k_v^i D_{v_2}^i + k_f^i D_f^i + k_f^i \left\| R^i \right\|$ and $k D_{x_d^i} + D_{v_d^i} + \hat{\delta}^i$, respectively. By following exactly the same method in the proof of Theorem 1, we obtain

$$\dot{V}_i(E^i) \leq -\tilde{c}_1^i \left\| E^i \right\|^2 + \tilde{c}_2^i \left\| E^i \right\| \tag{2.55}$$

and define $V(E) = \sum_{i=1}^{N} V_i(E^i)$ as the Lyapunov function for the whole error system, as specified in the proof of Theorem 1. Then the uniform ultimate boundedness of the error system and the set Ω_f are easily obtained via (2.55).

When (2.53) is satisfied, we can show that the cohesiveness of the swarm is conserved. To see this, note that for arbitrary i and j with $i \neq j$,

$$\begin{aligned} \left\|x^i - x^j\right\| &= \left\|\left(e_p^i + x_d^i\right) - \left(e_p^j + x_d^j\right)\right\| \\ &\leq \left\|e_p^i - e_p^j\right\| + \left\|x_d^i - x_d^j\right\| \\ &\leq \left\|E^i\right\| + \left\|E^j\right\| + D_x \end{aligned} \tag{2.56}$$

so from (2.50) and (2.56) we have (2.54). ■

Remark 17 *Comparing (2.19) with (2.55), we can see that the latter one does not include any cross term. This is because the errors for the swarm cohesion case are defined as the difference between an agent and the swarm centers ($\bar{x}$ and $\bar{v}$), which are affected by all the agents in the swarm, while the errors for the trajectory following case are defined as the difference between an agent and the given position and velocity trajectories, which are* not *affected by the behaviors of other agents. This absence of cross term significantly simplifies the proof for the theorem.*

Remark 18 *By comparing Theorem 1 and Theorem 4, we can see that Theorem 4 will hold whenever Theorem 1 holds, as long as $D_{x_d^i}$ and $D_{v_d^i}$ exist. This means cohesion property of a swarm in a certain environment guarantees the stability of that swarm in following* any *bounded trajectory in the same environment.*

Remark 19 *Similar to Remark 1, when (2.49) holds, the uniform ultimate boundedness is obtained. This condition only depends on k_p^i, k_v^i, D_{p_1}, and D_{v_1}. Although the remaining parameters, including k_r^i, r_s^i, k_f^i, D_{p_2}, D_{v_2}, D_f, and R^i, do not affect the boundedness of the error system, they do affect the ultimate bound. In the special*

case when $D^i_{p_1} = D^i_{v_1} = 0$ *for all* i*, (2.49) always holds and thus, the swarm error system is always bounded.*

Remark 20 *Smaller* $\|R^i\|$ *may decrease the bound. Smaller magnitude of the position and velocity trajectories also help in decreasing the ultimate bound. Our analysis includes the possibility that the resource profiles indicate that the agents should go in the opposite direction that is indicated by* $(x^i_d,\ v^i_d)$*. If there is an alignment between where the resource profiles say to go and the* $(x^i_d,\ v^i_d)$*, then the size of the bound decreases.*

Remark 21 *In the special case when* v^i_d *and all sensing errors are constant, we have that* $e^i_v \to 0$ *as* $t \to \infty$ *for all* i*, meaning* v^i *of each agent will be precisely following the given constant velocity trajectory ultimately in such a case. To see this, let* $\gamma^i = k^i_p d^i_p + k^i_v d^i_v - k v^i_d + k^i_f d^i_f - k^i_f R^i$ *and construct for all* i *a Lyapunov function*

$$\begin{aligned} V^o_i\left(E^i\right) &= \frac{1}{2}k^i_p\left(e^i_p - \frac{\gamma^i}{k^i_p}\right)^\top\left(e^i_p - \frac{\gamma^i}{k^i_p}\right) + \frac{1}{2}{e^i_v}^\top e^i_v \\ &\quad + k^i_r {r^i_s}^2 \sum_{j=1, j\neq i}^{N} \exp\left(\frac{-\frac{1}{2}\left\|\hat{e}^i_p - \hat{e}^j_p\right\|^2}{r^2_s}\right). \end{aligned}$$

Note $\dot{v}^i_d = 0$ *when* v^i_d *is constant. Then by following the method in the proof of Theorem 3, the above claim holds.*

2.5 Simulations

In this section, we will show some simulation results for both the no-noise and noise cases. Unless otherwise stated, in all the following simulations the parameters, which we refer to as "normal parameters," are: $N = 50$, $k^i_p = k_p = 1$, $k^i_v = k_v = 1$, $k = 0.1$, $k^i_f = k_f = 0.1$, $k^i_r = k_r = 10$, $r^i_s = r_s = 0.1$, and the three dimensional nutrient plane profile $\nabla J^i_p(x) = R^i = [1,\ 2,\ 3]^\top$ for all i.

2.5.1 No-Noise Case

All the simulations in this case are run for 20 seconds. The position and velocity trajectories of the swarm agents with the normal parameters are shown in Figure 2.2. All the agents are assigned initial velocities and positions randomly. At the beginning of the simulation, they appear to move around erratically. But soon, they swarm together and continuously reorient themselves as a group to slide down the plane profile. Note how these agents gradually catch up with each other while still keeping mutual spacing. Recall from the previous sections that for this case $v^i(t) \to -\frac{k_f}{k}R$ for all i as $t \to \infty$, and this can be seen from Figure 2.2(b) since the final velocity of each swarm agent is indeed $-[1,\ 2,\ 3]^\top$.

Next, we change the value of some of the parameters to show their impact on the system behavior.

Figures 2.3(a) and (b) show the results of keeping all normal parameters unchanged except for increases of k_r to 1000 and r_s to 1, respectively. Since both k_r and r_s are parameters affecting the repulsion range of each agent, as expected we find that the final swarm size becomes larger than in the previous case, while the swarm velocity and settling speed do not change much. We also investigated the number of collisions occurring between the agents. As expected, when k_r and r_s increase, the number of collisions decreases. Effects of other parameters are also as expected.

2.5.2 Noise Case

Now we will consider the case when noise exists. In our simulations the solutions of Duffing's Equation are used as "noise" so that the noise is guaranteed to be differentiable. Of course many other choices are possible, e.g., ones that lead to errors on

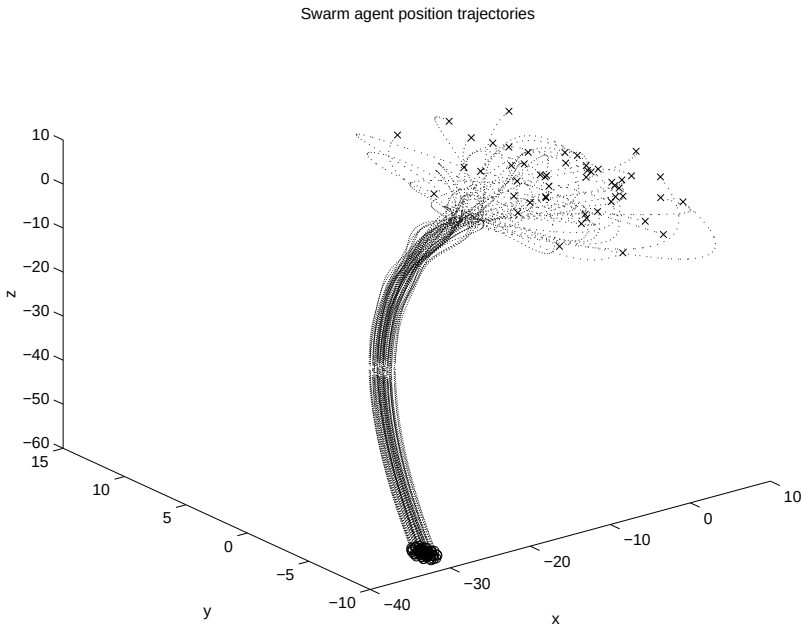

(a) Agent position trajectories.

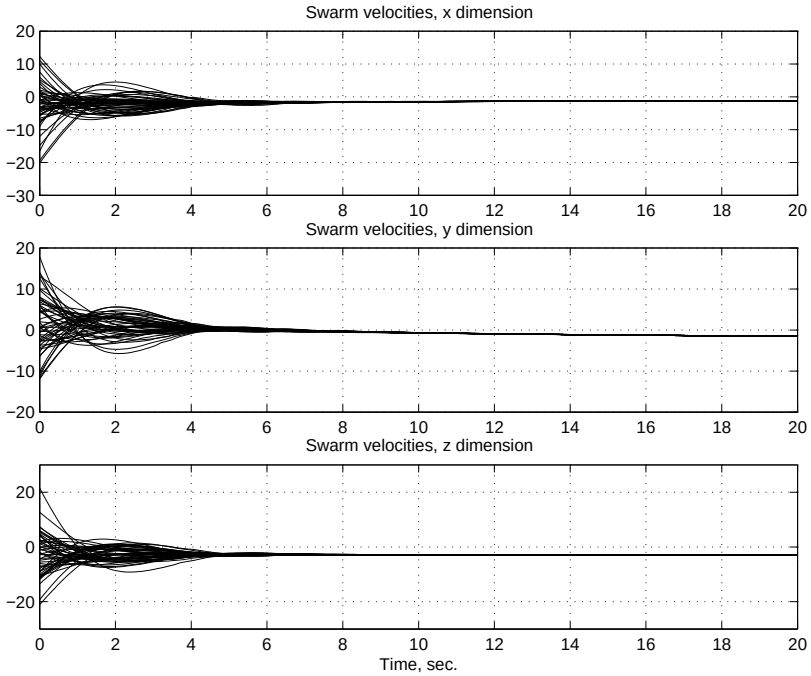

(b) Agent velocity trajectories.

Figure 2.2: No noise case with normal parameters.

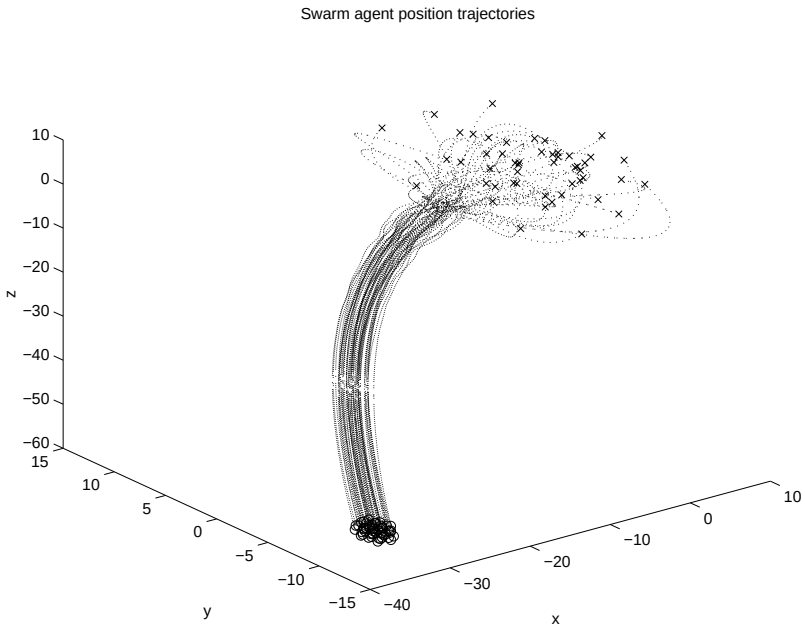

(a) Agent position trajectories ($k_r = 1000$, $r_s = 0.1$).

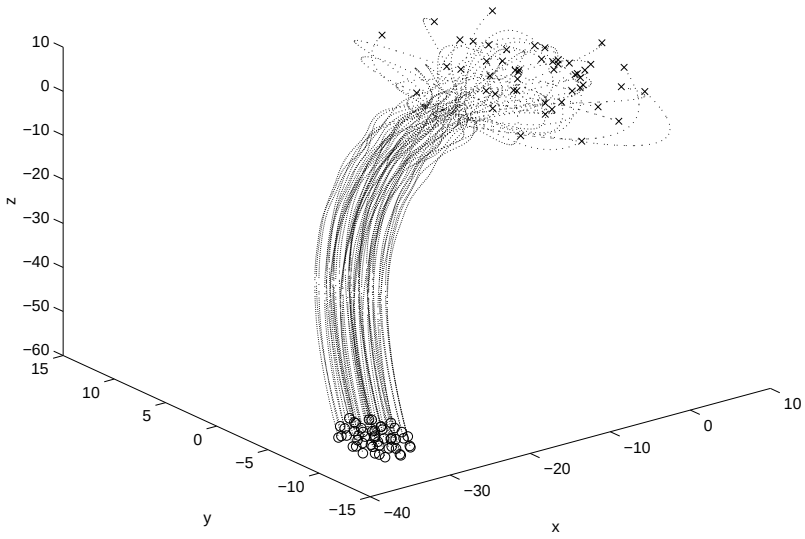

(b) Agent position trajectories ($r_s = 1$, $k_r = 10$).

Figure 2.3: No noise case with parameters changed.

a higher or lower frequency spectrum. Duffing's equation is in the form

$$\ddot{\vartheta} + \delta_D \dot{\vartheta} - \vartheta + \vartheta^3 = \gamma_D \cos(\omega_D t).$$

In the simulations we use $\delta_D = 0.25$, $\gamma_D = 0.30$ and $\omega_D = 1.0$ so that the solution ϑ of Duffing's Equation demonstrates chaotic behavior. We will simulate many such equations to generate noise on position, velocity, and resource profile gradient sensing. We denote by ϑ_i the solution to the i^{th} Duffing's Equation that we simulate. Note that the magnitude of ϑ is always bounded by a value of 1.5. Thus, we can easily change the noise bounds with some scaling factors. For example, in the case of noise with a linear bound, the position sensing noise is generated by $d_p^i = \frac{D_{p_1}\vartheta_1^i}{1.5}\|E^i\| + \frac{D_{p_2}\vartheta_2^i}{1.5}$ so that (2.12) is satisfied.

In this case, we run the simulations for 80 seconds. All the normal parameters used in the no-noise case are kept unchanged except the number of agents in the swarm in certain simulations, which is specified in the relevant figures. Figures 2.4 and 2.5 illustrate the case with linear noise bounds for a typical simulation run. The noise bounds are $D_{p_1} = D_{v_1} = 0.05$, $D_{p_2} = D_{v_2} = 1$, and $D_f = 10$, respectively. According to the Grunbaum principle [4, 51], forming a swarm may help the agents go down the gradient of the nutrient profile without being significantly distracted by noise. Figure 2.4 shows that the existence of noise does affect the swarm's ability to follow the profile, which is indicated by the oscillation of the position and velocity trajectories. But with all the agents working together, especially when the agents number N is large, they are able to move in the right direction and thus, minimize the negative effects of noise. In comparison, Figure 2.5 shows the case when there is only one agent. Since the single agent cannot benefit from the averaging effects

possible when there are many agents, the noise more adversely affects its performance in terms of accurately following the nutrient profile.

2.6 Concluding Remarks

In this chapter, we have derived conditions under which social foraging swarms maintain cohesiveness and follow a resource profile even in the presence of sensor errors and noise on the profile. We also studied special types of noise and the case where all agents are identical. Although we only studied one type of attraction and repulsion function, the results can be extended to other classes using approaches such as the ones in [35, 45]. Moreover, while we only studied the plane profile, extensions to profiles with other shapes such as those studied in [46] are possible. In fact any profile that is smooth and has a known bounded slope can be fit into the framework without changing our major results except part of Theorem 3. Specifically, the conclusion that the velocities of all agents approach a constant (prescribed by (2.44)) may not hold any more.

Our simulations illustrated advantages of social foraging in large groups relative to foraging alone since they show that a noisy resource profile can be more accurately tracked by a swarm than an individual [4, 51]. Moreover, the simulations produced agent trajectories that are curiously reminiscent of those seen in biology (e.g., by some insects). It would be interesting to determine if the model here, with appropriately chosen parameters, is an acceptably accurate representation for some social organisms and whether the predictions of the analysis would also accurately represent their group-level behavior.

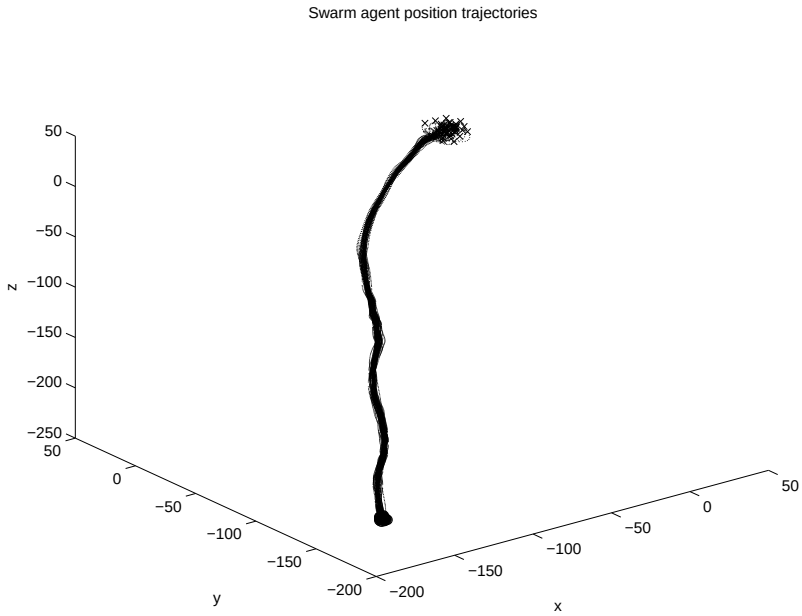

(a) Agent position trajectories.

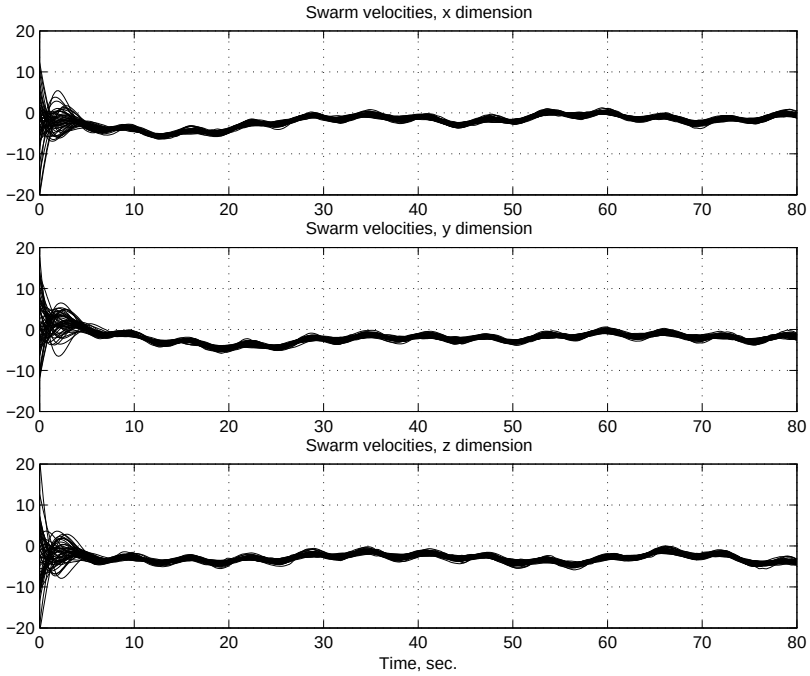

(b) Agent velocity trajectories.

Figure 2.4: Linear noise bounds case ($N = 50$).

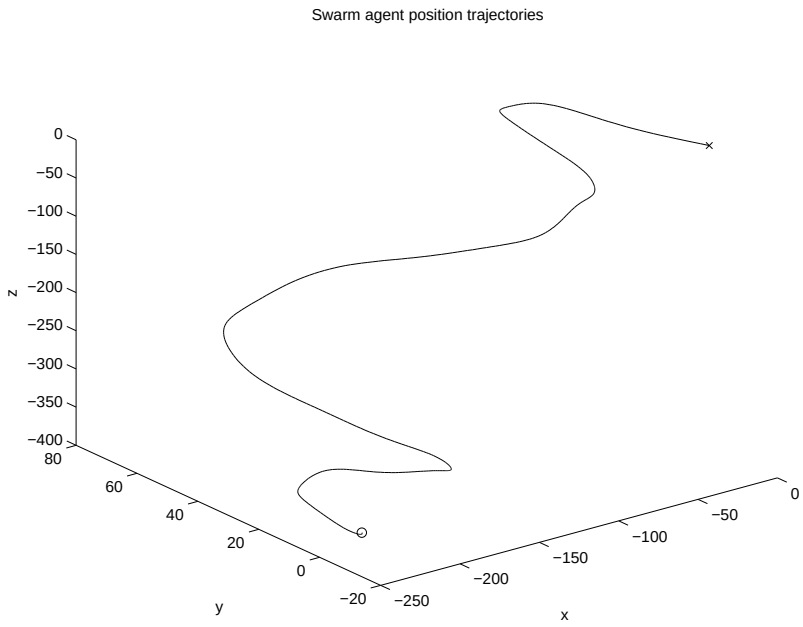

(a) Agent position trajectories.

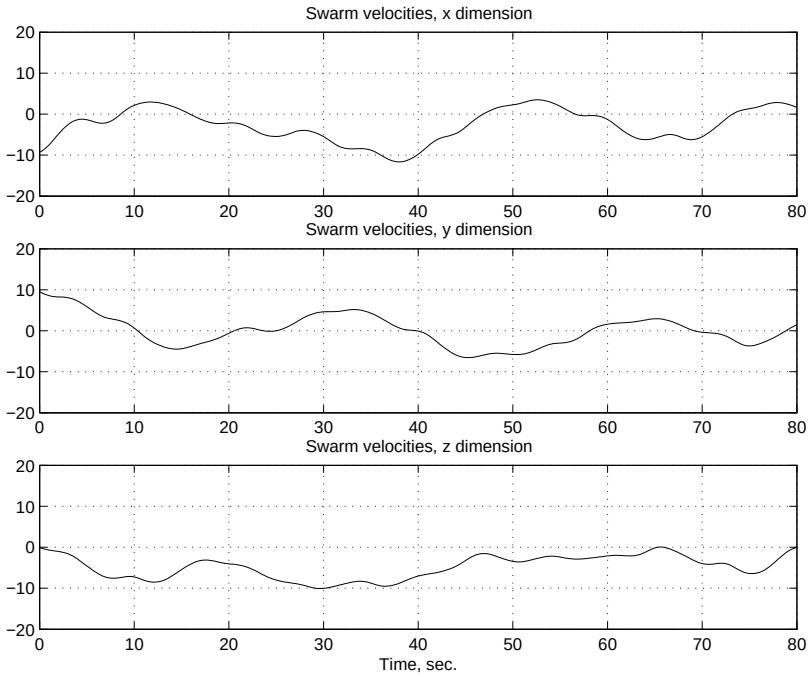

(b) Agent velocity trajectories.

Figure 2.5: Linear noise bounds case ($N = 1$).

CHAPTER 3

COHESIVE BEHAVIORS OF MULTIPLE COOPERATIVE MOBILE DISCRETE-TIME AGENTS IN A NOISY ENVIRONMENT

3.1 Introduction

Early work in swarm stability was done in a discrete-time framework [37, 38]. Subsequent work studied the one-dimensional discrete-time asynchronous case with time delays in [39, 54, 42, 40]. The higher dimensional case, where there is asynchronism, delays, and a fixed "line" communication topology, is considered in [55, 41].

In this chapter, we continue the work in Chapter 2 (also see [56, 57]) by studying stability properties of foraging swarms. The main difference with Chapter 2 is that we consider the effect of sensor errors and errors in sensing the gradient of a resource profile in the *discrete-time* case. We illustrate that in the discrete-time framework, the agents can forage in noisy environments more efficiently as a group than individually, a principle that has been identified for some organisms [4, 51] and verified in [56, 57]. For simplicity, we assume all agents are identical. It turns out that most results in this chapter can find their counterparts in Chapter 2.

The remainder of this chapter is organized as follows: In Section 3.2 we introduce a generic model for agents, interactions, and the foraging environment. Section 3.3

holds the main results on stability analysis of swarm cohesion. Section 3.4 holds the simulation results and some concluding remarks are provided in Section 3.5.

3.2 Basic Models

The basic models here include the models for agents, interactions, and environment, and the models for control and dynamics. Since they bear the same ideas as in Chapter 2, we will simply give out their mathematical form and define the notation in discrete time. Refer Chapter 2 for more explanations on these models.

3.2.1 Agents, Interactions, and Environment

Consider a swarm composed of an interconnection of N "agents," each of which has point mass dynamics given by

$$\begin{aligned} x^i((k+1)T) &= x^i(kT) + v^i(kT)T \\ v^i((k+1)T) &= v^i(kT) + \frac{1}{M_i}u^i(kT)T \end{aligned}$$

where $x^i \in \Re^n$ is the position, $v^i \in \Re^n$ is the velocity, M_i is the mass, $u^i \in \Re^n$ is the control input for the i^{th} agent, and T is the sampling time. To simplify notation, throughout the chapter we replace all "(kT)" with "(k)" whenever it does not lead to ambiguity. So we have

$$\begin{aligned} x^i(k+1) &= x^i(k) + v^i(k)T \\ v^i(k+1) &= v^i(k) + \frac{1}{M_i}u^i(k)T. \end{aligned} \tag{3.1}$$

Agent to agent interactions considered here are of the "attract-repel" type. Specifically, attraction here will be represented in u^i in a form like $-k'\left(x^i - x^j\right)$ where $k' > 0$

is a scalar that represents the strength of attraction. The repulsion term is of the form

$$k_r \exp\left(\frac{-\frac{1}{2}\|x^i - x^j\|^2}{{r_s}^2}\right)\left(x^i - x^j\right)$$

where $k_r > 0$ and $r_s > 0$. Other types of attraction and repulsion terms are also possible.

We consider the environment that the agents move in as a resource profile $J(x)$, where $x \in \Re^n$, and agents move in the direction of the negative gradient of $J(x)$ (i.e., in the direction of $-\nabla J(x) = -\partial J/\partial x$) in order to move away from "bad" areas and into "good" areas of the environment. One of the simplest profiles is a plane profile, i.e., $J(x) = J_p(x)$, where

$$J_p(x) = R^\top x + r_p \tag{3.2}$$

with $R \in \Re^n$ and $r_p \in \Re$. Below, we will study a family of profiles that is differentiable with bounded slope at all points.

3.2.2 Control and Error Dynamics

Let $\bar{x}(k) = \frac{1}{N}\sum_{i=1}^N x^i(k)$ and $\bar{v}(k) = \frac{1}{N}\sum_{i=1}^N v^i(k)$ be the centroid position and velocity of the swarm at the kth time step, respectively. The objective of each agent is to move so as to end up at $\bar{x}$ and $\bar{v}$. Since $\bar{x}$ and $\bar{v}$ are time-varying, in order to study the stability of swarm cohesion, we study the dynamics of an error system with $e_p^i(k) = x^i(k) - \bar{x}(k)$ and $e_v^i(k) = v^i(k) - \bar{v}(k)$. Then the error dynamics are given by

$$\begin{aligned} e_p^i(k+1) &= e_p^i(k) + e_v^i(k)T \\ e_v^i(k+1) &= e_v^i(k) + \frac{1}{M_i}u^i(k)T - \frac{1}{N}\sum_{j=1}^N \frac{1}{M_j}u^j(k)T. \end{aligned} \tag{3.3}$$

We assume that each agent can sense its position and velocity relative to $\bar{x}$ and $\bar{v}$, but with some errors. In particular, let $d_p^i \in \Re^n$ and $d_v^i \in \Re^n$ be these sensing errors

for agent i, respectively. We assume that $d_p^i(k)$ and $d_v^i(k)$ are any trajectories that are fixed a priori and and bounded by a known constant for all the time steps. Thus, each agent actually senses

$$\hat{e}_p^i(k) = e_p^i(k) - d_p^i(k)$$
$$\hat{e}_v^i(k) = e_v^i(k) - d_v^i(k)$$

and below we will also assume that it can sense its own velocity.

We assume the nutrient profile is continuous with bounded slope at all points, i.e., $\|\nabla J(x(k))\| \leq \Lambda$, where Λ is a known constant. We assume the i^{th} agent senses $\nabla J\left(x^i(k)\right)$, the gradient of the profile at its position, but with some bounded error $d_f^i(k)$ that is fixed a priori for all the time steps (as with d_p^i and d_v^i we will allow below d_f^i to be any in a certain class of trajectories) so each agent actually senses $\nabla J\left(x^i(k)\right) - d_f^i(k)$. For simplicity, we will write $\nabla J\left(x^i(k)\right)$ as ∇J^i from now on.

Suppose the general form of the control input for each agent at the kth step is

$$\begin{aligned} u^i(k) &= -M_i k_p \hat{e}_p^i(k) - M_i k_v \hat{e}_v^i(k) - M_i k_d v^i(k) \\ &\quad + M_i k_r \sum_{l=1, l\neq i}^{N} \exp\left(\frac{-\frac{1}{2}\left\|\hat{e}_p^i(k) - \hat{e}_p^l(k)\right\|^2}{{r_s}^2}\right)\left(\hat{e}_p^i(k) - \hat{e}_p^l(k)\right) \\ &\quad - M_i k_f\left(\nabla J^i(k) - d_f^i(k)\right) \end{aligned} \tag{3.4}$$

Here, similar to (2.4), we think of the scalars $k_p > 0$ and $k_v > 0$ as the "attraction gains" which indicate how aggressive each agent is in aggregating. The gain $k_d > 0$ works as a "velocity damping gain". The gain $k_r > 0$ is a "repulsion gain" which sets how much that agent wants to be away from others and r_s represents its repulsion range. The gain $k_f > 0$ indicates that agent's desire to move along the negative gradient of the resource profile.

To study stability properties, we will substitute the above choice for u^i into the error dynamics in Equation (3.3). To calculate $e_v^i(k+1)$, first notice that

$$\begin{aligned}\frac{1}{M_i}u^i(k) &= -k_p e_p^i(k) + k_p d_p^i(k) - k_v e_v^i(k) + k_v d_v^i(k) - k_d v^i(k) \\ &\quad + k_r \sum_{l=1,l\neq i}^{N} \exp\left(\frac{-\frac{1}{2}\left\|\hat{e}_p^i(k) - \hat{e}_p^l(k)\right\|^2}{{r_s}^2}\right)\left(\hat{e}_p^i(k) - \hat{e}_p^l(k)\right) \\ &\quad - k_f\left(\nabla J^i(k) - d_f^i(k)\right). \end{aligned} \tag{3.5}$$

Then we have

$$\begin{aligned}\frac{1}{N}\sum_{j=1}^{N}\frac{1}{M_i}u^j(k) &= \frac{1}{N}\sum_{j=1}^{N}k_p d_p^j(k) + \frac{1}{N}\sum_{j=1}^{N}k_v d_v^j(k) - k_d\bar{v}(k) \\ &\quad - \frac{1}{N}\sum_{j=1}^{N}k_f\left(\nabla J^j(k) - d_f^j(k)\right) \end{aligned} \tag{3.6}$$

where we used the facts of $\sum_{j=1}^{N} e_p^j = 0$, $\sum_{j=1}^{N} e_v^j = 0$ and

$$\frac{1}{N}\sum_{j=1}^{N}k_r \sum_{l=1,l\neq j}^{N} \exp\left(\frac{-\frac{1}{2}\left\|\hat{e}_p^j(k) - \hat{e}_p^l(k)\right\|^2}{{r_s}^2}\right)\left(\hat{e}_p^j(k) - \hat{e}_p^l(k)\right) = 0.$$

Define $E^i = [{e_p^i}^\top,\ {e_v^i}^\top]^\top$ and $E = [{E^1}^\top, {E^2}^\top, \ldots, {E^N}^\top]^\top$. From (3.3), (3.5) and (3.6) we have

$$e_v^i(k+1) = -k_p T e_p^i(k) + (1 - k_v T - k_d T)\, e_v^i(k) + g^i(k) + \phi(k) + \delta^i(E(k))$$

where

$$\begin{aligned} g^i(k) &= k_p T d_p^i(k) + k_v T d_v^i(k) + k_f T d_f^i(k) \\ \phi(k) &= -\frac{1}{N}\sum_{j=1}^{N}k_p T d_p^j(k) - \frac{1}{N}\sum_{j=1}^{N}k_v T d_v^j(k) - \frac{1}{N}\sum_{j=1}^{N}k_f T d_f^j(k) \\ \delta^i(E(k)) &= k_r T \sum_{j=1,j\neq i}^{N} \exp\left(\frac{-\frac{1}{2}\left\|\hat{e}_p^i - \hat{e}_p^j\right\|^2}{{r_s}^2}\right)\left(\hat{e}_p^i - \hat{e}_p^j\right) \\ &\quad - k_f T\left(\nabla J^i(k) - \frac{1}{N}\sum_{j=1}^{N}\nabla J^j(k)\right) \end{aligned}$$

which is a nonlinear non-autonomous system.

With I an $n \times n$ identity matrix, the error dynamics of the i^{th} agent may be written as

$$\begin{aligned} E^i(k+1) &= \overbrace{\begin{bmatrix} I & TI \\ -k_p TI & (1 - k_v T - k_d T)\, I \end{bmatrix}}^{A} E^i(k) \\ &\quad + \overbrace{\begin{bmatrix} 0 \\ I \end{bmatrix}}^{B} \overbrace{\left(g^i(k) + \phi(k) + \delta^i(E(k))\right)}^{C^i(k)}. \end{aligned} \tag{3.7}$$

If we regard the whole swarm as an interconnected system with each agent being a subsystem, then matrix A in (3.7) specifies the internal system dynamics for each agent/subsystem in the error coordinate system, and $C^i(k)$ gives the external input for each agent i at time step k.

3.3 Stability Analysis of Swarm Cohesion Properties with Noise

Consider a class of sensing errors that satisfy

$$\begin{aligned} \|d_f^i(k)\| &\leq D_f \\ \|d_p^i(k)\| &\leq D_{p_1} \left\|E^i(k)\right\| + D_{p_2} \\ \|d_v^i(k)\| &\leq D_{v_1} \left\|E^i(k)\right\| + D_{v_2} \end{aligned} \tag{3.8}$$

for all k and for any i, where D_{p_1}, D_{p_2}, D_{v_1}, D_{v_2} and D_f are as defined in (2.12). In this section, we will show some results which characterize the stability properties of the swarm system in the presence of noise. To do this, we use a Lyapunov approach to develop conditions under which local agent actions will lead to cohesive foraging.

3.3.1 Mathematical Preliminaries

Before we present our main results, we specify some mathematical properties which we will use in the remainder of the paper.

Lemma 1: *The matrix A in (3.7) is convergent if*

$$T < \begin{cases} \frac{4}{(k_v+k_d)+\sqrt{(k_v+k_d)^2-4k_p}} & if \ \ (k_v+k_d)^2-4k_p \geq 0 \\ \frac{k_v+k_d}{k_p} & if \ \ (k_v+k_d)^2-4k_p < 0 \end{cases} . \tag{3.9}$$

Proof: It can be proven that matrix A has n repeated values of the eigenvalues of matrix $\tilde{A} = \begin{bmatrix} 1 & T \\ -k_pT & 1-k_vT-k_dT \end{bmatrix}$. From $zI - \tilde{A} = \begin{bmatrix} z-1 & -T \\ k_pT & z-1+(k_v+k_d)T \end{bmatrix}$, we can write out the characteristic equation as

$$z^2 + \left[(k_v+k_d)\,T - 2\right] z + 1 - (k_v+k_d)T + k_pT^2 = 0.$$

Solving the equation gives the eigenvalues

$$z_{1,2} \ = \ \frac{1}{2}\left[2 - (k_v+k_d)\,T \pm T\sqrt{(k_v+k_d)^2 - 4k_p}\right].$$

To have a convergent A,

- If $(k_v+k_d)^2 - 4k_p \geq 0$, then we need

$$-1 < \frac{1}{2}\left[2 - (k_v+k_d)\,T \pm T\sqrt{(k_v+k_d)^2 - 4k_p}\right] < 1.$$

Notice that $z_{1,2} < 1$ always holds with $k_p > 0$. To have $-1 < z_{1,2}$, we need

$$-2 < 2 - (k_v+k_d)\,T - T\sqrt{(k_v+k_d)^2 - 4k_p}$$

that is

$$T < \frac{4}{(k_v+k_d) + \sqrt{(k_v+k_d)^2 - 4k_p}}.$$

- If $(k_v + k_d)^2 - 4k_p < 0$, we need $\|z_{1,2}\| < 1$. So

$$(2 - (k_v + k_d)\,T)^2 + T^2\left[4k_p - (k_v + k_d)^2\right] < 4$$

that is

$$4 - 4(k_v + k_d)T + 4k_pT^2 < 4.$$

So we have

$$0 < T < \frac{k_v + k_d}{k_p}.$$

This completes the proof. ■

From now on, we assume T is sufficiently small such that the condition in Lemma 1 holds.

Lemma 2: *For the error dynamics model described in (3.7), if the noise satisfies (3.8), then it holds that*

$$\begin{aligned}\sum_{i=1}^{N}\left\|C^i(k)\right\|^2 \;\leq\; & \gamma_1^2\sum_{i=1}^{N}\left\|E^i(k)\right\|^2 + 4\gamma_1\gamma_3\sum_{i=1}^{N}\left\|E^i(k)\right\| \\ & +3\gamma_1\gamma_2\sum_{i=1}^{N}\left\|E^i(k)\right\|\sum_{j=1}^{N}\left\|E^j(k)\right\| + N\gamma_3^2 \qquad (3.10)\end{aligned}$$

where $\gamma_1 = k_pTD_{p_1} + k_vTD_{v_1}$, $\gamma_2 = \gamma_1/N$, *and*

$$\gamma_3 = \left(2k_pD_{p_2} + 2k_vD_{v_2} + 2k_fD_f + (N-1)k_rT\exp\left(-\frac{1}{2}\right)r_s + 2k_f\Lambda\right)T$$

are constants.

Proof: Notice that any function $F(\psi) = \exp\left(-\|\psi\|^2/2{r_s}^2\right)\|\psi\|$, with ψ any real vector, has a unique maximum value of $\exp\left(-1/2\right)r_s$ which is achieved when $\|\psi\| = r_s$ [43]. So

$$\left\|\exp\left(\frac{-\frac{1}{2}\left\|\hat{e}_p^i - \hat{e}_p^j\right\|^2}{{r_s}^2}\right)\left(\hat{e}_p^i - \hat{e}_p^j\right)\right\| \leq \exp\left(-\frac{1}{2}\right)r_s.$$

Recall that we assume that the resource profile has bounded slope, i.e., $\|\nabla J(x(k))\| \leq \Lambda$, then

$$\left\|\delta^i(E(k))\right\| \leq (N-1)k_r T \exp\left(-\frac{1}{2}\right) r_s + 2k_f T\Lambda.$$

Thus, from (3.8) we have

$$\begin{aligned}
\left\|C^i(k)\right\| &\leq \left\|g^i(k)\right\| + \|\phi(k)\| + \left\|\delta^i(E(k))\right\| \\
&\leq k_p T\left(D_{p_1}\left\|E^i(k)\right\| + D_{p_2}\right) + k_v T\left(D_{v_1}\left\|E^i(k)\right\| + D_{v_2}\right) \\
&\quad + k_f T D_f + k_p T \frac{1}{N}\sum_{j=1}^{N}\left(D_{p_1}\left\|E^j(k)\right\| + D_{p_2}\right) \\
&\quad + k_v T \frac{1}{N}\sum_{j=1}^{N}\left(D_{v_1}\left\|E^j(k)\right\| + D_{v_2}\right) + k_f T \frac{1}{N}\sum_{j=1}^{N} D_f \\
&\quad + (N-1)k_r T \exp\left(-\frac{1}{2}\right) r_s + 2k_f T\Lambda \\
&= \gamma_1\left\|E^i(k)\right\| + \gamma_2 \sum_{j=1}^{N}\left\|E^j(k)\right\| + \gamma_3 \qquad (3.11)
\end{aligned}$$

with γ_1, γ_2 and γ_3 as given in the statement of the lemma. Then

$$\begin{aligned}
\left\|C^i(k)\right\|^2 &\leq \gamma_1^2\left\|E^i(k)\right\|^2 + \gamma_2^2\left(\sum_{j=1}^{N}\left\|E^j(k)\right\|\right)^2 + \gamma_3^2 + 2\gamma_3\gamma_1\left\|E^i(k)\right\| \\
&\quad + 2\gamma_1\gamma_2\left\|E^i(k)\right\|\sum_{j=1}^{N}\left\|E^j(k)\right\| + 2\gamma_2\gamma_3\sum_{j=1}^{N}\left\|E^j(k)\right\|.
\end{aligned}$$

So we have

$$\begin{aligned}\sum_{i=1}^{N}\left\|C^i(k)\right\|^2 &\leq \gamma_1^2\sum_{i=1}^{N}\left\|E^i(k)\right\|^2+N\gamma_2^2\left(\sum_{i=1}^{N}\left\|E^i(k)\right\|\sum_{j=1}^{N}\left\|E^j(k)\right\|\right)\\ &\quad +N\gamma_3^2+2\gamma_1\gamma_2\sum_{i=1}^{N}\left\|E^i(k)\right\|\sum_{j=1}^{N}\left\|E^j(k)\right\|\\ &\quad +2N\gamma_2\gamma_3\left(\sum_{i=1}^{N}\left\|E^i(k)\right\|\right)+2\gamma_3\gamma_1\sum_{i=1}^{N}\left\|E^i(k)\right\|\\ &= \gamma_1^2\sum_{i=1}^{N}\left\|E^i(k)\right\|^2+4\gamma_1\gamma_3\sum_{i=1}^{N}\left\|E^i(k)\right\|\\ &\quad +3\gamma_1\gamma_2\sum_{i=1}^{N}\left\|E^i(k)\right\|\sum_{j=1}^{N}\left\|E^j(k)\right\|+N\gamma_3^2\end{aligned}$$

where we used the fact that $\gamma_1 = N\gamma_2$. ■

Lemma 3: *Given an $L \times L$ matrix $\tilde{S}$ specified by*

$$\tilde{s}_{jk} = \begin{cases} -(\tilde{\sigma}+\tilde{a}), & j = n \\ -\tilde{a}, & j \neq n \end{cases} \tag{3.12}$$

where $\tilde{\sigma} < 0$ and $\tilde{a} > 0$. Then $\tilde{S} > 0$ ($\tilde{S} > 0$ is positive definite) if and only if $L\tilde{a} < -\tilde{\sigma}$.

Proof: A necessary and sufficient condition for $\tilde{S} > 0$ is that its eigenvalues are all positive. We have

$$\begin{aligned}
\left|\lambda I - \tilde{S}\right| &= \begin{vmatrix} \lambda+(\tilde{\sigma}+\tilde{a}) & \tilde{a} & \tilde{a} & \dots & \tilde{a} \\ \tilde{a} & \lambda+(\tilde{\sigma}+\tilde{a}) & \tilde{a} & \dots & \tilde{a} \\ \tilde{a} & \tilde{a} & \lambda+(\tilde{\sigma}+\tilde{a}) & \dots & \tilde{a} \\ \vdots & \vdots & \vdots & \ddots & \vdots \\ \tilde{a} & \tilde{a} & \tilde{a} & \dots & \lambda+(\tilde{\sigma}+\tilde{a}) \end{vmatrix} \\
&= \begin{vmatrix} \lambda+(\tilde{\sigma}+\tilde{a}) & \tilde{a} & \tilde{a} & \dots & \tilde{a} \\ -(\lambda+\tilde{\sigma}) & \lambda+\tilde{\sigma} & 0 & \dots & 0 \\ -(\lambda+\tilde{\sigma}) & 0 & \lambda+\tilde{\sigma} & \dots & 0 \\ \vdots & \vdots & \vdots & \ddots & \vdots \\ -(\lambda+\tilde{\sigma}) & 0 & 0 & \dots & \lambda+\tilde{\sigma} \end{vmatrix} \\
&= \begin{vmatrix} \lambda+\tilde{\sigma}+L\tilde{a} & \tilde{a} & \tilde{a} & \dots & \tilde{a} \\ 0 & \lambda+\tilde{\sigma} & 0 & \dots & 0 \\ 0 & 0 & \lambda+\tilde{\sigma} & \dots & 0 \\ \vdots & \vdots & \vdots & \ddots & \vdots \\ 0 & 0 & 0 & \dots & \lambda+\tilde{\sigma} \end{vmatrix} \\
&= (\lambda+\tilde{\sigma}+L\tilde{a})\,(\lambda+\tilde{\sigma})^{L-1}.
\end{aligned}$$

Since $-\tilde{\sigma} > 0$, to have all the eigenvalues positive we need $\tilde{\sigma} + L\tilde{a} < 0$, that is, $L\tilde{a} < -\tilde{\sigma}$. ■

The results of Lemma 2 and 3 will be used in the proof of our main result, which we present next.

Fact 1 *When matrix A is convergent, for any given matrix $\tilde{Q} = \tilde{Q}^\top > 0$, there exists a unique matrix $\tilde{P} = \tilde{P}^\top > 0$ which is the solution of the discrete Lyapunov equation $A^\top \tilde{P} A - \tilde{P} = -\tilde{Q}$.*

Definition 1 *Given $\tilde{P}$ and $\tilde{Q}$ that satisfy the discrete Lyapunov equation above, define $\beta_{M,m}$ respectively as twice the values of the maximum and minimum eigenvalues of $\tilde{P}$ given $\tilde{Q} = I$, i.e., $\beta_M = 2\lambda_{max}\left(\tilde{P}|_{\tilde{Q}=I}\right)$ and $\beta_m = 2\lambda_{min}\left(\tilde{P}|_{\tilde{Q}=I}\right)$.*

Fact 2 *With $\tilde{P}$, $\tilde{Q}$ and β_M defined above, the minimum of function $f(\tilde{P},\tilde{Q}) = 2\lambda_{max}(\tilde{P})/\lambda_{min}(\tilde{Q})$ is β_M, that is,*

$$\beta_M = \left.\frac{2\lambda_{max}(\tilde{P})}{\lambda_{min}(\tilde{Q})}\right|_{\tilde{Q}=I} = \min_{\tilde{Q}} f(\tilde{P},\tilde{Q}).$$

3.3.2 Uniform Ultimate Boundedness of Cohesive Social Foraging

Theorem 5: *Consider the error dynamics model described in (3.7) and assume the noise satisfies (3.8). Let β_M be defined in Fact 2. If we have*

$$k_p D_{p_1} + k_v D_{v_1} < \frac{1}{T}\left(\sqrt{\|A\|^2 + \frac{2}{\beta_M}} - \|A\|\right) \tag{3.13}$$

and there exists some constant $0 < \theta < 1$ such that

$$k_p D_{p_1} + k_v D_{v_1} < \frac{1}{T}\left(\frac{\sqrt{(2-\theta)^2\|A\|^2 + \frac{2(4-\theta)(1-\theta)}{\beta_M}}}{4-\theta} - \frac{2-\theta}{4-\theta}\|A\|\right) \tag{3.14}$$

then the trajectories of the error system are uniformly ultimately bounded (UUB).

Proof: To study the stability of the error dynamics, it is convenient to choose a Lyapunov function for each agent as

$$V_i(k) = E^i(k)^\top P E^i(k) \tag{3.15}$$

with $P = P^\top > 0$ a $2n \times 2n$ positive definite matrix. Then we have

$$\begin{aligned} V_i(k+1) &= E^i(k+1)^\top P E^i(k+1) \\ &= E^i(k)^\top A^\top P A E^i(k) + 2C^i(k)^\top B^\top P A E^i(k) \\ &\quad + C^i(k)^\top B^\top P B C^i(k). \end{aligned}$$

So

$$\begin{aligned}\Delta V_i(k) &= V_i(k+1) - V_i(k) \\ &= E^i(k)^\top \underbrace{\left(A^\top P A - P\right)}_{-Q} E^i(k) + 2C^i(k)^\top B^\top P A E^i(k) \\ &\quad + C^i(k)^\top B^\top P B C^i(k). \end{aligned} \tag{3.16}$$

Note that given any $Q = Q^\top > 0$, the existence of a desired P is stated in Fact 1. Choose for the composite system

$$V(k) = \sum_{i=1}^{N} V_i(k)$$

where $V_i(k)$ is given in (3.15). Since for any matrix $M = M^\top > 0$ and vector X

$$\lambda_{min}(M) X^\top X \leq X^\top M X \leq \lambda_{max}(M) X^\top X$$

where $\lambda_{min}(M)$ and $\lambda_{max}(M)$ denote the minimum and maximum eigenvalue of M, respectively, then we have

$$\sum_{i=1}^{N} \left(\lambda_{min}(P) \left\|E^i(k)\right\|^2\right) \leq V(k) \leq \sum_{i=1}^{N} \left(\lambda_{max}(P) \left\|E^i(k)\right\|^2\right). \tag{3.17}$$

Using (3.10) and (3.11) from Lemma 2 and the fact that $\|B\| = 1$ we have

$$\begin{aligned}\Delta V(k) &= \sum_{i=1}^{N} \Delta V_i(k) \\ &\leq \sum_{i=1}^{N} \Big[-\lambda_{min}(Q) \left\|E^i(k)\right\|^2 + 2\lambda_{max}(P) \left\|C^i(k)\right\| \|A\| \left\|E^i(k)\right\| \\ &\quad + \lambda_{max}(P) \left\|C^i(k)\right\|^2\Big] \\ &\leq \lambda_{min}(Q) \sum_{i=1}^{N} \Bigg[-\left(1 - \beta'_M \gamma_1 \|A\| - \beta'_M \frac{\gamma_1^2}{2}\right) \left\|E^i(k)\right\|^2 \\ &\quad + \beta'_M \gamma_3 \left(\|A\| + 2\gamma_1\right) \left\|E^i(k)\right\| + \frac{\beta'_M \gamma_3^2}{2} \\ &\quad + \left\|E^i(k)\right\| \sum_{j=1}^{N} \beta'_M \gamma_2 \left(\|A\| + \frac{3}{2}\gamma_1\right) \left\|E^j(k)\right\|\Bigg] \end{aligned}$$

where $\beta'_M = \frac{2\lambda_{max}(P)}{\lambda_{min}(Q)}$. By inspecting the above inequality, we can see that minimizing β'_M is desirable for achieving stability. Recall what is stated in Fact 2, we let $Q = I$ and thus, β'_M is minimized to β_M. Then with this choice of Q, we obtain

$$\begin{aligned}\Delta V(k) \;\leq\; & \sum_{i=1}^{N}\Bigg[-c_1\left\|E^i(k)\right\|^2 + c_2\left\|E^i(k)\right\| \\ & + \left\|E^i(k)\right\|\sum_{j=1}^{N}\left(a\left\|E^j(k)\right\|\right)\Bigg] + c_3 \end{aligned} \tag{3.18}$$

with c_1, c_2, c_3 and a constants and

$$\begin{aligned} c_1 &= 1 - \beta_M\gamma_1\|A\| - \beta_M\frac{\gamma_1^2}{2} \\ c_2 &= \beta_M\gamma_3\left(\|A\| + 2\gamma_1\right) \\ c_3 &= \frac{N\beta_M\gamma_3^2}{2} \\ a &= \beta_M\gamma_2\left(\|A\| + \frac{3}{2}\gamma_1\right). \end{aligned}$$

Obviously $c_2 > 0$, $c_3 > 0$, and $a > 0$. To have $c_1 > 0$, we need

$$\frac{\beta_M}{2}\gamma_1^2 + \beta_M\|A\|\gamma_1 - 1 < 0. \tag{3.19}$$

Solving this equation gives (3.13).

Now, return to (3.18) and note that for any θ, $0 < \theta < 1$,

$$\begin{aligned} -c_1\left\|E^i(k)\right\|^2 + c_2\left\|E^i(k)\right\| &\leq -(1-\theta)c_1\left\|E^i(k)\right\|^2,\ \forall\ \left\|E^i(k)\right\| \geq r \\ &= \sigma\left\|E^i(k)\right\|^2 \end{aligned} \tag{3.20}$$

where $r = \frac{c_2}{\theta c_1}$ and $\sigma = -(1-\theta)c_1 < 0$. This implies that as long as $\|E^i(k)\| \geq r$, the first two terms in (3.18) combined will give a negative contribution to $\Delta V(k)$.

Next, we seek conditions under which $\Delta V(k) < 0$. To do this, we consider the third term in the brackets of (3.18) and combine it with the above results. Note the

general situation where some of the $E^i(k)$ are such that $\|E^i(k)\| < r$ and others are not. Accordingly, define sets

$$\Pi_O(k) = \left\{i : \left\|E^i(k)\right\| \geq r,\ i \in 1, \ldots, N\right\} = \left\{i_O^1,\ i_O^2, \ldots,\ i_O^{N_O(k)}\right\}$$

and

$$\Pi_I(k) = \left\{i : \left\|E^i(k)\right\| < r,\ i \in 1, \ldots, N\right\} = \left\{i_I^1,\ i_I^2, \ldots,\ i_I^{N_I(k)}\right\}$$

where $N_O(k)$ and $N_I(k)$ are the size of $\Pi_O(k)$ and $\Pi_I(k)$ at time step k, respectively. Also, $\Pi_O(k) \bigcup \Pi_I(k) = \{1, \ldots, N\}$ and $\Pi_O(k) \bigcap \Pi_I(k) = \phi$. Of course, we do not know the explicit sets $\Pi_O(k)$ and $\Pi_I(k)$; all we know is that they exist. For now, we assume $N_O(k) > 0$, that is, the set $\Pi_O(k)$ is non-empty. We will later discuss the $N_O(k) = 0$ case. Then using analysis ideas from the theory of stability of interconnected systems [53] and using (3.18) and (3.20), we have

$$\begin{aligned}
\Delta V(k) \ \leq\ & \sum_{i \in \Pi_O(k)} \sigma \left\|E^i(k)\right\|^2 + \sum_{i \in \Pi_O(k)} \left(\left\|E^i(k)\right\| \sum_{j \in \Pi_O(k)} a \left\|E^j(k)\right\| \right) \\
& + \sum_{i \in \Pi_O(k)} \left(\left\|E^i(k)\right\| \sum_{j \in \Pi_I(k)} a \left\|E^j(k)\right\| \right) \\
& + \sum_{i \in \Pi_I(k)} \left(-c_1 \left\|E^i(k)\right\|^2 + c_2 \left\|E^i(k)\right\| \right) \\
& + \sum_{i \in \Pi_I(k)} \left(\left\|E^i(k)\right\| \sum_{j \in \Pi_O(k)} a \left\|E^j(k)\right\| \right) \\
& + \sum_{i \in \Pi_I(k)} \left(\left\|E^i(k)\right\| \sum_{j \in \Pi_I(k)} a \left\|E^j(k)\right\| \right) + c_3.
\end{aligned}$$

Note for each $N_O(k)$, with the corresponding $N_I(k) = N - N_O(k)$ there exist positive constants $K_1(N_I(k))$, $K_2(N_I(k))$ and $K_3(N_I(k))$ such that,

$$\begin{aligned} K_1(N_I(k)) &\geq \sum_{j\in\Pi_I(k)} a\left\|E^j(k)\right\| = \sum_{i\in\Pi_I(k)} \left\|E^i(k)\right\| a \\ K_2(N_I(k)) &\geq \sum_{i\in\Pi_I(k)} \left(-c_1\left\|E^i(k)\right\|^2 + c_2\left\|E^i(k)\right\|\right) \\ K_3(N_I(k)) &\geq \sum_{i\in\Pi_I(k)} \left(\left\|E^i(k)\right\| \sum_{j\in\Pi_I(k)} a\left\|E^j(k)\right\|\right). \end{aligned} \tag{3.21}$$

Then, we have

$$\begin{aligned} \Delta V(k) &\leq \sum_{i\in\Pi_O(k)} \sigma\left\|E^i(k)\right\|^2 + \sum_{i\in\Pi_O(k)} \left(\left\|E^i(k)\right\| \sum_{j\in\Pi_O(k)} a\left\|E^j(k)\right\|\right) \\ &\quad + K_1 \sum_{i\in\Pi_O(k)} \left\|E^i(k)\right\| + K_2 + K_1 \sum_{j\in\Pi_O(k)} \left\|E^j(k)\right\| + K_3 + c_3 \\ &= \sum_{i\in\Pi_O(k)} \sigma\left\|E^i(k)\right\|^2 + \sum_{i\in\Pi_O(k)} \left(\left\|E^i(k)\right\| \sum_{j\in\Pi_O(k)} a\left\|E^j(k)\right\|\right) \\ &\quad + \sum_{i\in\Pi_O(k)} 2K_1\left\|E^i(k)\right\| + K_2 + K_3 + c_3. \end{aligned}$$

Let $w(k)^\top = \left[\|E^{i_O^1}(k)\|, \|E^{i_O^2}(k)\|, \ldots, \|E^{i_O^{N_O(k)}}(k)\|\right]$ and the $N_O(k) \times N_O(k)$ matrix $S(k) = [s_{jk}]$ be specified by

$$s_{jk} = \begin{cases} -(\sigma + a), & j = n \\ -a, & j \neq n \end{cases}$$

so we have

$$\Delta V(k) \leq -w(k)^\top S(k) w(k) + \sum_{i\in\Pi_O(k)} 2K_1\left\|E^i(k)\right\| + K_2 + K_3 + c_3.$$

From Lemma 3 we know that $S(k) > 0$ as long as $N_O(k)a < -\sigma$, while this holds if we have $Na < -\sigma$ since $N_O(k) \leq N$. In fact it can be proven that when (2.15) holds, we have $Na < -\sigma$. This becomes clear when we write out $Na < -\sigma$ explicitly

$$N\beta_M\gamma_2\left(\|A\| + \frac{3}{2}\gamma_1\right) < (1-\theta)\left(1 - \beta_M\gamma_1\|A\| - \beta_M\frac{\gamma_1^2}{2}\right)$$

and solve the equation after manipulation

$$\frac{\beta_M(4-\theta)}{2}\gamma_1^2 + \beta_M\|A\|(2-\theta)\gamma_1 - (1-\theta) < 0.$$

So when (3.14) holds, we have $S(k) > 0$ and thus, $\lambda_{min}(S(k)) > 0$. Therefore

$$\Delta V(k) \leq -\lambda_{min}(S(k)) \sum_{i\in\Pi_O(k)} \left\|E^i(k)\right\|^2 + \sum_{i\in\Pi_O(k)} 2K_1 \left\|E^i(k)\right\| + K_2 + K_3 + c_3. \quad (3.22)$$

When the $\|E^i(k)\|$ for $i \in \Pi_O(k)$ are sufficiently large, the sign of $\Delta V(k)$ is determined by the term of $-\lambda_{min}(S(k)) \sum_{i\in\Pi_O(k)} \|E^i(k)\|^2$ and $\Delta V(k) < 0$. This analysis is valid for any value of $N_O(k)$, $1 \leq N_O(k) \leq N$; hence for any $N_O(k) \neq 0$ the system is uniformly ultimately bounded.

To complete the proof, we need to consider the case when $N_O(k) = 0$. Note that when $N_O(k) = 0$, $\|E^i(k)\| < r$ for all i. If we have $N_O(k) = 0$ persistently, then we could simply take r as the uniform ultimate bound. If otherwise, at certain moment the system changes such that some $\|E^i(k)\| \geq r$, then we have $N_O(k) \geq 1$ immediately, then all the analysis above, which holds for any $1 \leq N_O(k) \leq N$, applies. Thus, in either case we obtain the uniform ultimate boundedness. This concludes the proof. ■

Remark 22 *From (3.13) and (2.15) we can see that it is the attraction gains k_p and k_v and damping gain k_d that determine if boundedness can be achieved for given parameters that quantify the size of the noise. Other parameters (k_r, r_s and k_f, etc.) do not affect the boundedness but only the bound.*

Remark 23 *On the noise side, it is the D_{p_1} and D_{v_1} that affect the uniform ultimate boundedness of the error system, while D_{p_2} and D_{v_2} do not. Note that when D_{p_1} =*

$D_{v_1} = 0$, (3.13) and (2.15) are always satisfied, meaning when noise is constant or with constant bound, the trajectories of the error system are always UUB.

3.3.3 Special Case: Constant-Bound Noise and Plane Profile

In this section we assume the resource profile for each agent is a plane profile defined by $\nabla J^i(k) = R^i$, as seen in (3.2). Also we assume that $d_p^i(k)$ and $d_v^i(k)$ are bounded by some constants for all i,

$$\begin{aligned} \|d_p^i\| &\leq D_p \\ \|d_v^i\| &\leq D_v \end{aligned} \tag{3.23}$$

where $D_p \geq 0$ and $D_v \geq 0$ are known constants. The sensing error on the gradient of the nutrient profile is assumed to be bounded by known constant $D_f \geq 0$ such that for all i,

$$\|d_f^i\| \leq D_f. \tag{3.24}$$

Theorem 6: *Consider the error system described by the model in (3.3). Assume the noise satisfies (3.23) and (2.40). Let $\Lambda' = max_{1\leq i\leq N} \|R^i\|$. Then, the trajectories of the swarm error system are uniformly ultimately bounded, and E^i for all i will converge to the set Ω_b, where*

$$\Omega_b = \left\{ E : \ \left\|E^i\right\| \leq \frac{\gamma_3'}{2} \left(\beta_M + \sqrt{\|A\|^2 \beta_M^2 + 2\beta_M} \right), \ i = 1, 2, \ldots, N \right\} \tag{3.25}$$

is attractive and compact, with β_M defined in Fact 2 and

$$\gamma_3' = \left(2k_p D_p + 2k_v D_v + 2k_f D_f + (N-1) k_r T \exp\left(-\frac{1}{2}\right) r_s + 2k_f \Lambda' \right) T. \tag{3.26}$$

Moreover, the centroid velocity of the swarm $\bar{v}$ is uniformly ultimately bounded if we have

$$T < \frac{2}{k_d} \tag{3.27}$$

and $\bar{v}$ will converge to the set $\Omega_v = \{\bar{v} : \ \|v\| \leq v_M\}$, where

$$v_M = \begin{cases} \frac{\tau}{k_d} & \text{if } T \leq \frac{1}{k_d} \\ \frac{\tau T}{2 - k_d T} & \text{if } \frac{1}{k_d} < T < \frac{2}{k_d} \end{cases} \tag{3.28}$$

with $\tau = k_p D_p + k_v D_v + k_f D_f + k_f \Lambda'$.

Proof: To find the set Ω_b, we use the same idea as in the last section. Since now the noise has a constant bound, we have $\gamma_1 = 0$ and $\gamma_2 = 0$. So (3.11) is changed into $\|C^i(k)\| \leq \gamma_3'$ with γ_3' given by (3.26). From (3.18), we have

$$\Delta V_i(k) \leq -\left\|E^i(k)\right\|^2 + \beta_M \gamma_3' \|A\| \left\|E^i(k)\right\| + \frac{\beta_M {\gamma_3'}^2}{2} \tag{3.29}$$

where we let $Q = I$ by following the idea in Theorem 5 to obtain the above equation. Solving the equation gives that $\Delta V_i(k) < 0$ when

$$\left\|E^i(k)\right\| > \frac{\gamma_3'}{2}\left(\beta_M + \sqrt{\|A\|^2 \beta_M^2 + 2\beta_M}\right).$$

So the set

$$\Omega_b = \left\{E : \ \left\|E^i\right\| \leq \frac{\gamma_3'}{2}\left(\beta_M + \sqrt{\|A\|^2 \beta_M^2 + 2\beta_M}\right), \ i = 1, 2, \ldots, N\right\}$$

is attractive and compact.

To study the boundedness of $\bar{v}(k)$, choose a Lyapunov function $V_{\bar{v}}(k) = \bar{v}(k)^\top \bar{v}(k)$. Since

$$\begin{aligned} \bar{v}(k+1) &= \bar{v}(k) + \frac{1}{N}\sum_{j=1}^{N} \frac{1}{M_i} u^j(k) T \\ &= (1 - k_d T)\bar{v}(k) + \underbrace{\left(k_p \bar{d}_p + k_v \bar{d}_v + k_f \bar{d}_f - k_f \bar{R}\right)}_{d(k)} T \end{aligned} \tag{3.30}$$

where $\bar{d}_p(k) = \frac{1}{N}\sum_{i=1}^{N} d_p^i$. Similarly we define $\bar{d}_v(k)$ and $\bar{d}_f(k)$. Also $\bar{R} = \frac{1}{N}\sum_{i=1}^{N} R^i$. Obviously $\|d(k)\| \leq \tau$. Then we have

$$\begin{aligned}\Delta V_{\bar{v}}(k) &= \bar{v}(k+1)^\top \bar{v}(k+1) - \bar{v}(k)^\top \bar{v}(k) \\ &\leq \underbrace{k_d T(k_d T - 2)\|v(k)\|^2 + 2\tau T|1 - k_d T|\|v(k)\| + \tau^2 T^2}_{F(v)}.\end{aligned}$$

Obviously we need $k_d T - 2 < 0$, that is, $T < \frac{2}{k_d}$. Furthermore, it can be solved that the maximum root of $F(v) = 0$ are

$$\begin{aligned}v_M &= \frac{-2\tau T|1 - k_d T| - \sqrt{4\tau^2 T^2(1 - k_d T)^2 - 4k_d T(k_d T - 2)\tau^2 T^2}}{2k_d T(k_d T - 2)} \\ &= \frac{\tau|1 - k_d T| + \tau}{k_d(2 - k_d T)}.\end{aligned}$$

If $1 - k_d T \geq 0$, then $v_M = \frac{\tau}{k_d}$; if otherwise, $v_M = \frac{\tau T}{2 - k_d T}$. Since $\Delta V_{\bar{v}}(k) < 0$ when $\|v(k)\| > v_M$, we have the attractive and compact set $\Omega_v = \{\bar{v} : \|v\| \leq v_M\}$. ■

Remark 24 *The size of Ω_b in (3.25), which we denote by $|\Omega_b|$, is directly a function of several known parameters. If there are no sensing errors, i.e., $D_p = D_v = D_f = 0$, then Ω_b reduces to the set representing the no-noise case. If we increase r_s or k_r while keeping all other parameters unchanged, then each agent has a stronger repulsion effect to its neighbors so $|\Omega_b|$ is larger. If we let $N \to \infty$, then $|\Omega_b| \to \infty$ as expected.*

Remark 25 *Comparing (3.9) with (3.27) we can see that the boundedness of $\bar{v}$ and the convergency of the system matrix A are independent. That is, it is possible for an error system to have infinitely increasing norm $\|E^i\|$ while having $\bar{v}$ bounded, and vice versa. Also, from (3.28) we can see that the bound of $\|\bar{v}\|$ is affected by the noise bounds and the gradient of the plane profiles. Larger profile gradients or noise bounds will lead to larger v_M. Also when T is smaller than certain value ($\frac{2}{T}$ in this case),*

then the ultimate bound of $\|v(k)\|$ does not change with T any more; otherwise, it is a function of T.

Remark 26 *If there is no noise, from (3.30) we can see that it is the "averaged" profile gradient $\bar{R}$ that changes the moving directions of all the agents. That is, due to the desire to stay together, they each sacrifice following their own profile and compromise to follow the averaged profile. Furthermore, note that in this case (3.30) changes into*

$$\bar{v}(k+1) = (1 - k_d T)\bar{v}(k) - k_f \bar{R} T$$

when (3.27) is satisfied, using this equation recursively, we have $\bar{v}(k) = (1-k_d T)^k \bar{v}(0) - \frac{k_f \bar{R}}{k_d}$. This means as k goes to infinity, $\bar{v}(k)$ converges to a constant $-\frac{k_f \bar{R}}{k_d}$.

Remark 27 *In reality noise always exists, but in some cases when the swarm is large (N big) it can be that $\bar{d}_p \approx \bar{d}_v \approx \bar{d}_f \approx 0$ and thus, the group will still be able to follow the proper direction (i.e., the averaged profile). In the case when $N = 1$ (i.e., single agent), there is no opportunity for a cancellation of the sensor errors; hence an individual may not be able to climb a noisy gradient as easily as a group. This may be a reason why large group size is favorable for some organisms and this characteristic has been found in biological swarms [4, 51].*

3.4 Simulations

In this section, we will show some simulation results for both the no-noise and noise cases. Unless otherwise stated, in all the following simulations the parameters are: $N = 50$, $k_p = 1$, $k_v = 1$, $k_d = 0.1$, $k_f = 0.1$, $k_r = 1$, $r_s = 1$, and the three dimensional nutrient plane profile $\nabla J_p^i(x) = R^i = [2,\ 4,\ 6]^\top$ for all i.

3.4.1 No-Noise Case

All the simulations in this case are run for 20 seconds. The position and velocity trajectories of the swarm agents are shown in Figure 3.1. All the agents are assigned initial velocities and positions randomly. At the beginning of the simulation, they appear to move around erratically. But soon, they swarm together and continuously reorient themselves as a group to slide down the plane profile. Note how these agents gradually catch up with each other while still keeping mutual spacing. Recall from the previous section that for this case $\bar{v}(k) \to -\frac{k_f}{k_d} R$ as $k \to \infty$, and this can be seen from Figure 3.1(b) since the final velocity of each swarm agent is indeed $-[2,\ 4,\ 6]^\top$.

3.4.2 Noise Case

In this case, we run the simulations for 80 seconds. All the parameters used in the no-noise case are kept unchanged except the number of agents in the swarm in certain simulations, which is specified in the relevant figures. Figures 3.2 and 3.3 illustrate the case with linear noise bounds for a typical simulation run. The noise bounds are $D_{p_1} = D_{v_1} = 0.1$, $D_{p_2} = D_{v_2} = 3$, and $D_f = 30$, respectively. According to the "Grunbaum principle" [4, 51], forming a swarm may help the agents go down the gradient of the nutrient profile without being significantly distracted by noise. Figure 3.2 shows that the existence of noise does affect the swarm's ability to follow the profile, which is indicated by the oscillation of the position trajectories. But with all the agents working together, especially when the agents number N is large, they are able to move in the right direction and thus, minimize the negative effects of noise. In comparison, Figure 3.3 shows the case when there is only one agent. Since the single agent cannot benefit from the averaging effects possible when there are

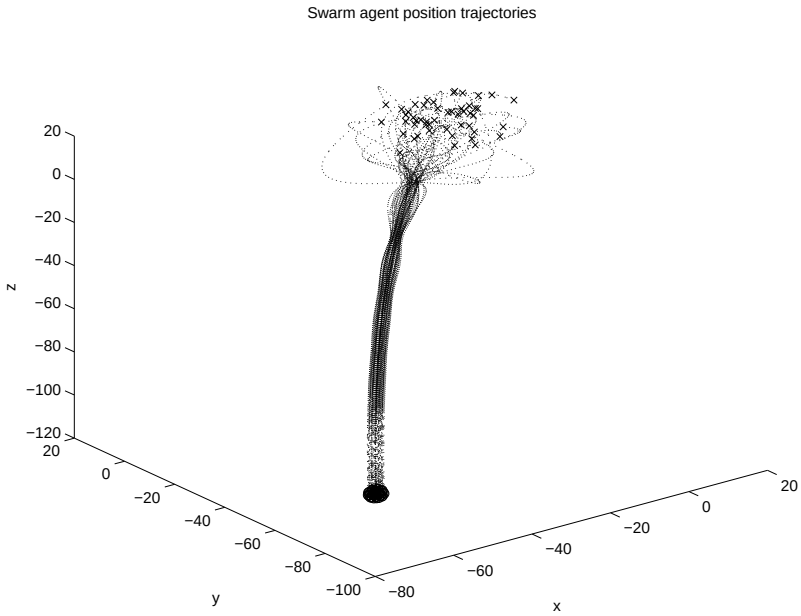

(a) Agent position trajectories.

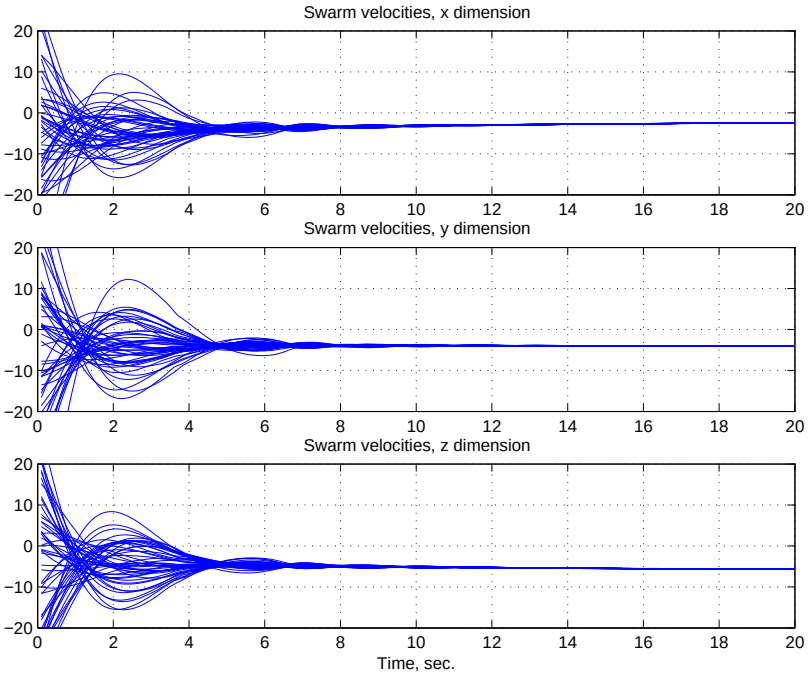

(b) Agent velocity trajectories.

Figure 3.1: No noise case.

many agents, the noise more adversely affects its performance in terms of accurately following the nutrient profile.

3.5 Concluding Remarks

In this chapter we focused on a discrete-time formulation and derived stability conditions under which social foraging swarms maintain cohesiveness and follow a resource profile even in the presence of sensor errors and noise on the profile. Our simulations illustrated advantages of social foraging in large groups relative to foraging alone since they show that a noisy resource profile can be more accurately tracked by a swarm than an individual.

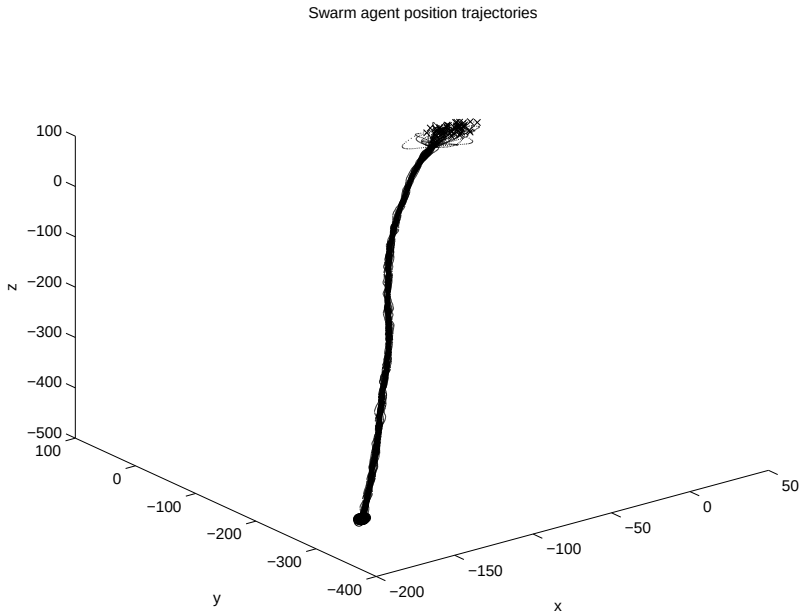

(a) Agent position trajectories.

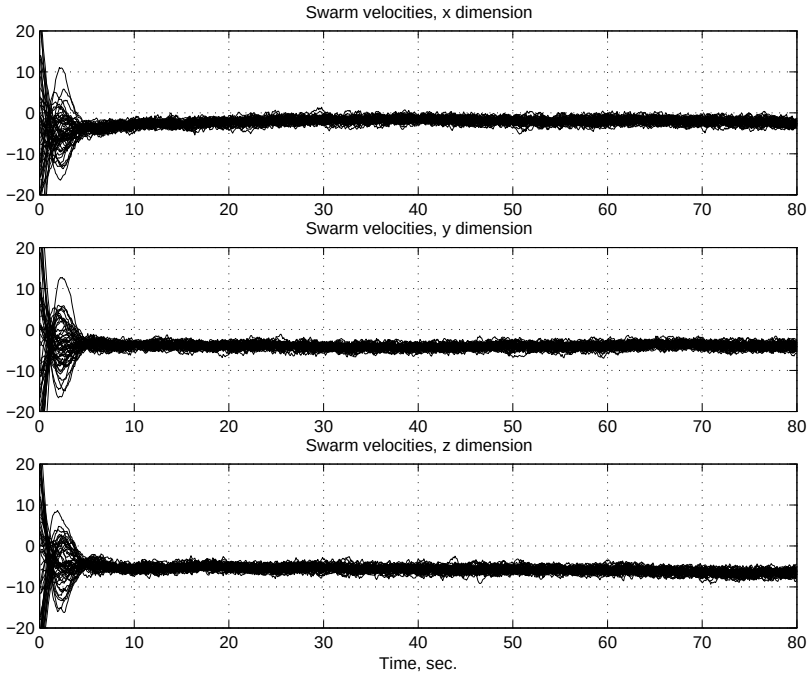

(b) Agent velocity trajectories.

Figure 3.2: Linear noise bounds case ($N = 50$).

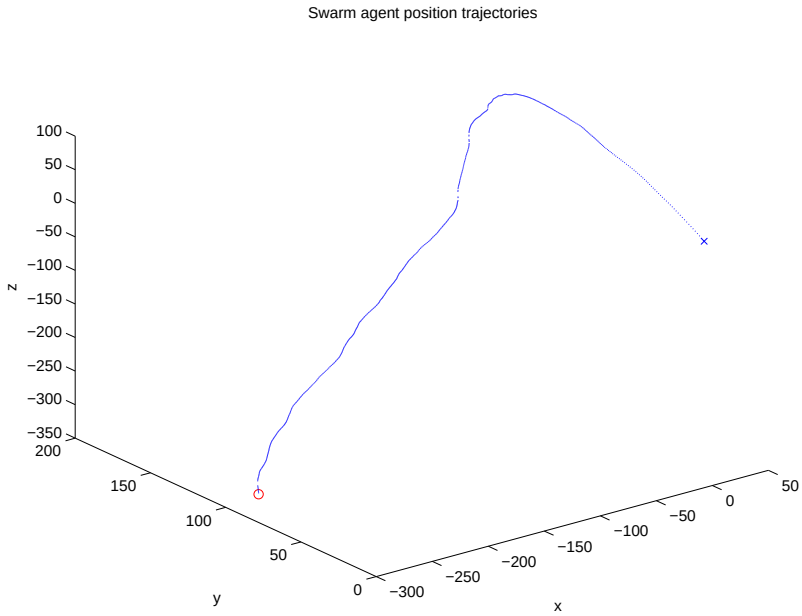

(a) Agent position trajectories.

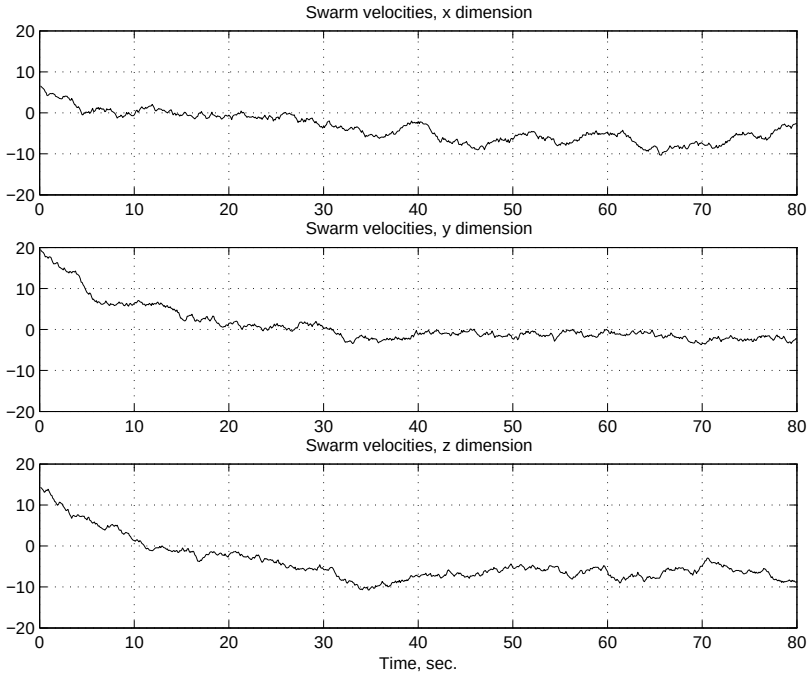

(b) Agent velocity trajectories.

Figure 3.3: Linear noise bounds case ($N = 1$).

CHAPTER 4

COHESIVE BEHAVIORS OF MULTIAGENT SYSTEMS WITH INFORMATION FLOW CONSTRAINTS

4.1 Introduction

In this chapter, we consider the effects of an interagent "sensing topology" and random but bounded sensing delays in an asynchronous discrete-time framework. The topology and delays both impose information flow constraints on the multiagent system (where by "information flow," we mean the sensing of positions and velocities of agents), which significantly complicate its ability to achieve cohesive and purposeful behavior. We are able to show that under certain conditions, even with noisy measurements and the group objective of following a resource profile, the group can become cohesive in the sense that interagent distances are uniformly ultimately bounded. Moreover, under some conditions a set of zero interagent distances is exponentially stable.

While in Chapter 2 (also see [56, 57]) we exploited a large-scale system stability methodology with scalar Lyapunov functions and M-matrices [53], here we extend some ideas from the theory of numerical methods in distributed computing [58] and use a Lyapunov framework for distributed discrete event systems [59]. To clarify

the relationship of our work to the work in [58], consider the "agreement algorithm" developed there. For it, consider N processors and suppose that the ith processor at time step $k = 0$ has a scalar $x^i(0)$ stored in its memory. These processors are to exchange values and eventually agree on an intermediate value x^f,

$$\min_{1\leq i\leq N}\{x^i(0)\} \leq x^f \leq \max_{1\leq i\leq N}\{x^i(0)\}.$$

The agreement algorithm in [58] is an asynchronous iterative process where each processor receives values from some other processors and combines them with its own value by forming a convex combination. If $x^i(k)$ is the value possessed by processor i at time step k, the asynchronous execution of the iteration is

$$x^i := \sum_{j=1}^{N} a_{ij}x^j,\ i = 1,\ldots,N$$

where the coefficients a_{ij} are nonnegative scalars such that $\sum_{j=1}^{N} a_{ij} = 1$ for all i. The agreement algorithm is given by

$$\begin{aligned} x^i(k+1) &= x^i(k),\ \text{if } k \notin \mathcal{K}^i \\ x^i(k+1) &= \sum_{j=1}^{N} a_{ij}x^j\left(\kappa_j^i(k)\right),\ \text{if } k \in \mathcal{K}^i \end{aligned} \tag{4.1}$$

where $\mathcal{K}^i$ is a set of time step indices at which the ith processor updates its value. Here, $\kappa_j^i(k)$ gives the amount by which the value used in an update of x^i is outdated. It is assumed that $k - B \leq \kappa_j^i(k) \leq k$, with $k \in \mathcal{K}^i$ and $B \in \mathcal{Z}^+ = \{0,1,2,\ldots\}$ some known constant. Bertsekas and Tsitsiklis [58] show that, under certain conditions, the sequence $\{x^i(k)\}$ converges and its limit is the same for each processor i, and particularly, there exist constants $C > 0$ and $\rho \in (0,1)$ such that

$$\begin{aligned} &\max_{1\leq i\leq N}\{x^i(k)\} - \min_{1\leq i\leq N}\{x^i(k)\} \\ \leq\ & C\rho^k\left(\max_{1\leq i\leq N}\left\{\max_{-B+1\leq\kappa\leq 0}\{x^i(\kappa)\}\right\} - \min_{1\leq i\leq N}\left\{\min_{-B+1\leq\kappa\leq 0}\{x^i(\kappa)\}\right\}\right). \end{aligned}$$

That is, the difference between the maximum and minimum values possessed by all the processors in a B-step-long "sliding" time slot decreases at the rate of a geometric progression.

To obtain some of the results in this chapter, we use similar methods to those in [58], and in the development below we will highlight how. However, it should be noted that there are significant differences between our model and the agreement algorithm model since (i) there are no dynamics for x^i in (4.1) like the second-order dynamics we use for our agents, (ii) all x^i in (4.1) are always bounded by the formulation of the agreement problem, (iii) there is no receiving (or passing) noise in (4.1), (iv) among their interactions there exists no "repulsion" effect among the values possessed by each processor, and (v) there exists no external effect on the processors analogous to our "resource profile" that models an environmental stimulus. Also, in our model we assume each agent updates its information on positions and velocities at each time step k, that is, the case of $k \notin \mathcal{K}^i$ in the agreement algorithm is not considered in our model. With all these differences, we are able to show that when the difference between the maximum and minimum agent position values in a fixed-length "sliding" time slot is sufficiently large, it decreases at the rate of a geometric progression until it enters certain "ball," with the ball's size determined by some system parameters. We show this via a general Lyapunov approach like in [59].

The remainder of this chapter is organized as follows: In Section 4.2 we introduce a generic model for agents, interactions, and the environment. Section 4.3 holds the main results on stability and boundedness analysis of cohesion. Section 4.4 holds the results of simulations and applications of the theory, and some concluding remarks are provided in Section 4.5.

Notation: $\Re^n$ denotes the n-dimensional Euclidean space, $\Re^+$ is the nonnegative reals, $\Re^{n\times m}$ denotes the set of all $n \times m$ real matrices, and $\mathcal{Z}^+$ is the nonnegative integers. $\|\cdot\|$ is the Euclidean vector norm. When x is a vector, x_i is the ith component of x. The notation $x > y$ ($x \geq y$), where x and y are vectors of the same dimension, means that $x_i > y_i$ (respectively, $x_i \geq y_i$) for all i. Similarly, if x, y and z are all vectors with the same dimension, $x = \max\{y, z\}$ ($x = \min\{y, z\}$) means its component $x_i = \max\{y_i, z_i\}$ (respectively, $x_i = \min\{y_i, z_i\}$) for all i, and x_i equals to either y_i or z_i when $y_i = z_i$. $|x|$ is the absolute value of x and it is taken componentwise when x is a vector. $\mathbf{1}_n$ denotes the vector $[1, 1, \ldots, 1]^\top \in \Re^n$. $\lceil x \rceil$ denotes the minimum integer that is larger than $x \in \Re^+$.

4.2 Mathematical Model

4.2.1 Agents, Sensing Topology, Interactions, and Environment

Here, similar to Chapter 3, we consider a system composed of an interconnection of N ($N \geq 2$) "agents," where the ith agent, $i = 1, \ldots, N$, has point mass dynamics defined in the same way as in (3.1). For convenience, we rewrite it below.

$$\begin{aligned} x^i(k+1) &= x^i(k) + v^i(k)T \\ v^i(k+1) &= v^i(k) + \frac{1}{M_i}u^i(k)T \end{aligned} \tag{4.2}$$

where $x^i \in \Re^n$ is the position, $v^i \in \Re^n$ is the velocity, $M_i > 0$ is the mass, $u^i \in \Re^n$ is the control input, and $T > 0$ is the sampling time. Throughout the chapter, we mainly consider the case of $k \in \mathcal{Z}^+$. We assume $x^i(k) = x^i(0)$, and thus, $v^i(k) = 0$, for $k < 0$, $i = 1, \ldots, N$.

Let $\mathcal{N} = \{1, \ldots, N\}$ be a set of indices that label the agents. Then, the sensing topology of the group of agents is characterized by a fixed (time-invariant) directed graph $\mathcal{G} = (\mathcal{N}, \mathcal{A})$, where $\mathcal{A} \subset \mathcal{N} \times \mathcal{N}$, and the positive direction of arc $(i, j) \in \mathcal{A}$ is from i to j. We say that i can *affect* j (or, j can *sense* i) only if $(i, j) \in \mathcal{A}$. So, the arc direction of $\mathcal{A}$ is the direction of information flow. Let Π^i for all $i \in \mathcal{N}$ be the set of "neighbors" of agent i such that all $j \in \Pi^i$ can have their information about positions and velocities be sensed by agent i (but possibly with some delays or errors). Clearly, by definition, $(i, j) \in \mathcal{A}$ means $i \in \Pi^j$ (instead of $j \in \Pi^i$). Also, it can be that $i \in \Pi^j$ but $j \notin \Pi^i$ so that agent j can sense agent i but agent i cannot sense agent j. We assume $i \in \Pi^i$ since it is reasonable to assume that an agent knows its own position and velocity. We also assume each Π^i includes at least one $j \neq i$, that is, each agent has at least one such neighbor. Define $N^i = |\Pi^i|$ as the size of Π^i, so $2 \leq N^i \leq N$.

Same as in Chapter 3, agent to agent interactions considered here are of the "attract-repel" type where each agent seeks to be in a position that is "comfortable" relative to its neighbors. Attraction indicates that each agent wants to be close to all its neighbors and it provides the mechanism for achieving grouping and cohesion of the group of agents. Repulsion provides the mechanism where each agent does not want to be too close to other agents. Attraction here will be represented in u^i in a form like $-k'\left(x^i - x^j\right)$ where $k' > 0$ is a scalar that represents the strength of attraction. For repulsion, we use a repulsion term in u^i of the form

$$k_r \exp\left(\frac{-\frac{1}{2}\|x^i - x^j\|^2}{{r_s}^2}\right)\left(x^i - x^j\right) \tag{4.3}$$

where $k_r \geq 0$ and $r_s > 0$. Other types of attraction and repulsion terms are also possible.

Next, for the environment that the agents move in, we will simply consider the case where they move (forage) over a "resource profile" $J(x)$, where $x \in \Re^n$. Agents move in the direction of $-\nabla J(x) = -\partial J/\partial x$, the negative gradient of $J(x)$, in order to move away from "bad" areas and into "good" areas of the environment [60]. To achieve this, a term that holds $\nabla J(x)$ will be used in u^i for each agent i. The goal of the multiagent system is to stay cohesive and move in the direction specified by $J(x)$. Clearly there are many possible shapes for $J(x)$, including ones with many peaks and valleys. Below, we will study a family of profiles such that they are differentiable everywhere and $\|\nabla J(x)\| \leq \Lambda_0$ for all $x \in \Re^n$, where Λ_0 is a known constant.

4.2.2 Sensing Delays, Noise, and Asynchronism

We assume that the ith agent, $i \in \mathcal{N}$, can sense the positions and velocities of all its neighbors, but with some time delay. In particular, let $\tau_j^i(k) \in [0, B_s] \subset \mathcal{Z}^+$ indicate the amount by which the position and velocity of agent j sensed by agent i at the kth step is outdated, with $B_s \in \mathcal{Z}^+$ a known constant. Thus, the position and velocity of agent j sensed by i at the kth step are written as $x^j(k - \tau_j^i(k))$ and $v^j(k - \tau_j^i(k))$, respectively. Note that by this definition, it is possible that for $k' > k$, $k - \tau_j^i(k) > k' - \tau_j^i(k')$. That is, if we think of the position and velocity information about agent j as data indexed by k, then these data could arrive at agent i (suppose $j \in \Pi^i$) in a "shuffled" order. For simplicity of notation, hereafter we will write $\tau_j^i(k)$ as τ_j^i. But, it should be remembered that it is a *time-varying* integer-valued term. We will also assume that each agent can sense its own position and velocity without any delay, i.e., $\tau_i^i = 0$ for all i. Note that with the topology defined in Section 4.2.1,

if $j \notin \Pi^i$, i can never sense j and this can be thought of as having an infinite delay, while if $j \in \Pi^i$, then the sensing delay is bounded by B_s.

We assume that there exist sensing errors when each agent senses its own and other agents' positions and velocities. In particular, let $d_p^{ij} \in \Re^n$ and $d_v^{ij} \in \Re^n$ be these sensing errors (e.g., noise) for agent i with respect to agent j, respectively. Thus, if $j \in \Pi^i$, agent i actually senses agent j's position and velocity as

$$\hat{x}^j(k - \tau_j^i) = x^j(k - \tau_j^i) - d_p^{ij}(k)$$
$$\hat{v}^j(k - \tau_j^i) = v^j(k - \tau_j^i) - d_v^{ij}(k).$$

(In fact, precisely speaking, each agent i need not sense the *absolute* position and velocity but the *relative* ones of agent j. We will discuss more on this in Section 4.2.3.) Notice that, different from time delays, we allow errors for an agent in sensing its own position and velocity, i.e., it could happen that $d_p^{ii}(k) \neq 0$ and $d_v^{ii}(k) \neq 0$. We assume the sensing error magnitudes are bounded by some constants, that is, $\|d_p^{ij}\| \leq \delta_p \in \Re^+$ and $\|d_v^{ij}\| \leq \delta_v \in \Re^+$ for all i and $j \in \Pi^i$, where δ_p and δ_v are known.

Besides the position and velocity sensing errors, we also assume there are some errors for agent i in sensing $\nabla J\left(x^i(k)\right)$, the gradient of the profile at its position at the kth step. Note that sensing errors related to profile could originate either from position sensing errors (i.e., $\hat{x}^i$ instead of x^i) or from gradient sensing errors (i.e., $\nabla \hat{J}$ instead of ∇J). For simplicity, we do not distinguish between these two cases and write the profile-related sensing error at the kth step as $d_f^i(k)$, i.e., we assume that $\nabla \hat{J}\left(\hat{x}^i(k)\right) = \nabla J(x^i(k)) - d_f^i(k)$. It is assumed that $\|d_f^i(k)\| \leq \delta_f \in \Re^+$ for all i, with δ_f a known constant. To simplify notation, we will write $\nabla \hat{J}\left(\hat{x}^i(k)\right)$ as $\nabla \hat{J}^i(k)$ from now on. We also assume $\nabla \hat{J}^i(k) = \nabla \hat{J}^i(0)$ for $k < 0$, $i \in \mathcal{N}$.

Next, we explain how our random delays lead to a type of asynchronous operation for our multiagent system. Of course, the motions of the agents are synchronous in the sense that the time step T is fixed. However, the time delays τ_j^i are random, but only fall on the boundaries of time intervals quantified by T. So, we are considering a restricted form of asynchronism, with B_sT the maximum sensing delay in real time. This is further illustrated by the following example. Suppose for agent i, $j_1 \in \Pi^i$ and $j_2 \in \Pi^i$. Also, suppose $B_s \geq 2$, and $\tau_{j_1}^i \in \{0,1\}$ and $\tau_{j_2}^i \in \{0,1,2\}$, with specific values from these sets chosen randomly at each k. It is possible that agent i senses agent j_1 according to $\tau_{j_1}^i(k) = 0,1,1,0,1,0,0,\ldots$, and agent j_2 according to $\tau_{j_2}^i(k) = 1,0,1,2,2,0,1,\ldots$, where both sequences are random. This means that agent i can sense the positions and velocities of agents j_1 and j_2 at different time steps. Asynchronism of information flow is obvious in this example.

4.2.3 Controls and Dynamics

Suppose that the general form of the control input for each agent i at the kth step is

$$\begin{aligned} u^i(k) \;=\; & -M_i k_p \sum_{j\in\Pi^i} \left(\hat{x}^i(k) - \hat{x}^j(k-\tau_j^i)\right) - M_i k_v \sum_{j\in\Pi^i} \left(\hat{v}^i(k) - \hat{v}^j(k-\tau_j^i)\right) \\ & -M_i k_d \hat{v}^i(k) \\ & +M_i k_r \sum_{j\in\Pi^i} \exp\left(\frac{-\frac{1}{2}\left\|\hat{x}^i(k) - \hat{x}^j(k-\tau_j^i)\right\|^2}{{r_s}^2}\right)\left(\hat{x}^i(k) - \hat{x}^j(k-\tau_j^i)\right) \\ & -M_i k_f \nabla \hat{J}^i(k). \end{aligned} \tag{4.4}$$

with all system parameters as defined in (3.4).

By writing the control input as in (4.4), we are assuming that each agent i can sense its own position and velocity, but with some errors. Also, we assume agent i can

sense the profile gradient at its position, but with some error. Recall in Section 4.2.2, to initiate the description of our problem, we also assumed that agent i can sense the (absolute) positions and velocities (possibly with some delays and errors) of all its neighbor $j \in \Pi^i$. But, it should be noted that this is *not* required. In particular, only the *relative* position $\hat{x}^i(k) - \hat{x}^j(k-\tau_j^i)$ and the *relative* velocity $\hat{v}^i(k) - \hat{v}^j(k-\tau_j^i)$ need to be known by agent i, as one can see from (4.4).

When sensing delays and errors are present, after some manipulations, Equation (4.2) becomes, for each i,

$$\begin{aligned} x^i(k+1) &= 2x^i(k) - x^i(k-1) + \frac{1}{M_i}u^i(k-1)T^2 \\ &= 2x^i(k) - x^i(k-1) - k_p T^2 \sum_{j\in\Pi^i} \left(x^i(k-1) - x^j(k-1-\tau_j^i)\right) \\ &\quad -k_v T^2 \sum_{j\in\Pi^i} \left(v^i(k-1) - v^j(k-1-\tau_j^i)\right) - k_d T^2 v^i(k-1) \\ &\quad +\psi^i(k-1)T^2 - k_f \nabla J^i(k-1)T^2 + \delta^i(k-1)T^2 \end{aligned}$$

where

$$\begin{aligned} \psi^i(k-1) &= k_r \sum_{j\in\Pi^i} \exp\left(-\frac{\left\|\hat{x}^i(k-1) - \hat{x}^j(k-1-\tau_j^i)\right\|^2}{2{r_s}^2}\right) \\ &\quad \times \left(\hat{x}^i(k-1) - \hat{x}^j(k-1-\tau_j^i)\right) \end{aligned}$$

and

$$\begin{aligned} \delta^i(k-1) &= k_p \sum_{j\in\Pi^i} \left(d_p^{ii}(k-1) - d_p^{ij}(k-1)\right) \\ &\quad +k_v \sum_{j\in\Pi^i} \left(d_v^{ii}(k-1) - d_v^{ij}(k-1)\right) \\ &\quad +k_d d_v^{ii}(k-1) + k_f d_f^i(k-1). \end{aligned}$$

Using $x^i(k+1) = x^i(k) + v^i(k)T$ as in (4.2) and eliminating all v-related terms, we have

$$\begin{aligned}
x^i(k+1) &= 2x^i(k) - x^i(k-1) - k_p T^2 \sum_{j\in\Pi^i} \left(x^i(k-1) - x^j(k-1-\tau_j^i)\right) \\
&\quad -k_v T^2 \sum_{j\in\Pi^i} \left(\frac{x^i(k) - x^i(k-1)}{T} - \frac{x^j(k-\tau_j^i) - x^j(k-1-\tau_j^i)}{T} \right) \\
&\quad -k_d T^2 \frac{x^i(k) - x^i(k-1)}{T} + \psi^i(k-1)T^2 - k_f \nabla J^i(k-1)T^2 \\
&\quad +\delta^i(k-1)T^2 \\
&= (2 - k_v N^i T - k_d T)x^i(k) + (-1 - k_p N^i T^2 + k_v N^i T + k_d T)x^i(k-1) \\
&\quad +k_v T \sum_{j\in\Pi^i} x^j(k-\tau_j^i) + (k_p T^2 - k_v T) \sum_{j\in\Pi^i} x^j(k-1-\tau_j^i) \\
&\quad +\psi^i(k-1)T^2 - k_f \nabla J^i(k-1)T^2 + \delta^i(k-1)T^2. \qquad (4.5)
\end{aligned}$$

Note that for any i and k, we have

$$\|\psi^i(k)\| \le (N^i - 1)\exp(-\frac{1}{2})k_r r_s \le \psi_0 \qquad (4.6)$$

where we used the fact that $x^i(k) - x^i(k-\tau_i^i) = 0$, and $\psi_0 = (N-1)\exp(-1/2)k_r r_s$. Since for any given vector z we have $\max_j |z_j| \le \|z\|$, $\max_j |\psi_j^i(k)| \le \psi_0$. Thus, for all i and k we have

$$|\psi^i(k)| \le \bar{\psi} = \psi_0 \mathbf{1}_n \in \Re^n. \qquad (4.7)$$

Sometimes we know a constant integer $\bar{N}$ such that $N^i \le \bar{N} \le N$ for all i. Then, let $\psi_0' = (\bar{N} - 1)\exp(-1/2)k_r r_s$, and we have

$$|\psi^i(k)| \le \bar{\psi}' = \psi_0' \mathbf{1}_n \in \Re^n. \qquad (4.8)$$

Generally, using (4.8) instead of (4.7) helps alleviate conservativeness in the results, especially when $\bar{N} \ll N$. Nevertheless, for brevity, we use (4.7) throughout the chapter.

Similarly, we have

$$|k_f \nabla J^i(k)| \leq \bar{\Lambda} = k_f \Lambda_0 \mathbf{1}_n \in \Re^n \tag{4.9}$$

for all i and k. Sometimes it is possible to know the upper bound of the profile slope in all the n directions in the $\Re^n$ space, i.e., $|\nabla J^i(k)| < \Lambda'$ for all i and k, with $\Lambda' = [\Lambda_1, \Lambda_2, \ldots, \Lambda_n]^\top \in \Re^n$ a known constant vector. Then we have

$$|k_f \nabla J^i(k)| \leq \bar{\Lambda}' = [k_f \Lambda_1, \ldots, k_f \Lambda_n]^\top \in \Re^n. \tag{4.10}$$

Generally, using (4.10) instead of (4.9) helps alleviate conservativeness in the results. Nevertheless, in either case the methodology for stability analysis is the same. Hereafter, we assume only $\bar{\Lambda}$ is known and (4.9) is used in the remainder of the chapter.

For the last term in (4.5) we have

$$|\delta^i(k-1)| \leq \bar{\Delta} = \Delta_0 \mathbf{1}_n \in \Re^n \tag{4.11}$$

where $\Delta_0 = 2k_p N \delta_p + (2k_v N + k_d)\delta_v + k_f \delta_f$.

4.3 Stability Analysis of Cohesion Properties

In this section we give the main results on stability analysis of cohesion. In Section 4.3.1 we specify some mathematical properties we use in the remainder of the chapter. In Section 4.3.2 we quantify several properties of the dynamics of agent position trajectories relative to the sensing topology. In Section 4.3.3 we provide our main results on uniform ultimate boundedness and exponential stability characterizations of cohesiveness. In Section 4.3.4 we interpret the results and give insights into how system parameters and information flow constraints affect cohesiveness.

4.3.1 Mathematical Preliminaries

Let

$$\begin{aligned} c_1 &= 2 - k_v NT - k_d T \\ c_2 &= -1 - k_p NT^2 + k_v NT + k_d T \\ c_3 &= k_v T \\ c_4 &= k_p T^2 - k_v T. \end{aligned}$$

Also, let $c_1^i = 2 - k_v N^i T - k_d T$ and $c_2^i = -1 - k_p N^i T^2 + k_v N^i T + k_d T$, $i \in \mathcal{N}$. Then, we can write (4.5) as

$$\begin{aligned} x^i(k+1) &= c_1^i x^i(k) + c_2^i x^i(k-1) + c_3 \sum_{j \in \Pi^i} x^j(k - \tau_j^i) + c_4 \sum_{j \in \Pi^i} x^j(k-1-\tau_j^i) \\ &\quad + \psi^i(k-1)T^2 - k_f \nabla J^i(k-1)T^2 + \delta^i(k-1)T^2. \end{aligned} \tag{4.12}$$

Next, we present an assumption which will be used throughout the remainder of the chapter.

Assumption 1 *The system parameters k_p, k_v, k_d, N and T are such that $c_1 > 0$, $c_2 > 0$, $c_3 > 0$ and $c_4 \geq 0$.*

Before we proceed, we prove the following two Lemmas which will be useful in our proofs later.

Lemma 4: *If Assumption 1 holds, then*

(i) $c_1 \in (0,1)$, $c_2 \in (0,1)$, $c_3 \in (0,1)$, *and* $c_4 \in [0,1)$.

(ii) $c_1^i \in [c_1, 1)$ *and* $c_2^i \in [c_2, 1)$ *for all* $i \in \mathcal{N}$.

Proof: Note that $c_1 + c_2 + c_3 N + c_4 N = 1$. Since c_1, c_2 and c_3 are all positive and $c_4 \geq 0$, we must have $c_1 \in (0,1)$, $c_2 \in (0,1)$, $c_3 \in (0,1)$, and $c_4 \in [0,1)$.

Note that $c_1^i + c_2^i + c_3 N^i + c_4 N^i = 1$ for all i, we have $c_1^i \in (0,1)$ and $c_2^i \in (0,1)$. Since $N^i \leq N$ for all i, $c_1^i \geq c_1$, also $c_2^i \geq c_2$ by using the assumption of $c_4 \geq 0$. That is, $c_1^i \in [c_1, 1)$ and $c_2^i \in [c_2, 1)$. ■

Lemma 5: *Suppose u, v, w and z are real vectors of the same dimension, and z is nonnegative componentwise. If $u \geq \min\{v, w\} + z$, then $\min\{u, v\} \geq \min\{v, w\} - z$. Also, if $u \leq \max\{v, w\} + z$, then $\max\{u, v\} \leq \max\{v, w\} + z$.*

Proof: For the first part, consider the ith entry of each vector, where i is picked arbitrarily. Then we have $u_i \geq \min\{v_i, w_i\} + z_i$.

(i) If $v_i < w_i$, then $\min\{v_i, w_i\} = v_i$. Thus, $u_i \geq v_i + z_i \geq v_i - z_i = \min\{v_i, w_i\} - z_i$. Since $v_i \geq v_i - z_i = \min\{v_i, w_i\} - z_i$, we have $\min\{u_i, v_i\} \geq \min\{v_i, w_i\} - z_i$.

(ii) If $v_i \geq w_i$, then $\min\{v_i, w_i\} = w_i$. Thus, $u_i \geq w_i + z_i \geq w_i - z_i = \min\{v_i, w_i\} - z_i$. Since $v_i \geq w_i \geq w_i - z_i = \min\{v_i, w_i\} - z_i$, we have $\min\{u_i, v_i\} \geq \min\{v_i, w_i\} - z_i$.

Since i is picked arbitrarily, we have $\min\{u, v\} \geq \min\{v, w\} - z$. The second part is proven similarly. ■

4.3.2 Properties of Agent Position Dynamics Relative to Sensing Topology

Define the state $X(k) \in \Re^{Nn \times (B_s+2)}$ for the system as

$$X(k) = \begin{bmatrix} x^{11}(k) & x^{12}(k) & \dots & x^{1(B_s+2)}(k) \\ x^{21}(k) & x^{22}(k) & \dots & x^{2(B_s+2)}(k) \\ \vdots & \vdots & & \vdots \\ x^{N1}(k) & x^{N2}(k) & \dots & x^{N(B_s+2)}(k) \end{bmatrix} \tag{4.13}$$

where $x^{ij}(k) = x^i(k-j+1) \in \Re^n$, with $i \in \mathcal{N}$ and $j \in \mathcal{B}$, $\mathcal{B} = \{1, \ldots, B_s+2\}$. Define $M(k) \in \Re^n$, the maximum displacement from the origin of any agent over the last $B_s + 2$ time steps in each dimension, as

$$\begin{aligned} M(k) &= \max_{i\in\mathcal{N}} \left\{ \max_{j\in\mathcal{B}} \left\{ x^{ij}(k) \right\} \right\} \\ &= \max_{i\in\mathcal{N}} \left\{ \max_{0\le\tau\le B_s+1} \left\{ x^i(k-\tau) \right\} \right\}. \end{aligned} \tag{4.14}$$

Similarly, let $m(k) \in \Re^n$ be the minimum such displacement, defined as

$$\begin{aligned} m(k) &= \min_{i\in\mathcal{N}} \left\{ \min_{j\in\mathcal{B}} \left\{ x^{ij}(k) \right\} \right\} \\ &= \min_{i\in\mathcal{N}} \left\{ \min_{0\le\tau\le B_s+1} \left\{ x^i(k-\tau) \right\} \right\}. \end{aligned} \tag{4.15}$$

First, we show that the rates of increase (decrease) of elements of $M(k)$ (respectively, $m(k)$) are bounded.

Lemma 6: *If Assumption 1 holds, then for any integer n_2 and n_1, with $n_2 \geq n_1 > 0$, we have*

$$\begin{aligned} M(n_2) &\leq M(n_1) + (n_2 - n_1)\Theta T^2 \\ m(n_2) &\geq m(n_1) - (n_2 - n_1)\Theta T^2 \end{aligned} \tag{4.16}$$

where $\Theta = \bar{\psi}+\bar{\Lambda}+\bar{\Delta}$, with $\bar{\psi}$, $\bar{\Lambda}$ and $\bar{\Delta}$ defined in (4.7), (4.9), and (4.11), respectively.

Proof: If Assumption 1 holds, then by Lemma 4, $c_1^i > 0$ and $c_2^i > 0$. Since $\tau_j^i \in [0, B_s]$, by the definition of $M(k)$, we have from (4.7), (4.9), (4.11) and (4.12)

that

$$\begin{aligned} x^i(k+1) &\leq c_1^i M(k) + c_2^i M(k) + c_3 \sum_{j\in\Pi^i} M(k) + c_4 \sum_{j\in\Pi^i} M(k) \\ &\quad + \psi^i(k-1)T^2 - k_f \nabla J^i(k-1)T^2 + \delta^i(k-1)T^2 \\ &\leq M(k) + \bar{\psi}T^2 + \bar{\Lambda}T^2 + \bar{\Delta}T^2 \end{aligned}$$

for all $k \geq 0$, where we used the fact that $c_1^i + c_2^i + c_3 N^i + c_4 N^i = 1$. Since the above equation holds for all i, we have

$$\begin{aligned} \max_{i\in\mathcal{N}} \left\{x^i(k+1)\right\} &\leq M(k) + \Theta T^2 \\ &= \max\left\{\max_{i\in\mathcal{N}}\left\{\max_{0\leq\tau\leq B_s}\left\{x^i(k-\tau)\right\}\right\},\ \max_{i\in\mathcal{N}}\left\{x^i(k-1-B_s)\right\}\right\} \\ &\quad + \Theta T^2. \end{aligned}$$

With Lemma 5, we have from the above equation that

$$\begin{aligned} &\max\left\{\max_{i\in\mathcal{N}}\left\{x^i(k+1)\right\},\ \max_{i\in\mathcal{N}}\left\{\max_{0\leq\tau\leq B_s}\left\{x^i(k-\tau)\right\}\right\}\right\} \\ \leq\ &\max\left\{\max_{i\in\mathcal{N}}\left\{\max_{0\leq\tau\leq B_s}\left\{x^i(k-\tau)\right\}\right\},\ \max_{i\in\mathcal{N}}\left\{x^i(k-1-B_s)\right\}\right\} + \Theta T^2. \end{aligned}$$

By definition of $M(k)$, this is

$$M(k+1) \leq M(k) + \Theta T^2. \tag{4.17}$$

Now, for the case of $n_2 > n_1 > 0$, we have by using (4.17) repeatedly

$$M(n_2) \leq M(n_1) + (n_2 - n_1)\Theta T^2.$$

Since the above equation also holds when $n_2 = n_1$, we have $M(n_2) \leq M(n_1) + (n_2 - n_1)\Theta T^2$ for all $n_2 \geq n_1 > 0$.

Using a similar approach, we can show that

$$m(k+1) \geq m(k) - \Theta T^2 \tag{4.18}$$

and thus, for $n_2 \geq n_1 > 0$,

$$m(n_2) \geq m(n_1) - (n_2 - n_1)\Theta T^2.$$

■

Next, we will prove three Lemmas, with our ultimate objective to show that there exist constants $\eta_1 > 0$, $\eta_1 \in \mathcal{Z}^+$, $\eta_2 \in (0,1) \subset \Re$ and $\eta_3 \in \Re^+$ such that $M(k+\eta_1) - m(k+\eta_1) \leq (1-\eta_2)(M(k) - m(k)) + \eta_3 \mathbf{1}_n$ for all $k \in \mathcal{Z}^+$. This shows that $M(k) - m(k)$ decreases (componentwise) at the rate of a geometric progression, but with some "perturbation" term characterized by η_3. In proving these Lemmas, we use Lemma 6 and ideas similar to those in [58]. Next, we present another assumption that is needed by the following Lemmas.

Assumption 2 *There exists a fixed nonempty set $\mathcal{D} \subseteq \mathcal{N}$ of "distinguished" agents such that for every $i \in \mathcal{D}$ and every $j \in \mathcal{N}$, there exists a positive path from i to j in the directed graph $\mathcal{G}$, defined in Section 4.2.1.*

Recall that in Section 4.2.1 we define the concept of sensing topology and the corresponding directed graph $\mathcal{G}$ of our system, but the connectivity of the topology is not defined. As expected, such connectivity cannot be arbitrary. Assumption 2 above gives a constraint on it. This assumption means that the position and velocity information of every distinguished agent i can, through certain positive paths, affect every agent j, even if i and j are not directly connected to each other. Intuitively, if we think of $\mathcal{G}$ as a "tree," then its "branches" are those positive arcs of $\mathcal{A}$, and its "roots" form the distinguished set $\mathcal{D}$. (Notice that one should not think of this "tree" as the same as the *tree* concept in graph theory [61] since in graph theory, a *tree* is a connected acyclic graph, while in our case, the graph $\mathcal{G}$ could have cycles.) Note that

for a graph, having such a distinguished set is a much milder condition than being completely connected.

Throughout the next three Lemmas, we fix some $l \in \mathcal{D}$. Define D_p, $1 \leq p \leq N-1$, as the set of $i \in \mathcal{N}$ and $i \neq l$ such that p is the minimum number of arcs in a positive path from l to i in $\mathcal{G}$. Also, let $D_0 = \{l\}$. Then there exists an integer P, $1 \leq P \leq N-1$, such that $D_0 \bigcup D_1 \bigcup \ldots \bigcup D_P = \mathcal{N}$ and every $i \in \mathcal{N}$ belongs (and only belongs) to one of the sets $D_0, D_1, \ldots, D_P$. Also, for every $i \in D_p$, $p \in \{1, \ldots, P\}$, there must exist some $j \in D_{p-1}$ such that, by the definition of $\mathcal{A}$ in Section 4.2.1, $(j, i) \in \mathcal{A}$, i.e., i can sense j. One illustrative example is given as follows. Figure 4.1 shows the sensing topology of five agents, where the direction of each arrow indicates the positive direction of an arc in $\mathcal{A}$. For example, arc $(1, 2) \in \mathcal{A}$, meaning the position and velocity information of agent 1 affects agent 2 (or, agent 2 can sense agent 1). Arc $(i, i) \in \mathcal{A}$, $i \in \{1, \ldots, 5\}$, since all agents can sense their own positions and velocities. Moreover, agents 1 and 5 can sense each other, and so can agents 2 and 4. Also, by Assumption 2, $\mathcal{D} = \{1, 5\}$. If we choose $l = 1$, then $P = 2$, $\mathcal{D}_0 = \{1\}$, $\mathcal{D}_1 = \{2, 5\}$, and $\mathcal{D}_2 = \{3, 4\}$. If we choose $l = 5$, then $P = 3$, $\mathcal{D}_0 = \{5\}$, $\mathcal{D}_1 = \{1\}$, $\mathcal{D}_2 = \{2\}$, and $\mathcal{D}_3 = \{3, 4\}$.

In the next Lemma, we will show that in a n_0-indexed fixed-length time slot $\mathcal{K}_0 \subset \mathcal{Z}^+$, with n_0 any nonnegative integer, the position trajectory of agent l, $l \in \mathcal{D}$, is bounded in terms of $M(n_0)$, $m(n_0)$, $x^l(n_0)$, and system parameters.

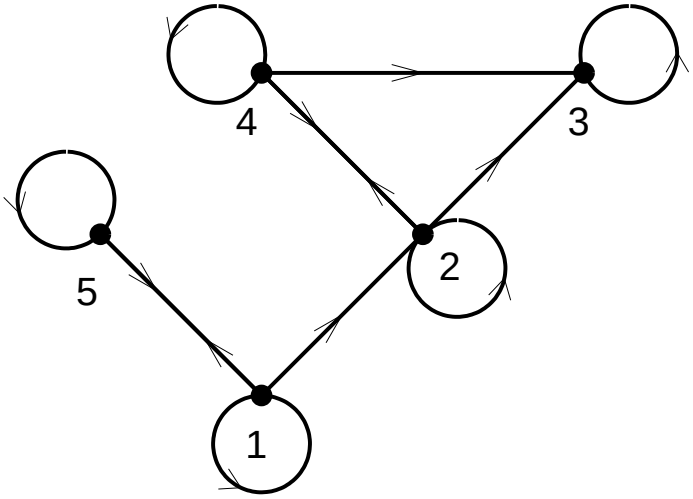

Figure 4.1: A simple sensing topology with five agents.

Lemma 7: *If Assumptions 1 and 2 hold, then for any agent $l \in \mathcal{D}$, and for every $k \in \mathcal{K}_0 = [n_0,\ n_0 + (P+1)(B_s+1)]$, with any $n_0 \in \mathcal{Z}^+$, we have*

$$\begin{aligned} x^l(k+1) &\leq M(n_0) - \alpha\left(M(n_0) - x^l(n_0)\right) - \beta_1\gamma\Theta T^2 \\ x^l(k+1) &\geq m(n_0) + \alpha\left(x^l(n_0) - m(n_0)\right) + \beta_1\gamma\Theta T^2 \end{aligned} \tag{4.19}$$

where $\alpha = c_1^{(P+1)(B_s+1)+1}$, $\beta_1 = (1 - k_v NT - k_d T)(P+1)(B_s+1) - 2 + k_d T$, and

$$\gamma = \frac{1 - (2 - k_d T)^{(P+1)(B_s+1)+1}}{k_d T - 1}.$$

Proof: Knowing $c_1^l + c_2^l + c_3 N^l + c_4 N^l = 1$, we have from (4.12)

$$\begin{aligned} M(n_0) - x^l(k+1) \;=\; & c_1^l(M(n_0) - x^l(k)) + c_2^l(M(n_0) - x^l(k-1)) \\ & + c_3 \sum_{j\in\Pi^l} \left(M(n_0) - x^j(k - \tau_j^l)\right) \\ & + c_4 \sum_{j\in\Pi^l} \left(M(n_0) - x^j(k - 1 - \tau_j^l)\right) \\ & - \psi^l(k-1)T^2 + k_f \nabla J^l(k-1)T^2 - \delta^l(k-1)T^2. \end{aligned} \tag{4.20}$$

Note that $1 - k_dT < 0$ since $c_2^l + c_4N^l > 0$. Thus, $(1 - k_dT)((P + 1)(B_s + 1) - 1) < 0 < k_vNT(P + 1)(B_s + 1)$, that is, $\beta_1 = (1 - k_vNT - k_dT)(P + 1)(B_s + 1) - 2 + k_dT < -1$. Since $c_1 + c_3N > 0$, we have $2 - k_dT \in (0, 1)$ and thus, $\gamma = \left(1 - (2 - k_dT)^{(P+1)(B_s+1)+1}\right)/(1 - (2 - k_dT)) > 1$. Therefore, $\beta_1\gamma < \beta_1 < -1$. In the proof we consider two cases separately: $k = n_0$ and $k \in [n_0+1, n_0+(P+1)(B_s+1)]$.

Case (i): $\mathbf{k = n_0}$.

When $k = n_0$, all x-related terms on the right hand side of (4.20) have time indices in the range of $[n_0 - B_s - 1, n_0]$ (where $n_0 - B_s - 1$ could be negative) and thus, are less than or equal to $M(n_0)$ by definition. Therefore (4.20) can be immediately written as

$$\begin{aligned} M(n_0) - x^l(k+1) &\geq c_1^l(M(n_0) - x^l(k)) - \Theta T^2 \\ &\geq c_1^l(M(n_0) - x^l(k)) + \beta_1\Theta T^2. \end{aligned} \tag{4.21}$$

Since $c_1^l \geq c_1 > \alpha$ and $\beta_1\gamma < \beta_1 < -1$, we have

$$M(n_0) - x^l(k+1) \geq \alpha\left(M(n_0) - x^l(n_0)\right) + \beta_1\gamma\Theta T^2.$$

Case (ii): $\mathbf{k \in [n_0 + 1, n_0 + (P + 1)(B_s + 1)]}$.

Before we proceed, for each fixed l and n_0 define two sets $\Pi_L^l(k)$ and $\Pi_G^l(k)$, which will be used in our deduction below. Specifically, let

$$\Pi_L^l(k) = \left\{j : k - \tau_j^l \leq n_0,\ j \in \Pi^l\right\}$$

which is the set of agents that satisfy $x^j(k - \tau_j^l) \leq M(n_0)$ by the definition of $M(k)$, and let

$$\Pi_G^l(k) = \left\{j : k - \tau_j^l > n_0,\ j \in \Pi^l\right\}$$

which is the set of agents that, though they may or may not satisfy $x^j(k-\tau_j^l) \leq M(n_0)$, have Lemma 6 applicable to $M(k-\tau_j^l)$ and $M(n_0)$ with $n_2 = k-\tau_j^l$ and $n_1 = n_0$. Also, let $N_L^l(k)$ and $N_G^l(k)$ be the sizes of $\Pi_L^l(k)$ and $\Pi_G^l(k)$, respectively. Then $N_L^l(k) + N_G^l(k) = N^l$. Obviously, for all $j \in \Pi_L^l(k)$ we have $k-1-\tau_j^l < n_0$ (and thus, $x^j(k-1-\tau_j^l) \leq M(n_0)$ by definition), and for all $j \in \Pi_G^l(k)$ we have $k-1-\tau_j^l \geq n_0$ (and thus, we can apply Lemma 6 to $M(k-1-\tau_j^l)$ and $M(n_0)$) since all the numbers involved here are integers. These facts will be used in our deduction below. Note that we do not know the explicit sets $\Pi_L^l(k)$ and $\Pi_G^l(k)$; all we know is that they exist for any $k \in \mathcal{Z}^+$. The explicit values in the sets clearly depend on k but we allow k to be arbitrary in the time slot $[n_0+1, n_0+(P+1)(B_s+1)]$, so the analysis below is valid for all k in this time slot.

Now (4.20) can be rewritten as

$$\begin{aligned} M(n_0) - x^l(k+1) &= c_1^l(M(n_0) - x^l(k)) + c_2^l(M(n_0) - x^l(k-1)) \\ &\quad + c_3 \sum_{j \in \Pi_G^l(k)} \big(M(n_0) - x^j(k-\tau_j^l)\big) \\ &\quad + c_3 \sum_{j \in \Pi_L^l(k)} \big(M(n_0) - x^j(k-\tau_j^l)\big) \\ &\quad + c_4 \sum_{j \in \Pi_G^l(k)} \big(M(n_0) - x^j(k-1-\tau_j^l)\big) \\ &\quad + c_4 \sum_{j \in \Pi_L^l(k)} \big(M(n_0) - x^j(k-1-\tau_j^l)\big) \\ &\quad - \psi^l(k-1)T^2 + k_f \nabla J^l(k-1)T^2 - \delta^l(k-1)T^2. \end{aligned}$$

By definition of $\Pi_L^l(k)$ and $M(k)$, the $j \in \Pi_L^l(k)$ terms are nonnegative. Thus,

$$\begin{aligned}
M(n_0) - x^l(k+1) &\geq c_1^l(M(n_0) - x^l(k)) + c_2^l(M(n_0) - x^l(k-1)) \\
&\quad + c_3 \sum_{j \in \Pi_G^l(k)} \big(M(n_0) - x^j(k - \tau_j^l)\big) \\
&\quad + c_4 \sum_{j \in \Pi_G^l(k)} \big(M(n_0) - x^j(k - 1 - \tau_j^l)\big) - \Theta T^2 \\
&\geq c_1^l(M(n_0) - x^l(k)) + c_2^l(M(n_0) - x^l(k-1)) \\
&\quad + c_3 \sum_{j \in \Pi_G^l(k)} \big(M(n_0) - M(k - \tau_j^l)\big) \\
&\quad + c_4 \sum_{j \in \Pi_G^l(k)} \big(M(n_0) - M(k - 1 - \tau_j^l)\big) - \Theta T^2 \\
&\geq c_1^l(M(n_0) - x^l(k)) + c_2^l(M(n_0) - M(k-1)) \\
&\quad + c_3 \sum_{j \in \Pi_G^l(k)} \big(M(n_0) - M(k - \tau_j^l)\big) \\
&\quad + c_4 \sum_{j \in \Pi_G^l(k)} \big(M(n_0) - M(k - 1 - \tau_j^l)\big) - \Theta T^2.
\end{aligned}$$

Next, using Lemma 6 and the fact that $k \geq n_0 + 1$, we have

$$\begin{aligned}
M(n_0) - x^l(k+1) &\geq c_1^l(M(n_0) - x^l(k)) + c_2^l(n_0 - k + 1)\Theta T^2 \\
&\quad + c_3 \sum_{j \in \Pi_G^l(k)} (n_0 - k + \tau_j^l)\Theta T^2 \\
&\quad + c_4 \sum_{j \in \Pi_G^l(k)} (n_0 - k + 1 + \tau_j^l)\Theta T^2 - \Theta T^2 \\
&\geq c_1^l(M(n_0) - x^l(k)) + \big[c_2^l(n_0 - k + 1) + c_3 N_G^l(k)(n_0 - k) \\
&\quad + c_4 N_G^l(k)(n_0 - k + 1) - 1\big]\Theta T^2 \\
&\geq c_1^l(M(n_0) - x^l(k)) + \big[c_2^l(n_0 - k + 1) + c_3 N^l(n_0 - k) \\
&\quad + c_4 N^l(n_0 - k + 1) - 1\big]\Theta T^2 \\
&= c_1^l(M(n_0) - x^l(k)) + \big[(c_2^l + c_3 N^l + c_4 N^l)(n_0 - k) \\
&\quad + c_2^l + c_4 N^l - 1\big]\Theta T^2.
\end{aligned}$$

By the assumption of $k \leq n_0 + (P+1)(B_s+1)$ and the fact that $N^l \leq N$,

$$\begin{aligned} M(n_0) - x^l(k+1) &\geq c_1^l(M(n_0) - x^l(k)) + \big[-(c_2^l + c_3 N^l + c_4 N^l)(P+1)(B_s+1) \\ &\quad + c_2^l + c_4 N^l - 1\big]\,\Theta T^2 \\ &= c_1^l(M(n_0) - x^l(k)) + \big[(1 - k_v N^l T - k_d T)(P+1)(B_s+1) \\ &\quad - 2 + k_d T\big]\,\Theta T^2 \\ &\geq c_1^l(M(n_0) - x^l(k)) + \beta_1 \Theta T^2. \end{aligned} \tag{4.22}$$

Recall $k \in [n_0+1,\ n_0+(P+1)(B_s+1)]$ in (4.22). For now, consider $k = n_0 + 1$, then from (4.22) we have

$$M(n_0) - x^l(n_0+2) \geq c_1^l(M(n_0) - x^l(n_0+1)) + \beta_1 \Theta T^2. \tag{4.23}$$

Since (4.21) gives

$$M(n_0) - x^l(n_0+1) \geq c_1^l(M(n_0) - x^l(n_0)) + \beta_1 \Theta T^2$$

we have from (4.23) that

$$M(n_0) - x^l(n_0+2) \geq (c_1^l)^2(M(n_0) - x^l(n_0)) + c_1^l \beta_1 \Theta T^2 + \beta_1 \Theta T^2.$$

Repeating this procedure for all $k \in [n_0+1,\ n_0+(P+1)(B_s+1)]$ and using the facts that $c_1 \leq c_1^l \leq 2 - k_d T < 1$ and $\beta_1 < 0$, we have

$$\begin{aligned} M(n_0) - x^l(k+1) &\geq (c_1^l)^{(P+1)(B_s+1)+1}(M(n_0) - x^l(n_0)) + \sum_{z=0}^{(P+1)(B_s+1)} (c_1^l)^z \beta_1 \Theta T^2 \\ &\geq c_1^{(P+1)(B_s+1)+1}(M(n_0) - x^l(n_0)) + \sum_{z=0}^{(P+1)(B_s+1)} (2 - k_d T)^z \beta_1 \Theta T^2 \\ &= c_1^{(P+1)(B_s+1)+1}(M(n_0) - x^l(n_0)) \\ &\quad + \frac{1 - (2 - k_d T)^{(P+1)(B_s+1)+1}}{1 - (2 - k_d T)} \beta_1 \Theta T^2 \end{aligned}$$

where in the last step we used the fact that for a geometric series, with $c \in (0,1)$, the sum

$$\sum_{z=0}^{m} c^z = (1-c^{m+1})/(1-c). \tag{4.24}$$

This proves the first part of the Lemma. The second part is proven similarly. ■

So far we have shown that in an n_0-indexed time slot $\mathcal{K}_0$, the position trajectory of any agent $l \in \mathcal{D}$ is bounded in terms of $M(n_0)$, $m(n_0)$, $x^l(n_0)$ and system parameters. In the next Lemma, we will show that for the same agent l as in Lemma 7, for any agent $i \in \mathcal{N}$ there exists a $p \in \{0,1,\ldots,P\}$ and correspondingly, an n_0-indexed fixed-length time slot $\mathcal{K}_p \subseteq \mathcal{K}_0$, such that in $\mathcal{K}_p$ the position trajectory of agent i is bounded in terms of $M(n_0)$, $m(n_0)$, $x^l(n_0)$ and system parameters, n_0 as defined in Lemma 7.

Lemma 8: *If Assumptions 1 and 2 hold, then for every $p \in \{0,1,\ldots,P\}$, there exists some α_p such that for every $k \in \mathcal{K}_p = [n_0 + p(B_s+1),\ n_0 + (P+1)(B_s+1)]$, with $n_0 \in \mathcal{Z}^+$, and for every $i \in D_p$, we have*

$$\begin{aligned} x^i(k+1) &\leq M(n_0) - \alpha_p \left(M(n_0) - x^l(n_0)\right) - \gamma_p \Theta T^2 \\ x^i(k+1) &\geq m(n_0) + \alpha_p \left(x^l(n_0) - m(n_0)\right) + \gamma_p \Theta T^2. \end{aligned} \tag{4.25}$$

where $\alpha_p = c_3^p \alpha$ and $\gamma_p = c_3^p \beta_1 \gamma + \sum_{z=0}^{p-1} c_3^z \beta_2$ (and particularly, $\gamma_0 = \beta_1 \gamma$), with α, β_1 and γ as defined in Lemma 7, and $\beta_2 = -(1-k_v T)(P+1)(B_s+1) - 2 + k_d T < 0$.

Proof: We show this by induction. From Lemma 7, obviously this holds for $p = 0$ case, where $i = l$ and $D_0 = \{l\}$. Suppose it holds for the case of $p = p'$, $1 \leq p' < P$, then we need to show that it also holds for any $i \in D_{p'+1}$. By Assumption 2, for any $i \in D_{p'+1}$ there must exist some $i' \in D_{p'}$ such that $i' \in \Pi^i$. Note that for i', by the

induction hypothesis, it satisfies

$$x^{i'}(k'+1) \leq M(n_0) - \alpha_{p'}\left(M(n_0) - x^l(n_0)\right) - \gamma_{p'}\Theta T^2 \tag{4.26}$$

where $k' \in \mathcal{K}_{p'} = [n_0 + p'(B_s+1),\ n_0 + (P+1)(B_s+1)]$.

Now, for $k \in \mathcal{K}_{p'+1} = [n_0 + (p'+1)(B_s+1),\ n_0 + (P+1)(B_s+1)]$, we have from (4.12)

$$\begin{aligned}
M(n_0) - x^i(k+1) &= c_1^i(M(n_0) - x^i(k)) + c_2^i(M(n_0) - x^i(k-1)) \\
&\quad + c_3 \sum_{j\in\Pi^i}\left(M(n_0) - x^j(k-\tau_j^i)\right) \\
&\quad + c_4 \sum_{j\in\Pi^i}\left(M(n_0) - x^j(k-1-\tau_j^i)\right) \\
&\quad - \psi^i(k-1)T^2 + k_f\nabla J^i(k-1)T^2 - \delta^i(k-1)T^2 \\
&\geq c_1^i(M(n_0) - M(k)) + c_2^i(M(n_0) - M(k-1)) \\
&\quad + c_3 \sum_{j\in\Pi^i, j\neq i'}\left(M(n_0) - M(k-\tau_j^i)\right) \\
&\quad + c_3(M(n_0) - x^{i'}(k-\tau_{i'}^i)) \\
&\quad + c_4 \sum_{j\in\Pi^i}\left(M(n_0) - M(k-1-\tau_j^i)\right) - \Theta T^2.
\end{aligned}$$

Since $k \in \mathcal{K}_{p'+1}$, $n_0 < k - \tau_j^i$ for all possible τ_j^i. By Lemma 6,

$$\begin{aligned}
M(n_0) - x^i(k+1) &\geq c_1^i(n_0-k)\Theta T^2 + c_2^i(n_0-k+1)\Theta T^2 \\
&\quad + c_3 \sum_{j\in\Pi^i, j\neq i'} (n_0 - k + \tau_j^i)\Theta T^2 \\
&\quad + c_3(M(n_0) - x^{i'}(k-\tau_{i'}^i)) \\
&\quad + c_4 \sum_{j\in\Pi^i} (n_0 - k + 1 + \tau_j^i)\Theta T^2 - \Theta T^2 \\
&\geq c_3(M(n_0) - x^{i'}(k-\tau_{i'}^i)) + [c_1^i(n_0-k) + c_2^i(n_0-k+1) \\
&\quad + c_3(N^i - 1)(n_0-k) + c_4 N^i(n_0-k+1) - 1]\Theta T^2 \\
&= c_3(M(n_0) - x^{i'}(k-\tau_{i'}^i)) + \left[(c_1^i + c_2^i + c_3 N^i + c_4 N^i)(n_0-k)\right. \\
&\quad \left. + c_2^i - c_3(n_0-k) + c_4 N^i - 1\right]\Theta T^2 \\
&= c_3(M(n_0) - x^{i'}(k-\tau_{i'}^i)) + \left[(n_0-k) + c_2^i - c_3(n_0-k)\right. \\
&\quad \left. + c_4 N^i - 1\right]\Theta T^2 \\
&= c_3(M(n_0) - x^{i'}(k-\tau_{i'}^i)) + [(1-k_v T)(n_0-k) \\
&\quad -2 + k_d T]\,\Theta T^2.
\end{aligned}$$

Note that $k \in \mathcal{K}_{p'+1}$, so $n_0 - k \geq -(P+1)(B_s+1)$, and thus, the above equation can be written as

$$M(n_0) - x^i(k+1) \geq c_3(M(n_0) - x^{i'}(k-\tau_{i'}^i)) + \beta_2 \Theta T^2. \tag{4.27}$$

Let $\tilde{k} = k' + 1$. Recall $k' \in \mathcal{K}_{p'}$, then $\tilde{k} \in \tilde{\mathcal{K}}_{p'} = [n_0 + p'(B_s+1) + 1, n_0 + (P+1)(B_s + 1) + 1]$. Rewrite (4.26) as

$$M(n_0) - x^{i'}(\tilde{k}) \geq c_3^{p'}\alpha\left(M(n_0) - x^l(n_0)\right) + c_3^{p'}\beta_1\gamma\Theta T^2 + \sum_{z=0}^{p'-1} c_3^z \beta_2 \Theta T^2. \tag{4.28}$$

By assumption, $k \in \mathcal{K}_{p'+1} = [n_0 + (p'+1)(B_s+1),\ n_0 + (P+1)(B_s+1)]$, therefore in (4.27) we have $k - \tau_{i'}^i \in \tilde{\mathcal{K}}_{p'+1} = [n_0 + p'(B_s+1) + 1, n_0 + (P+1)(B_s+1)] \subset \tilde{\mathcal{K}}_{p'}$.

Since (4.28) is valid on $\tilde{\mathcal{K}}_{p'}$, it must also be valid on $\tilde{\mathcal{K}}_{p'+1}$. Thus, we can plug (4.28) into (4.27) directly by replacing $x^{i'}(\tilde{k})$ with $x^{i'}(k-\tau^i_{i'})$, and this gives

$$\begin{aligned} M(n_0) - x^i(k+1) &\geq c_3^{p'+1}\alpha(M(n_0) - x^l(n_0)) + c_3^{p'+1}\beta_1\gamma\Theta T^2 + \sum_{z=0}^{p'} c_3^z\beta_2\Theta T^2 \\ &= \alpha_{p'+1}(M(n_0) - x^l(n_0)) + \gamma_{p'+1}\Theta T^2. \end{aligned}$$

This proves the first part of the Lemma. The second part is proven similarly. ■

Intuitively, Lemma 7 means that if agent $l \in \mathcal{D}$ has its position and velocity changed at any time step $n_0 \in \mathcal{Z}^+$, then its position trajectory will be affected by that change thereafter since it can sense its own information without delay, while in comparison, Lemma 8 means, when agent l changes its position and velocity at n_0, for an agent $i \in \mathcal{D}_p$ (meaning it is p arcs away from agent l on the topology), possibly it cannot be affected by this change until time step $n_0 + p(B_s + 1)$ since the sensing delay on each arc could be up to $B_s + 1$ steps. (Note that it is "$B_s + 1$" instead of "B_s" because our system is a second-order one. In other words, if we were dealing with a first-order system, then it will be "B_s.") Take the system in Figure 4.1 for example. If we choose $l = 1$, then for agent 3, (4.25) holds on the time slot $\mathcal{K}_2$ since agent 3 is two arcs away from the "distinguished" agent 1 (so $3 \in \mathcal{D}_2$) and thus, it may take up to a $2(B_s + 1)$-time-step delay for the changes in position and velocity of agent 1 (happened at n_0) to affect agent 3.

Notice that $\mathcal{K}_P \subset \mathcal{K}_{P-1} \subset \ldots \subset \mathcal{K}_0$. Thus, given an agent $l \in \mathcal{D}$, Lemma 8 holds in time slot $\mathcal{K}_P$ for any agent $i \in \mathcal{N}$. This means that with respect to agent l, the position trajectory of any agent $i \in \mathcal{N}$ is bounded in $\mathcal{K}_P$ in terms of $M(n_0)$, $m(n_0)$, $x^l(n_0)$, and system parameters. This gives us the following Lemma, which,

as we stated earlier, shows that $M(k) - m(k)$ decreases at the rate of a geometric progression, but with some "perturbation" term.

Lemma 9: *If Assumptions 1 and 2 hold, then for every $n_0 \in \mathcal{Z}^+$, we have*

$$\begin{aligned} & M(n_0 + (P+1)(B_s+1)+1) - m(n_0 + (P+1)(B_s+1)+1) \\ \leq \; & (1 - c_3^P \alpha)(M(n_0) - m(n_0)) + 2\beta\Theta T^2 \end{aligned} \tag{4.29}$$

where $\beta = \max\{-\gamma_0, -\gamma_P\} > 0$, with γ_p defined in Lemma 8.

Proof: We first show that $\beta = \max_{0\leq p\leq P}\{-\gamma_p\}$. To see this, pick any $p \in \{1, \ldots, P-1\}$, then from the parameters defined in Lemma 8 and (4.24)

$$\begin{aligned} \gamma_{p+1} - \gamma_p &= \left(c_3^{p+1}\beta_1\gamma + \frac{1-c_3^{p+1}}{1-c_3}\beta_2\right) - \left(c_3^p\beta_1\gamma + \frac{1-c_3^p}{1-c_3}\beta_2\right) \\ &= c_3^p(c_3-1)\beta_1\gamma + \frac{c_3^p(1-c_3)}{1-c_3}\beta_2 \\ &= c_3^p\left((c_3-1)\beta_1\gamma + \beta_2\right). \end{aligned}$$

Since $\gamma_0 = \beta_1\gamma$ and $\gamma_1 = c_3\beta_1\gamma + \beta_2$, we have

$$\gamma_{p+1} - \gamma_p = c_3^p\left(\gamma_1 - \gamma_0\right).$$

Thus, if $\gamma_1 \geq \gamma_0$, then $\gamma_{p+1} \geq \gamma_p$ for all $p \in \{1, \ldots, P-1\}$ and $\gamma_P = \max_{0\leq p\leq P}\{\gamma_p\}$ and $\gamma_0 = \min_{0\leq p\leq P}\{\gamma_p\}$. If $\gamma_1 < \gamma_0$, then $\gamma_0 = \max_{0\leq p\leq P}\{\gamma_p\}$ and $\gamma_P = \min_{0\leq p\leq P}\{\gamma_p\}$. Therefore,

$$\beta = \max\{-\gamma_0, -\gamma_P\} = \max_{0\leq p\leq P}\{-\gamma_p\}.$$

Note that $\beta > 0$ since $\gamma_p < 0$ for all p.

Now, given $\mathcal{K}_P = [n_0 + P(B_s+1),\ n_0 + (P+1)(B_s+1)]$, for every $n_0 \in \mathcal{Z}^+$ we have by the definition of $M(k)$

$$M(n_0 + (P+1)(B_s+1)+1) = \max_{i\in\mathcal{N}}\left\{\max_{k\in\mathcal{K}_P}\{x^i(k+1)\}\right\}.$$

Note that for each $x^i(k+1)$, $i \in \mathcal{N}$ and $k \in \mathcal{K}_P$, from Lemma 8 we have for any fixed $l \in \mathcal{D}$ that

$$x^i(k+1) \leq M(n_0) - c_3^P \alpha(M(n_0) - x^l(n_0)) + \beta\Theta T^2 \tag{4.30}$$

where we used the facts that $c_3^P \alpha = \min_{0\leq p\leq P}\{\alpha_p\}$ and $\beta = \max_{0\leq p\leq P}\{-\gamma_p\}$. Therefore

$$M(n_0 + (P+1)(B_s+1)+1) \leq M(n_0) - c_3^P \alpha(M(n_0) - x^l(n_0)) + \beta\Theta T^2.$$

Similarly,

$$m(n_0 + (P+1)(B_s+1)+1) \geq m(n_0) + c_3^P \alpha(x^l(n_0) - m(n_0)) - \beta\Theta T^2.$$

Subtracting these two equations, we obtain

$$\begin{aligned} & M(n_0 + (P+1)(B_s+1)+1) - m(n_0 + (P+1)(B_s+1)+1) \\ \leq\ & (1 - c_3^P \alpha)(M(n_0) - m(n_0)) + 2\beta\Theta T^2. \end{aligned}$$

■

Note that $2\beta\Theta T^2$ is only affected by system parameters, sensing errors and resource profiles and thus, is bounded. So from (4.29), intuitively we can see that when $M(n_0) - m(n_0)$ is sufficiently large, the first term on the right hand side of (4.29) will dominate the second term and thus, $M(n_0) - m(n_0)$ will decrease in time. Next, we will quantify this idea and provide a uniform ultimate bound on the position trajectories.

4.3.3 Cohesion: Uniform Ultimate Boundedness and Exponential Stability

Before we proceed, we define an error coordinate system. Let

$$\bar{x}(k) = \frac{1}{N(B_s+2)} \sum_{i=1}^{N} \sum_{j=1}^{B_s+2} x^{ij}(k) = \frac{1}{N(B_s+2)} \sum_{i=1}^{N} \sum_{\tau=0}^{B_s+1} x^{i}(k-\tau) \tag{4.31}$$

be the averaged centroid position of all the agents during the last B_s+2 time steps, with $x^{ij}(k)$ as defined in (4.13). By definition, $m(k) \leq \bar{x}(k) \leq M(k)$. Define $e^{ij}(k) = x^{ij}(k) - \bar{x}(k) = x^{i}(k-j+1) - \bar{x}(k) \in \Re^n$ as the position error (i.e., relative displacement) of agent i with respect to $\bar{x}(k)$ at time step $k-j+1$, with $i \in \mathcal{N}$ and $j \in \mathcal{B}$. Thus, e_l^{ij}, $l = 1, \ldots, n$, is the lth component of the error vector. In this error coordinate system, we define $E(k) \in \mathcal{E} = \Re^{Nn \times (B_s+2)}$ for the system as

$$E(k) = \begin{bmatrix} e^{11}(k) & e^{12}(k) & \ldots & e^{1(B_s+2)}(k) \\ e^{21}(k) & e^{22}(k) & \ldots & e^{2(B_s+2)}(k) \\ \vdots & \vdots & & \vdots \\ e^{N1}(k) & e^{N2}(k) & \ldots & e^{N(B_s+2)}(k) \end{bmatrix}.$$

In this error coordinate system, define the set

$$\mathcal{E}_0 = \left\{ E(k) \in \mathcal{E} : \; e_l^{ij} = 0, \; i \in \mathcal{N}, j \in \mathcal{B}, 1 \leq l \leq n \right\} = \left\{ \mathbf{0}^{Nn \times (B_s+2)} \right\}. \tag{4.32}$$

Let $\rho : \mathcal{E} \times \mathcal{E} \to \Re^+$ denote a metric on $\mathcal{E}$ and $\rho(E(k), \mathcal{E}_0)$ be the distance between $E(k)$ and the set $\mathcal{E}_0$. Since $\mathcal{E}_0$ has only one element, and it is the zero element, a valid choice for the metric is

$$\rho(E(k), \mathcal{E}_0) = \max_{1 \leq l \leq n} \left\{ \max_{i \in \mathcal{N}} \left\{ \max_{j \in \mathcal{B}} \left\{ \left| e_l^{ij}(k) \right| \right\} \right\} \right\}. \tag{4.33}$$

For convenience, we collect some relevant parameters from Lemma 7, 8 and 9:

(Lemma 7) $\alpha = c_1^{(P+1)(B_s+1)+1}$, $\beta_1 = (1 - k_v N T - k_d T)(P+1)(B_s+1) - 2 + k_d T < 0$, and $\gamma = [1 - (2 - k_d T)^{(P+1)(B_s+1)+1}]/(k_d T - 1)$, with $\gamma > 1$.

(Lemma 8) $\gamma_p = c_3^p\beta_1\gamma + \sum_{z=0}^{p-1} c_3^z\beta_2$ for $p \in \{0, 1, \ldots, P\}$ (and particularly, $\gamma_0 = \beta_1\gamma$), with $\beta_2 = -(1 - k_vT)(P + 1)(B_s + 1) - 2 + k_dT < 0$.

(Lemma 9) $\beta = \max\{-\gamma_0, -\gamma_P\} > 0$.

Next, we present our main results, which indicate that the system trajectories are uniformly ultimately bounded in the error coordinate system, and that under certain conditions the set of zero interagent distances is exponentially stable. We show this via a general Lyapunov approach like that in [59].

Theorem 7: *Given a multiagent system described by (4.12), if Assumptions 1 and 2 hold, then the trajectories of (4.12) are uniformly ultimately bounded in the error coordinate system. Let*

$$\eta = 2\left(\frac{\beta}{c_3^P\alpha - \epsilon} + (P + 1)(B_s + 1) + 1\right)$$

where α is defined in Lemma 7, β is defined in Lemma 9, and ϵ is any constant such that $0 < \epsilon < c_3^P\alpha < 1$. Let $W(k) = M(k) - m(k)$ and $l'(k) = \arg\max_{1\leq l\leq n}\{W_l(k)\}$. Then, there exists a finite $k^0 \in \mathcal{Z}^+$ such that

$$W_{l'(k)}(k) = M_{l'(k)}(k) - m_{l'(k)}(k) < \eta\Theta_0T^2 + \theta \tag{4.34}$$

for all $k \geq k^0$, with $\Theta_0 = \psi_0 + k_f\Lambda_0 + \Delta_0$ and $\theta > 0$ any positive real number. In particular, $k^0 = \max_{1\leq l\leq n}\{k_l^0\}$, where

$$k_l^0 = \begin{cases} 0, & \text{if } W_l(0) < c_\epsilon + \theta \\ \left\lceil \log_{1-\epsilon}\left(\frac{c_\epsilon+\theta}{W_l(0)}\right)\right\rceil c_0, & \text{otherwise} \end{cases}$$

with $c_0 = (P + 1)(B_s + 1) + 1$ and $c_\epsilon = 2\beta\Theta_0T^2/(c_3^P\alpha - \epsilon)$.

Proof: We employ a Lyapunov stability theoretic approach to prove this theorem. Choose Lyapunov function $V(k) = W_{l'(k)}(k)$. Obviously, $l'(k)$ is time-varying, which

is allowed in the following analysis. In the error coordinate system, we have

$$\begin{aligned} W(k) &= \max_{i,j}\left\{x^{ij}(k)-\bar{x}(k)\right\}-\min_{i,j}\left\{x^{ij}(k)-\bar{x}(k)\right\} \\ &= \max_{i,j}\left\{e^{ij}(k)\right\}-\min_{i,j}\left\{e^{ij}(k)\right\} \end{aligned}$$

and thus,

$$\begin{aligned} V(k) &= \max_{l}\left\{\max_{i,j}\left\{e_l^{ij}(k)\right\}-\min_{i,j}\left\{e_l^{ij}(k)\right\}\right\} \\ &= \max_{i,j}\left\{e_{l'(k)}^{ij}(k)\right\}-\min_{i,j}\left\{e_{l'(k)}^{ij}(k)\right\}. \end{aligned}$$

Next, we show $V(k)$ is bounded from above and below by two $\mathcal{KR}$ functions[1]. Since

$$\begin{aligned} \max_{i,j}\left\{\left|e^{ij}(k)\right|\right\} &\geq \max_{i,j}\left\{x^{ij}(k)-\bar{x}(k)\right\} = M(k)-\bar{x}(k) \\ \max_{i,j}\left\{\left|e^{ij}(k)\right|\right\} &\geq \max_{i,j}\left\{\bar{x}(k)-x^{ij}(k)\right\} = \bar{x}(k)-m(k) \end{aligned}$$

with $|\cdot|$ a componentwise absolute value, we have $M(k)-m(k) \leq 2\max_{i,j}\{|e^{ij}(k)|\}$. Then, by the definition of $V(k)$ and (4.33)

$$V(k) = M_{l'(k)}(k)-m_{l'(k)}(k) \leq 2\max_{i,j}\left\{\left|e_{l'(k)}^{ij}(k)\right|\right\} \leq 2\max_{i,j,l}\left\{\left|e_l^{ij}(k)\right|\right\} = 2\rho\left(E(k),\mathcal{E}_0\right).$$

Also by definition, $\rho(E(k),\mathcal{E}_0) \leq M_{l'(k)}(k)-m_{l'(k)}(k)$. In summary, we have

$$\rho(E(k),\mathcal{E}_0) \leq V(k) \leq 2\rho(E(k),\mathcal{E}_0). \tag{4.35}$$

Next, we will show that for arbitrary l, $1 \leq l \leq n$, there exists a finite $k_l^0 \in \mathcal{Z}^+$ such that $W_l(k) < \eta\Theta_0 T^2+\theta$ for all $k \geq k_l^0$. To do this, we first show that there must exist a finite k_l^0 such that $W_l(k_l^0) < c_\epsilon+\theta$, with $c_\epsilon = 2\beta\Theta_0 T^2/(c_3^P\alpha-\epsilon)$ as defined

[1]Consider a continuous function $f:\Re^+\to\Re^+$. If $f(0)=0$, f is strictly increasing on $[0,\infty)$, and $\lim_{r\to\infty} f(r)=\infty$, then f is said to belong to class $\mathcal{KR}$ [59].

earlier. Obviously, $c_\epsilon \leq \eta\Theta T^2$. Since $c_0 = (P+1)(B_s+1)+1$, from Lemma 9, we have for all $k \geq 0$,

$$W(k+c_0) \leq (1-c_3^P\alpha)W(k) + 2\beta\Theta T^2.$$

Notice that $\Theta = \Theta_0\mathbf{1}_n$, we have for each l

$$W_l(k+c_0) \leq (1-c_3^P\alpha)W_l(k) + 2\beta\Theta_0 T^2. \tag{4.36}$$

If $W_l(k) \geq c_\epsilon$, we have from (4.36) that

$$W_l(k+c_0) \leq (1-\epsilon)W_l(k). \tag{4.37}$$

Since $0 < \epsilon < c_3^P\alpha < 1$, given arbitrary $\theta > 0$, there must exist a finite $k_l^0 \in \mathcal{Z}^+$ such that $W_l(k_l^0) < c_\epsilon + \theta$. In particular, if $W_l(0) < c_\epsilon + \theta$, then $k_l^0 = 0$; otherwise, $W_l(0) \geq c_\epsilon + \theta$ and there exists an integer k_l such that $W_l(0)(1-\epsilon)^{k_l} < c_\epsilon + \theta$, where

$$k_l = \left\lceil \log_{1-\epsilon}\left(\frac{c_\epsilon+\theta}{W_l(0)}\right)\right\rceil \tag{4.38}$$

and thus, $k_l^0 = k_l c_0$.

Next, we prove by induction that $W_l(k) < \eta\Theta_0 T^2 + \theta$ for all intervals of $[k_l^0 + sc_0, k_l^0 + (s+1)c_0]$, $s \in \mathcal{Z}^+$. When $s = 0$, from Lemma 6 we have for all $k \in [k_l^0, k_l^0 + c_0]$

$$W_l(k) \leq W_l(k_l^0) + 2c_0\Theta_0 T^2 < \eta\Theta_0 T^2 + \theta$$

since $W_l(k_l^0) < c_\epsilon + \theta$. Suppose it holds for $s = s'$. Then for each $k \in [k_l^0 + s'c_0, k_l^0 + (s'+1)c_0]$, it must satisfy either of following two cases:

(i) $c_\epsilon \leq W_l(k) < \eta\Theta_0 T^2 + \theta$.

(ii) $0 \leq W_l(k) < c_\epsilon$.

If k is such that case (i) holds, then we have $W_l(k+c_0) \leq (1-\epsilon)W_l(k)$ from (4.37); if k is such that case (ii) holds, then we have, from Lemma 6, $W_l(k+c_0) \leq W_l(k) + 2c_0\Theta_0 T^2$. In either case, $W_l(k+c_0) < \eta\Theta_0 T^2 + \theta$, $k \in [k_l^0 + s'c_0, k_l^0 + (s'+1)c_0]$. That is, $W_l(k) < \eta\Theta_0 T^2 + \theta$ for all $k \in [k_l^0 + (s'+1)c_0, k_l^0 + (s'+2)c_0]$.

Finally, since l is picked arbitrarily, we have $V(k) = W_{l'(k)}(k) = \max_l W_l(k) < \eta\Theta_0 T^2 + \theta$ for all $k \geq k^0 = \max_{1\leq l\leq n}\{k_l^0\}$. ■

From Theorem 7 we have the following corollary.

Corollary 2 *Given a multiagent system described by (4.12), if Assumptions 1 and 2 hold, then the velocities of all the agents are uniformly ultimately bounded and there exists a finite $k^0 > 0$ such that $|v^i(k)| < \eta\Theta T + \theta/T$ for all $k \geq k^0$, with η and θ as defined in Theorem 7.*

Proof: From Theorem 7, there exists a finite $k^0 > 0$ such that $M(k) - m(k) < \eta\Theta T^2 + \theta$ for all $k \geq k^0$. By definition, $x^i(k) \geq m(k+1)$ for all i and k. Thus, we have

$$v^i(k) = \frac{x^i(k+1) - x^i(k)}{T} \leq \frac{M(k+1) - m(k+1)}{T} \leq \eta\Theta T + \frac{\theta}{T}$$

for all $k \geq k^0$ and all $i \in \mathcal{N}$. Similarly, $v^i(k) \geq -\eta\Theta T - \theta/T$. ■

For some applications, it is possible that the terms related to noise, repulsion and profile are negligible. That is, $\Theta = 0$. So, (4.12) can be rewritten as

$$x^i(k+1) = c_1^i x^i(k) + c_2^i x^i(k-1) + c_3 \sum_{j\in\Pi^i} x^j(k-\tau_j^i) + c_4 \sum_{j\in\Pi^i} x^j(k-1-\tau_j^i). \quad (4.39)$$

Then, the stability property of this system is given by the following theorem.

Theorem 8: *Given a multiagent system described by (4.39), if Assumptions 1 and 2 hold, then the set $\mathcal{E}_0$, defined in (4.32), is invariant and exponentially stable. Moreover, $v^i(k) \to 0$ for all i as $k \to \infty$.*

Proof: To see why $\mathcal{E}_0$ is invariant, note that in $\mathcal{E}_0$ we have $e_l^{ij} = 0$ for all i, j, and l. Correspondingly, $x^{i_1 j_1}(k) = x^{i_2 j_2}(k) = \bar{x}(k)$ for all $i_1, i_2 \in \mathcal{N}$ and $j_1, j_2 \in \mathcal{B}$, with $x^{ij}(k)$ defined in (4.13). Recall that $c_1^i + c_2^i + c_3 N^i + c_4 N^i = 1$, so we have from (4.39)

$$x^i(k+1) = c_1^i \bar{x}(k) + c_2^i \bar{x}(k) + c_3 \sum_{j \in \Pi^i} \bar{x}(k) + c_4 \sum_{j \in \Pi^i} \bar{x}(k) = \bar{x}(k)$$

for all i at any time step $k \in \mathcal{Z}^+$. Thus, $x^i(k+1)$ is such that all $e_l^{ij}(k+1)$ are still in $\mathcal{E}_0$. So, $\mathcal{E}_0$ is invariant.

Before we proceed, we define a Lyapunov function in the error coordinate system. As in Theorem 7, let $l'(k) = \arg\max_{1 \le l \le n} \{M_l(k) - m_l(k)\}$. Let $W(k) = M(k) - m(k)$. Choose Lyapunov function $V(k) = W_{l'(k)}(k)$. Note that by definition, if $k' \neq k$, then $W_{l'(k)}(k) \ge W_{l'(k')}(k)$. That is, at time step k, W_l gives the maximum when $l = l'(k)$, though possibly W_l reaches the maximum with some $l = l'(k') \neq l'(k)$ at some k' other than k.

To prove that $\mathcal{E}_0$ is exponentially stable, note that (4.35) holds here and we first show that $V(k)$ is nonincreasing in time. Notice when $\Theta = 0$, Lemma 6 gives $M(k+1) \le M(k)$ and $m(k+1) \ge m(k)$ and thus, $W_l(k+1) \le W_l(k)$ for all l. Therefore

$$V(k+1) = W_{l'(k+1)}(k+1) \le W_{l'(k+1)}(k) \le W_{l'(k)}(k) = V(k).$$

This means $V(k)$ is nonincreasing.

Next, we will show that there exist some constants c_v and α_v such that $\rho(E(k), \mathcal{E}_0) \le c_v \exp(-\alpha_v k) \rho(E(0), \mathcal{E}_0)$, which means $\mathcal{E}_0$ is exponentially stable. When $\Theta = 0$,

Equation (4.36) gives $W_l(k + c_0) \leq (1 - c_3^P \alpha) W_l(k)$ for all l and all $k \in \mathcal{Z}^+$. So, $W_l(c_0) \leq (1 - c_3^P \alpha) W_l(0)$ and by induction, we have for any $s \in \mathcal{Z}^+$ that

$$W_l(sc_0) \leq (1 - c_3^P \alpha)^s W_l(0).$$

Recall that $W_l(k)$ is non-increasing, so for any $k \in [sc_0, (s+1)c_0]$, and for any $s \in \mathcal{Z}^+$, we have

$$W_l(k) \leq W_l(sc_0) \leq (1 - c_3^P \alpha)^s W_l(0) \leq (1 - c_3^P \alpha)^{\frac{k}{c_0} - 1} W_l(0).$$

That is, $W_l(k) \leq c_v \exp(-\alpha_v k) W_l(0)/2$, where $c_v = 2(1 - c_3^P \alpha)^{-1}$, and $\alpha_v > 0$ is such that $\exp(-\alpha_v) = (1 - c_3^P \alpha)^{\frac{1}{c_0}}$. Such choice of α_v is feasible since $1 - c_3^P \alpha \in (0, 1)$. Since l is picked arbitrarily, by the definition of $V(k)$, we have

$$V(k) = W_{l'(k)}(k) \leq \frac{c_v}{2} \exp(-\alpha_v k) W_{l'(k)}(0) \leq \frac{c_v}{2} \exp(-\alpha_v k) W_{l'(0)}(0) = \frac{c_v}{2} \exp(-\alpha_v k) V(0).$$

Finally, since $\rho(E(k), \mathcal{E}_0) \leq V(k) \leq 2\rho(E(k), \mathcal{E}_0)$, the above equation gives

$$\rho(E(k), \mathcal{E}_0) \leq c_v \exp(-\alpha_v k) \rho(E(0), \mathcal{E}_0).$$

So far we have proven the set $\mathcal{E}_0$ is exponentially stable, which means as $k \to \infty$,

$$e_l^{ij}(k) = x_l^{ij}(k) - \bar{x}_l(k) = x_l^i(k - j + 1)(k) - \bar{x}_l(k) \to 0 \tag{4.40}$$

for all $i \in \mathcal{N}$, $j \in \mathcal{B}$, and $1 \leq l \leq n$. From (4.39) and (4.40), $x^i(k+1) \to \bar{x}(k)$ for all i. Since (4.40) holds for all l, we have $x^i(k+1) - x^{ij}(k) \to 0$ (componentwise) for all $i \in \mathcal{N}$ and $j \in \mathcal{B}$ as $k \to \infty$. Thus, as $k \to \infty$,

$$v^i(k) = \frac{x^i(k+1) - x^i(k)}{T} \to 0.$$

■

4.3.4 Discussion: Parameters, Sensing Topology, and Extensions

Effects of Parameters

Before we proceed, it should be noted that the uniform ultimate bound we obtain in (4.34) can be quite conservative since we have to take overbounds of many terms during the deduction. Therefore, one has to be careful not to be too ambitious in interpreting the results. Nevertheless, as we discuss next, the above results are still useful for providing insights into the effects of system parameters on dynamics and cohesiveness.

If Assumption 1 holds, we have $1 < k_d T < 2$ or alternatively, $1/k_d < T < 2/k_d$, meaning that when k_d is fixed, the sampling time T can be neither too large nor too small. Also, $c_3 \in (0, 1)$ gives $k_v < 1/T < k_d$. Recall that k_v is the "velocity attraction gain" and k_d is the "velocity damping gain;" hence, this means that if the damping term dominates the velocity attraction effect this could help to achieve uniform ultimate boundedness.

The parameters k_r, r_s and k_f do not affect the boundedness (i.e., Lagrange stability) of the system trajectories. Neither do the noise bounds δ_p, δ_v and δ_f and the magnitude of resource profile gradient Λ_0. But, all these parameters do affect the size of the ultimate bound on the system trajectories (if it is bounded at all). In fact, increasing these parameters could increase the uniform ultimate bound $\eta\Theta_0 T^2 + \theta$ since Θ_0 is increased. This makes sense because (i) large k_r and r_s means that the agents want to stay further away from each other, (ii) large noise amplitudes, as quantified by δ_p, δ_v, and δ_f, can distract the agents and make it harder for them to stay close, and (iii) a large profile gradient and profile tracking gain (∇J and k_f)

could aggravate the impact of time delay since it leads to large accelerations (in magnitude) of agents and thus, with the same delay magnitudes, the amount by which position information of other agents gets outdated may increase.

Note that with a repulsion term of the form defined in Equation (4.3), collision avoidance is not guaranteed. But large k_r and r_s, meaning strong repulsion effects, may help reduce collisions between the agents. Moreover, as in [35, 45, 62] it is possible to extend the results of this chapter to consider a "hard repel" case by using a different form for the repel term. Also, note that each agent can only sense its neighbors' positions, and thus the repulsion term only takes effect in this "neighborhood." In other words, if agent $j \notin \Pi^i$, then agent i will not "repel" agent j even if they are close to each other.

From the proof of Theorem 7, we have $k_l^0 = k_l c_0$ if $(c_\epsilon + \theta)/W_l(0) \in (0, 1]$, with k_l defined in (4.38). Notice that $1 - \epsilon \in (0, 1)$, so for all l, if $W_l(0)$ increases, k_l and thus, k_l^0, increases. This means that if initially the agents are spatially far away from each other, then it will take a longer time for the system trajectories to converge and enter the "ball" that has a radius quantified by $\eta\Theta_0 T^2 + \theta$. Also, if Θ_0 decreases with other parameters unchanged, then c_ϵ decreases and thus, k_l^0 increases, meaning it will take a longer time for the system trajectories to enter the "ball." This makes sense because a smaller Θ_0 quantifies a smaller radius of the "ball," and thus, more time steps are needed before the trajectories can enter it.

Corollary 2 indicates that the velocity magnitudes of all agents are bounded and their velocities can oscillate within the bound. This bound is affected by noise amplitudes, the gradient of profile, and other system parameters in a way similar to how the uniform ultimate bound on the system trajectories is affected.

The bound on the sensing delay, B_s, and the maximum number of arcs P on the positive path between any two agents in directed graph $\mathcal{G}$, do not affect the boundedness of the system trajectories. But, they may affect the ultimate bound on the system trajectories in that they affect η. To see this, first note that

$$-\gamma_0 = -\beta_1\gamma = ((-1 + k_v NT + k_d T)(c_0 - 1) + 2 - k_d T)\,\frac{1 - (2 - k_d T)^{c_0}}{k_d T - 1} > 0$$

with c_0 as defined in Theorem 7. When B_s increases, c_0 increases and thus, $-\gamma_0$ increases. Recall that $\beta = \max\{-\gamma_0, -\gamma_P\}$, so β increases as B_s increases. As a result, η increases. This means that a large B_s could lead to large ultimate bound on the system trajectories.

Note that although P affects η in a similar way as B_s does, one should not jump too quickly to the conclusion that a large P increases the bound. This is because, as discussed earlier, we overbound many terms and this leads to conservativeness. Specifically, recall that by definition, large P may mean that there are fewer neighbors (small N^i) for an agent i, which further means that the repulsion effect, quantified by ψ^i, on agent i could be small since $\psi^i \leq (N^i - 1)\exp(-1/2)k_r r_s$ from (4.6). In other words, although large P could increase the trajectory bound by increasing η, it could also decrease the trajectory bound by decreasing the upper bound of the repulsion term. Thus, without knowing the specific topology, we cannot say too much about the effect of P on the uniform ultimate bound.

In some special cases, there are no sensing delays and all the agents can sense each other, as is the case studied in [63]. Then, we have $P = 1$ and $B_s = 0$. Substituting these values into all the previous deductions, we can easily obtain a uniform ultimate bound $\eta'\Theta_0 T^2 + \theta$, which is not provided in [63]. In particular, let $\beta_1' = -2k_v NT - k_d T$,

$\gamma' = 3 - k_d T + (2 - k_d T)^2$, and $\beta_2' = -4 + 2k_v T + k_d T$. Then we have η' as follows.

$$\eta' = 2\left(\frac{\beta'}{c_3\alpha' - \epsilon} + 3\right)$$

where $\alpha' = c_1^3$ and $\beta' = \max\{-\gamma_0', -\gamma_1'\}$, with $\gamma_0' = \beta_1'\gamma'$ and $\gamma_1' = c_3\beta_1'\gamma' + \beta_2'$.

Furthermore, recall that we fixed some $l \in \mathcal{D}$ in proving Lemma 7 to 9. It should be noted that P, and thus, $\{D_p\}$, $p = 1, \ldots, P$, are generally functions of l, that is, picking a different $l \in \mathcal{D}$ could result in different P and $D_0, D_1, \ldots, D_P$. Thus, if one wants to calculate a uniform ultimate bound of the system explicitly, choosing different l (and thus, P) could result in different values of the bound. By choosing the minimum one from these values, we alleviate conservativeness on the bound.

The values of B_s and P also affect the convergence speed of the system. To see this, we assume for simplicity that Θ is so small that $2\beta\Theta T^2$ is negligible. Then (4.29) can be written as

$$M(n_0+(P+1)(B_s+1)+1) - m(n_0+(P+1)(B_s+1)+1) < (1-c_3^P\alpha)(M(n_0) - m(n_0)).$$

Note that when c_1 and c_3 are fixed, both c_3^P and $\alpha = c_1^{(P+1)(B_s+1)+1}$ decrease as P and B_s increase, meaning the system trajectory convergence speed decreases.

Theorem 8 indicates that for the multiagent system described by (4.39) a certain set is exponentially stable in the error coordinate system despite the existence of sensing delays and topology. In particular, all agents will converge to one point and ultimately stop. The effects of P and B_s on convergence speed are the same as stated above.

Note that in Assumption 1, $c_3 > 0$ and $c_4 \geq 0$ are equivalent to $c_3' = k_v NT > 0$ and $c_4' = k_p NT^2 - k_v NT \geq 0$. Inspecting c_1, c_2, c_3' and c_4' shows that all k_p and k_v

appear with "N," which means by choosing $k_p = k'_p/N$ and $k_v = k'_v/N$, Assumption 1 can be made free of N. In other words, consider the Assumption below.

Assumption 3 *Let* $c'_1 = 2 - k'_v T - k_d T$, $c'_2 = -1 - k'_p T^2 + k'_v T + k_d T$, $c'_3 = k'_v T$, *and* $c'_4 = k'_p T^2 - k'_v T$. *The parameters* k'_p, k'_v, k_d, *and* T *are such that* $c'_1 > 0$, $c'_2 > 0$, $c'_3 > 0$ *and* $c'_4 \geq 0$.

If Assumption 3 holds and if k_p and k_v are free to change by design, then Assumption 1 holds for any N ($N \geq 2$). This is because we can choose k_p and k_v such that the effect of N is counteracted and thus, satisfaction of Assumption 1 holds independent of N. Accordingly, the uniform ultimate boundedness of the system is independent of the number of agents N, presuming Assumption 2 still holds. It is not surprising that $c'_1 + c'_2 + c'_3 + c'_4 = 1$, and in particular, $c'_1 \in (0, 1)$, $c'_2 \in (0, 1)$, $c'_3 \in (0, 1)$, and $c'_4 \in [0, 1)$.

Moreover, the parameter triplet (k'_p, k'_v, k_d) such that Assumption 3 holds is nonempty for any $T > 0$. In other words, for any $\tilde{T} > 0$, there exist $\tilde{k}_p > 0$, $\tilde{k}_v > 0$, and $\tilde{k}_d > 0$ such that $\tilde{c}_1 = 2 - \tilde{k}_v \tilde{T} - \tilde{k}_d \tilde{T} > 0$, $\tilde{c}_2 = -1 - \tilde{k}_p \tilde{T}^2 + \tilde{k}_v \tilde{T} + \tilde{k}_d \tilde{T} > 0$, $\tilde{c}_3 = \tilde{k}_v \tilde{T} > 0$, and $\tilde{c}_4 = \tilde{k}_p \tilde{T}^2 - \tilde{k}_v \tilde{T} \geq 0$. To see this, first note that for a specific T, it is easy to verify that Assumption 3 holds for certain (k'_p, k'_v, k_d). For instance, given $T = 0.3$, then one valid triplet is $k'_p = 8$, $k'_v = 2$, and $k_d = 4$. Then, for an arbitrary $\tilde{T}$, simply let $\tilde{k}_p = k'_p \tilde{T}^2/T^2$, $\tilde{k}_v = k'_v \tilde{T}/T$ and $\tilde{k}_d = k_d \tilde{T}/T$, and we have $\tilde{c}_1 > 0$, $\tilde{c}_2 > 0$, $\tilde{c}_3 > 0$ and $\tilde{c}_4 \geq 0$ as expected.

Effects of Sensing Topology and Relations to a Switching Topology

It should be noted that some types of classical network topologies can easily fit into our model. For example, when their graphs are directed, (i) a *line* topology can

be characterized by $N^i = 2$ (recall $i \in \Pi^i$) for all $i \in \mathcal{N}$, $P = N - 1$, and $\mathcal{D} = \{1\}$, presuming agent 1 is one end of the topology, (*ii*) a *ring* topology can be characterized by $N^i = 2$ for all $i \in \mathcal{N}$, $P = N - 1$, and $\mathcal{D} = \mathcal{N}$, and (*iii*) a *completely connected* topology can be characterized by $N^i = N$ for all $i \in \mathcal{N}$, $P = 1$, and $\mathcal{D} = \mathcal{N}$.

As defined in Section 4.2.1, the sensing topology in our model is a fixed (time-invariant) topology coupled with sensing delays and sensing errors. Next, we relate our sensing topology to a switching topology by comparing it with that in [48], where the authors define a switching topology to study Vicsek's model [15].

First, there are similarities between both topologies. Specifically, in [48] the authors use some switching signal $\sigma(t)$ to characterize the switching topology and, for any agents i and j, agent i cannot obtain the latest information ("heading angle") of agent j when the interconnection is broken. In our sensing topology, the inclusion of time-varying sensing delays and sensing errors represents that for any agents i and j, but $j \in \Pi^i$ and $j \neq i$, there is no guarantee that agent i obtains the latest information (position and velocity) of agent j accurately. So, this captures some features observed in a switching topology. Also, to achieve convergence, it is assumed in [48] that the switching signal $\sigma(t)$ is such that the agents are "linked together" across contiguous time intervals of *arbitrary but finite* length. Basically this means the information ("heading angle") of any agent j can affect, through certain path, any agent i in a finite-length time interval. In other words, j can affect i sufficiently frequently, although i and j possibly are not directly connected. Our results in earlier parts of Section 4.3 indicate that when some assumptions are satisfied, convergence can be achieved for *arbitrary but finite* B_s, which quantifies the largest amount of information outdate. Basically, this means it must take a finite-length time for the

information (position and velocity) of j to affect i (suppose there exists a positive path from j to i) or, in other words, j can affect i sufficiently frequently, although i and j possibly are not directly connected.

There are also significant differences between our sensing topology and the one in [48]. First, the authors in [48] restrict to the topology to one characterized by some *undirected* graph, which means at any instant, if agent i can sense j, then j must be able to sense i. In our sensing topology, we allow the topology characterized by some *directed* graph, which means it is possible that agent i can sense j while j *cannot* sense i. Obviously, one can regard undirected graph as a special case of directed graph. However, to achieve this, we *require* the existence of a set of "distinguished" agents, i.e., some special type of agent. Next, for the switching topology in [48], at any time instant, agent i either senses the latest information of agent j or senses nothing about j. Our topology is different in that the sensing topology is a fixed topology, where at any time instant, agent i *always* has the potential to sense some position and velocity information about agent $j \in \Pi^i$, but such information could be always outdated (but the outdate amount is bounded). That is, it is possible that i *never* senses the latest information of j. Finally, by our definition of τ_j^i, or more explicitly, $\tau_j^i(k)$, it is possible that for $k' > k$, $k - \tau_j^i(k) > k' - \tau_j^i(k')$. (Of course, a necessary condition to have this happen is $k' - k < B_s$ since τ_j^i is bounded by B_s.) That is, suppose the position and velocity information about agent j are data indexed by k, then these data could arrive at agent i (suppose $j \in \Pi^i$) in a "shuffled" order. From our deduction, clearly this "order shuffling" phenomenon, with the constraint of $\tau_j^i \in [0, B_s]$, does not affect the uniform ultimate boundedness of the system. In comparison, the topology in [48]

does not include a time delay, so it is not immediately clear whether "order shuffling" could be allowed in that framework.

Extensions

Here, we discuss some possible generalizations of our results. First, recall that in Section 4.2.3 we assumed that, to achieve cohesion, each agent i can sense its own (absolute) position and velocity (though it only needs to measure the *relative* position and velocity of agent j, $j \in \Pi^i$). This assumption can be difficult to satisfy in certain applications. In fact, it is possible for us to relax the assumption so that each agent only needs to sense its own position and velocity information *relative* to certain "common moving base" $x_b(k)$. One possible way to do so is to choose $x_b(k) = \bar{x}(k)$, with $\bar{x}(k)$ defined in (4.31). Alternatively, one could use the idea in [59] and define $x_b(k) \in \mathcal{X}_b$, where

$$\mathcal{X}_b = \left\{ X(k) \in \Re^{Nn \times (B_s+2)} : \; x_l^{i_1 j_1}(k) = x_l^{i_2 j_2}(k), \; i_1, i_2 \in \mathcal{N}, \; j_1, j_2 \in \mathcal{B}, \; 1 \leq l \leq n \right\}$$

with $X(k)$ and $x^{ij}(k)$ defined in (4.13). Similar to Section 4.3.3, define position error $e_b^{ij}(k) = x^{ij}(k) - x_b(k)$, then we can rewrite (4.12) and study the system behaviors in this error coordinate system. In this way, there is no need for the agents to have access to any *absolute* information on positions and velocities. It should be noted that similar ideas of converting to error coordinate systems are used in [56, 57, 63].

Next, it is possible to generalize the form of control input, as given in (4.4), to accommodate a class of attraction functions that include a nonlinearity and obtain some results similar to those in [45]. In particular, consider the function $g : \Re^n \to \Re^n$, $g(x) = [g_1(x_1), g_2(x_2), \ldots, g_n(x_n)]^\top$ for $x \in \Re^n$. Suppose for all $1 \leq l \leq n$, the component function $g_l : \Re \to \Re$ is odd, continuous, and satisfies $\mu_1 \leq g_l(y)/y \leq \mu_2$

for all $y \in \Re$, $y \neq 0$, with μ_1 and μ_2 some known positive constants, and $g_l(0) = 0$. Then, the generalized control input can have the following form

$$\begin{aligned} u^i(k) &= -M_i k_p \sum_{j \in \Pi^i} g\left(\hat{x}^i(k) - \hat{x}^j(k - \tau_j^i)\right) - M_i k_v \sum_{j \in \Pi^i} g\left(\hat{v}^i(k) - \hat{v}^j(k - \tau_j^i)\right) \\ &\quad -M_i k_d \hat{v}^i(k) \\ &\quad +M_i k_r \sum_{j \in \Pi^i} \exp\left(\frac{-\frac{1}{2}\left\|\hat{x}^i(k) - \hat{x}^j(k - \tau_j^i)\right\|^2}{{r_s}^2}\right)\left(\hat{x}^i(k) - \hat{x}^j(k - \tau_j^i)\right) \\ &\quad -M_i k_f \nabla \hat{J}^i(k). \end{aligned}$$

Obviously, when $\mu_1 = \mu_2 = 1$, the equation above changes into (4.4).

Finally, it is possible to cope with gradient following and trajectory following with our model. For gradient following, the agents only try to have the gradient of their position trajectories be the same as that of the desired trajectory, $J_d(k)$, and to achieve this, we just need to change $\nabla J^i(k)$ (where for simplicity, we ignore the noise effect) in (4.4) into $-\nabla J_d^i(k)$. For trajectory following, the agents try to have their position trajectories track the desired trajectory, and to achieve this, one possible way is to replace $\nabla J^i(k)$ in (4.4) with $x^i(k) - J_d^i(k)$. As one can imagine, generally, the agent position trajectories generated by gradient following and trajectory following will both have the same *shape* as $J_d(k)$, though possibly are scaled by some factor. But, gradient following also allows some offset (or translation) on the agent position trajectories with respect to $J_d(k)$, i.e., in *location* the position trajectories of all the agents can be quite different from $J_d(k)$, though they have the same *orientation*. In comparison, trajectory following guarantees that the agent position trajectories and $J_d(k)$ are at the same location. It is clear that gradient following can be accommodated in our model without any change, and all our previous proofs hold. While for trajectory following, some changes in the control input equation (4.4) and thus,

system equation (4.12), are required, and the proofs would need to change. Nevertheless, it should be noted that with either gradient following or trajectory following, the resultant multiagent model is closely related to models of *coupled synchronization*, a phenomenon ubiquitous in nature and one that is attracting increasing research interest [64, 65, 66, 67]. In Section 4.4.2, we will show some simulation results which will help to make connections between multiagent system cohesion and synchronization.

4.4 Applications

The swarm models given in [56, 57, 63] and this chapter can have different applications. Some candidates, as indicated in [56, 57, 63], include groups of robots designed to coordinate their activities, networked cooperative UAVs developed for commercial and military purposes, platooning of vehicles in IVHS, and so on. Also, from the theory in this chapter, we can see that the idea of the agreement problem [58] is also reflected in the models. Moreover, as we stated in Section 4.3.4, the models are also related to models of synchronization. Next, we will show in Section 4.4.1 some simulations where each agent is regarded as a vehicle with second-order dynamics. The simulation results verify some of our earlier observations in Section 4.3. Then, in Section 4.4.2, we will give some simulation results on synchronization, with gradient/trajectory following included in the model, which we hope will motivate future research in understanding the relations between multiagent systems and coupled oscillators.

4.4.1 Multivehicle Cohesion

In this section, we will show some simulation results where we view the agents as vehicles. First, we show some plots related to the parameter triplet (k'_p, k'_v, k_d) in Assumption 3. As mentioned in Section 4.3.4, such a parameter set is nonempty for any $T > 0$ and our plots will show this. For comparison, we arbitrarily pick $T = 0.1$ and $T = 0.5$. The corresponding parameter surfaces are shown in Figure 4.2, with each point on the surface corresponding to a triplet. For a triplet, if none of the three components is zero, then it satisfies Assumption 3. Consider the $T = 0.1$ case in Figure 4.2(a). Obviously k_d has its valid range in $(10, 20)$, which reflects our earlier observation of $1/T < k_d < 2/T$. Similarly, $k'_p \in (0, 1/T^2) = (0, 100)$ since $c'_1 + c'_2 > 0$, and $k'_v \in (0, 1/T) = (0, 10)$ since $c'_1 + c'_2 + c'_4 > 0$.

Before we proceed, we shall specify how to construct a sensing topology with a given P since different P will be used in the following simulations. Recall that for agent i, Π^i is the set of its neighbors, and $i \in \Pi^i$. Suppose each agent i has (including itself) c_P neighbors in a "circulant" manner, that is, $\Pi^1 = \{1, 2, \ldots, c_P\}$, $\Pi^2 = \{2, 3, \ldots, c_P + 1\}$, ..., and $\Pi^N = \{N, 1, \ldots, c_P - 1\}$. Obviously, we have $\mathcal{D} = \mathcal{N}$ in this case. Choose $c_P = \lceil N/P \rceil$, then the resultant sensing topology has the desired P. Of course, other approaches, including some that allow randomly assigned connections, to construct a sensing topology such that it has the desired P, are possible.

In all the following simulations, unless otherwise stated, the system parameters are $N = 20$, $k_p = 0.2$, $k_v = 0.06$, $k_d = 6$, $k_r = 1$, $r_s = 0.8$, $k_f = 1.1$, and $T = 0.2$. The noise bounds are $\delta_p = \delta_v = \delta_f = 2\sqrt{3}$, assuming that the noise d_p^{ij}, d_v^{ij} and d_f^i are uniformly distributed and zero-mean for all $i, j \in \mathcal{N}$. Also, the profile gradient

$\nabla J = [\cos(x) + 2,\ 2\sin(y) + 4,\ 3\cos(z) + 4.5]^\top \in \Re^3$, $P = 4$, and sensing delay $B_s = 20$. All the simulations in this section are run for 350 time steps. All the agents are assigned initial positions randomly. For simplicity, their positions are kept constant for $k \leq 0$ and correspondingly, all agents have zero velocities for $k < 0$.

Figure 4.3 shows the position and velocity trajectories of the system. From Figure 4.3(a), we can see that at the beginning of the simulation, the agents appear to move around erratically. But soon, they get close to each other and move cohesively in spite of the existence of noise, sensing delays, and topology characterized by an incompletely connected graph. Figure 4.3(b) shows that the velocities of the agents oscillate but are bounded.

Figure 4.4 shows the effects of changing some parameters of the system. Specifically, Figure 4.4(a) is for the no-noise case. Obviously, the ultimate bound on the system trajectories decreases comparing to Figure 4.3(a). Figure 4.4(b) is for the case where $r_s = 2$ instead of the previously used $r_s = 0.8$, so that there are larger repulsion effects. As expected, the ultimate bound of the system trajectories increases.

Next, we illustrate the effects of P and B_s. Figure 4.5 shows the position trajectories in three dimensions versus time, with no changes on the originally given parameters (i.e., the parameters are the same as those for Figure 4.3). Figure 4.6(a) is for the case of no sensing delay ($B_s = 0$), and Figure 4.6(b) is for the case where we further have a completely connected sensing topology, i.e., $B_s = 0$ and $P = 1$. Comparing Figure 4.5 with Figure 4.6(a) and Figure 4.6(b), we can see that decreasing B_s and P helps increase convergence speed as expected.

4.4.2 Synchronization of Coupled Oscillators

In this part, we show an example where the agents, though starting with randomly assigned positions and velocities and being affected by sensing delays and topology, achieve a type of synchronization through gradient following or trajectory following, as discussed in Section 4.3.4, and slide down a spiral line in a cohesive manner. The three-dimensional spiral line, which is the desired trajectory, is defined as

$$J_d(k) = [\cos(z(k)), \sin(z(k)), z(k)]^\top \subset \Re^3$$

with $z(k) = -R_z kT$, and R_z some known positive constant. Projected onto the (x, y) plane, this is a circle and we think of each agent's position in (x, y) as representing the phase of an oscillator. To illustrate the key idea of synchronization of coupled oscillators, we remove sensing errors and interagent repulsion from the model. So, $k_r = \delta_p = \delta_v = \delta_f = 0$. Also, we let $R_z = 0.1$, $B_s = 10$, $k_f = 8.5$ for gradient following, and $k_f = 2$ for trajectory following. Other parameters, and the sensing topology, are as defined in Section 4.4.1. Simulations in this section are run for 1000 steps. The simulation results for both gradient following and trajectory following are shown below. In all the following figures, the initial and final positions of an agent are represented by a cross sign and a black dot, respectively. (Note that only one black dot is shown in the figures since they are all on top of one another.) For comparison, the plot of $J_d(k)$ is superimposed in the figures as a dashed line with square markers.

Figure 4.7 shows the results with gradient following, where each agent only tries to track the gradient of $J_d(k)$. Figure 4.7(a) shows that, although their initial positions and velocities are assigned randomly, the agents soon move together, achieve

synchronization, and slide down along a spiral line as a group. Clearly, the projection of $J_d(k)$ on (x, y) plane is simply a unit circle, with the origin its center. Since gradient following does not enforce alignment of the agent trajectories and the desired trajectory, the projection of the agent position trajectories on (x, y) plane has an offset on its center with respect to the one formed by $J_d(k)$, as shown in Figure 4.7(b). Figure 4.8 shows the results with trajectory following. Similar to the case shown in Figure 4.7, the agents manage to achieve synchronization and slide down a spiral line. As expected, the agent position trajectories and $J_d(k)$ are aligned with each other, except that the radius of their (x, y) plane projection is scaled by certain factor, which is determined by the system parameters. Overall, Figures 4.7 and 4.8 clearly illustrate the complicated nature of the dynamics of the distributed systems we are studying.

It should be noted that the synchronization shown by the above simulations is different from that found in [65, 67] since (i) the agent trajectories here initially do not have to stay on a circle in the (x, y) plane, even though ultimately they must, in order to be synchronized, and (ii) the underlying dynamics are different. Still, there are interesting analogies between the attraction terms and the sinusoidal terms in the Kuramoto model [64], and the velocity damping term along with the desired trajectory profile and the natural frequencies of the oscillators in [64].

4.5 Concluding Remarks

In this chapter we focused on a discrete-time formulation and, using a Lyapunov approach, derived stability conditions under which a multiagent system achieves cohesiveness even in the presence of (i) a fixed sensing topology, characterized by an

incompletely connected directed graph that constrains information flow, (*ii*) a random but bounded delay and "noise" in sensing other agents' positions and velocities, and (*iii*) noise in sensing a resource profile that the agents are moving on. An agent sensing topology characterized by a completely connected *undirected* graph might be easy to analyze, but may rarely be found in nature. By defining a directed graph $\mathcal{G}$ as in Section 4.2.1, we remove the requirement (as in [56]) that each agent has to be able to detect all other agents. Although Assumption 2 requires the existence of some special set $\mathcal{D}$, but it is not a strong assumption. Thus, the results in this chapter represent our progress in studying multiagent systems that demonstrate certain global "emergent" behaviors through local interactions. As discussed in Section 4.3.4, our sensing topology with time-varying sensing delays and sensing errors captures some features observed in a switching (or time-varying) topology. Thus, we view the results in this chapter as representing some progress toward establishment of stability properties of multiagent systems with a switching topology.

Finally, as explained in Section 4.3.4, our approach may also help make progress in studying the problem of synchronization of coupled oscillators with a sensing topology, time delays, and asynchronism. In fact, we hope that the ideas there will motivate the future study of relationships between multiagent system stability and synchronization.

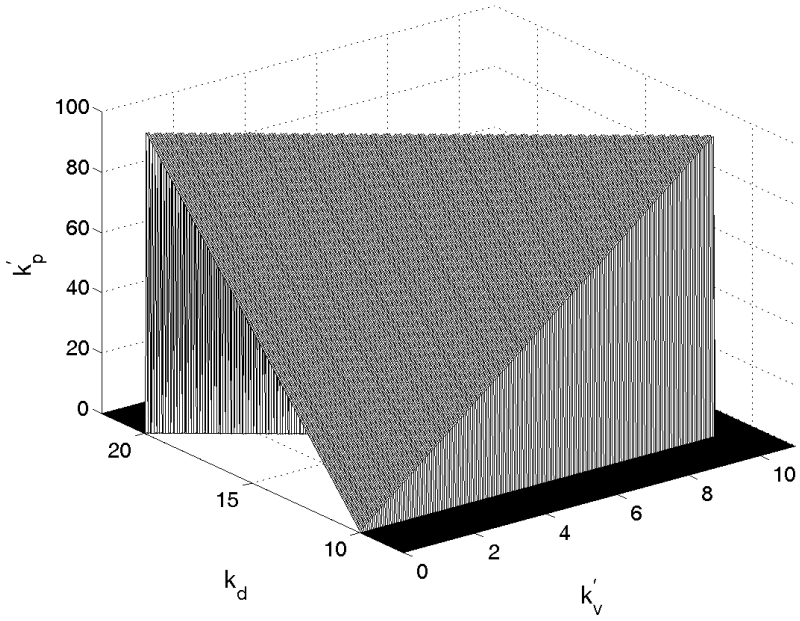

(a) $T = 0.1$.

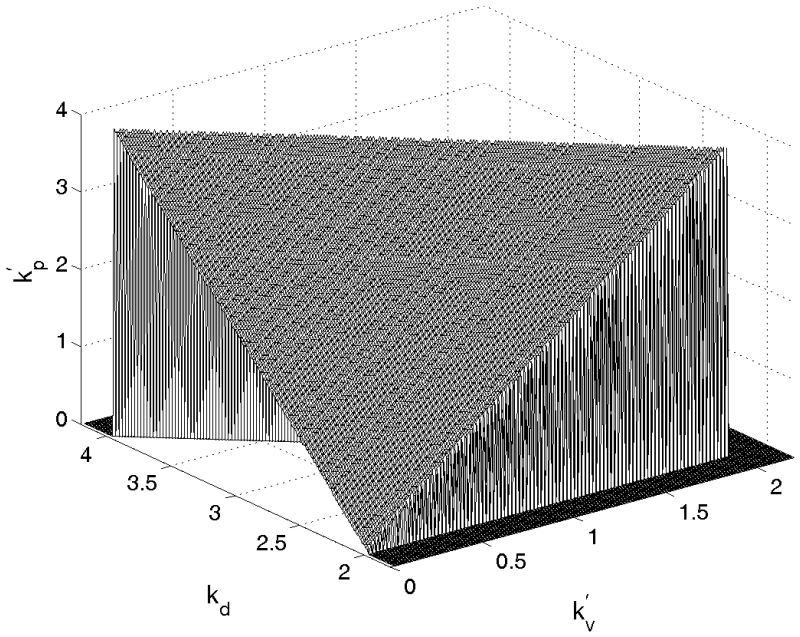

(b) $T = 0.5$.

Figure 4.2: Parameter surface qualified for Assumption 3.

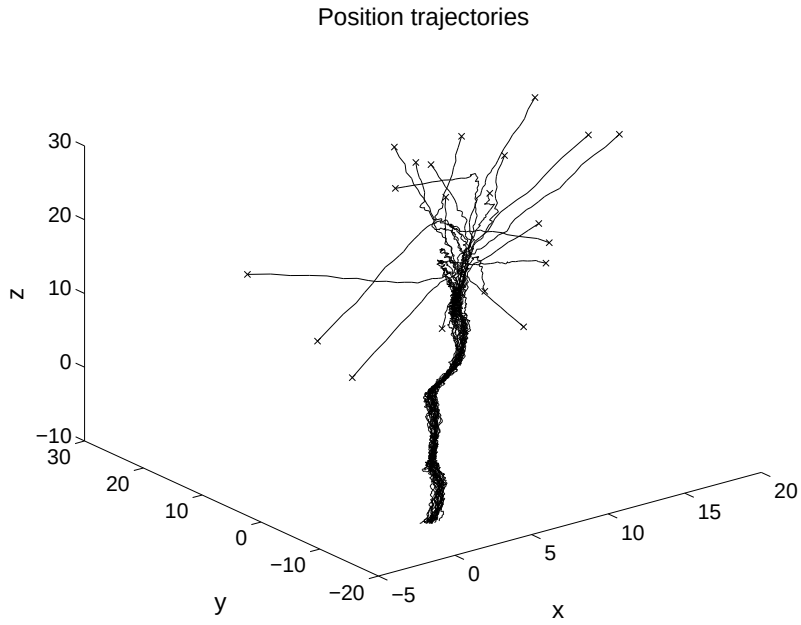

(a) Position trajectories.

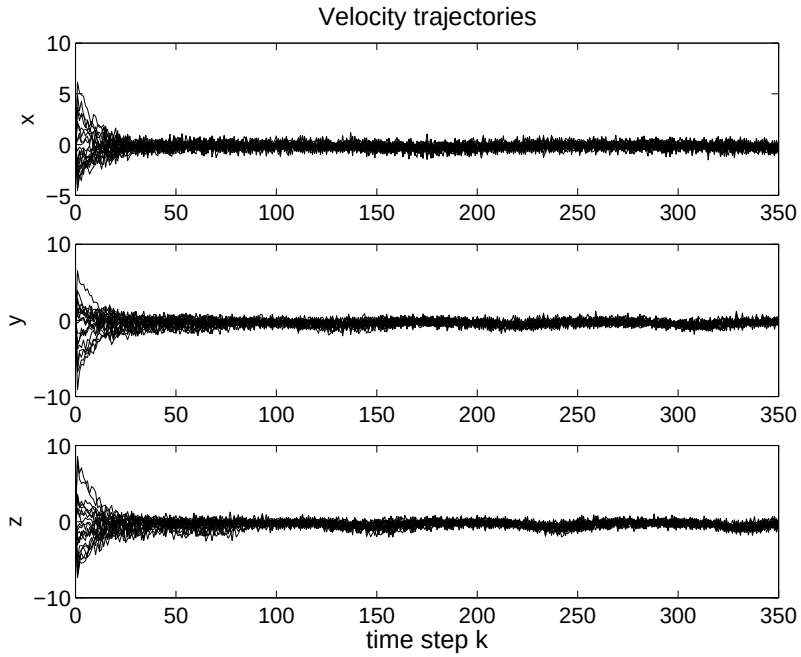

(b) Velocity trajectories.

Figure 4.3: Position and velocity trajectories ((x, y, z) denotes the three dimensions).

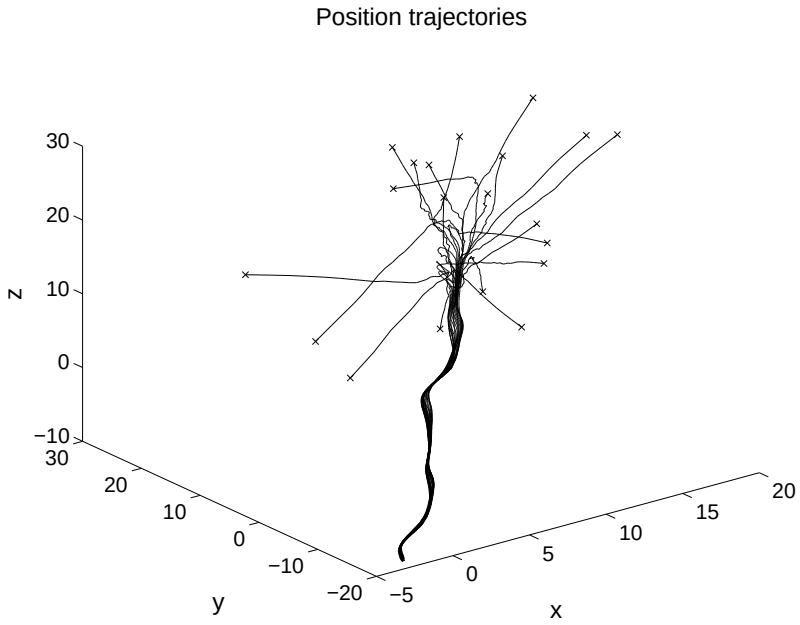

(a) No noise case.

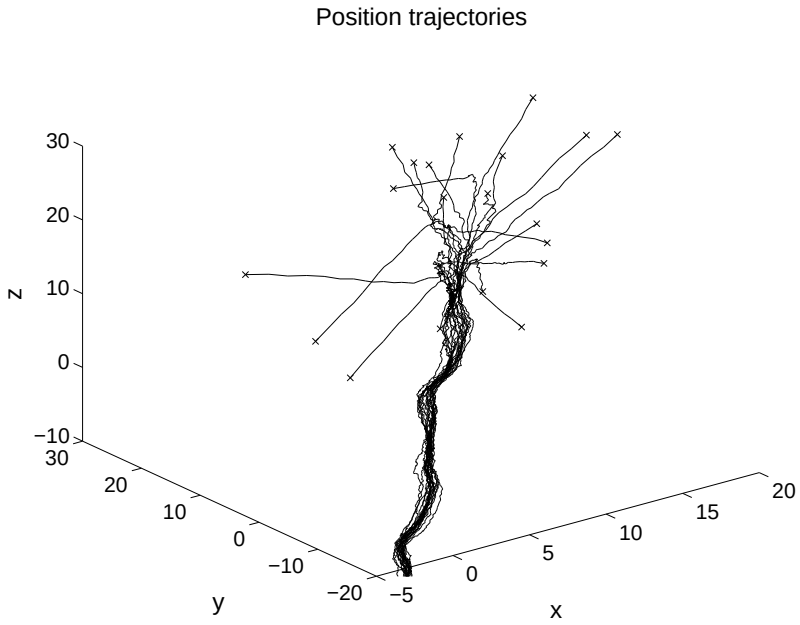

(b) Large repulsion case ($r_s = 2$).

Figure 4.4: Position and velocity trajectories ((x, y, z) denotes the three dimensions).

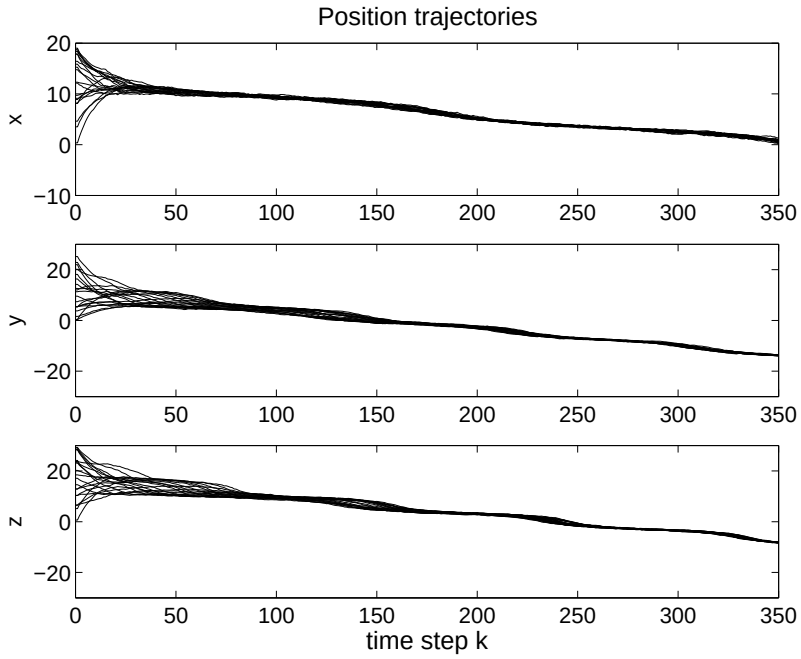

Figure 4.5: Position trajectories with no parameter changes.

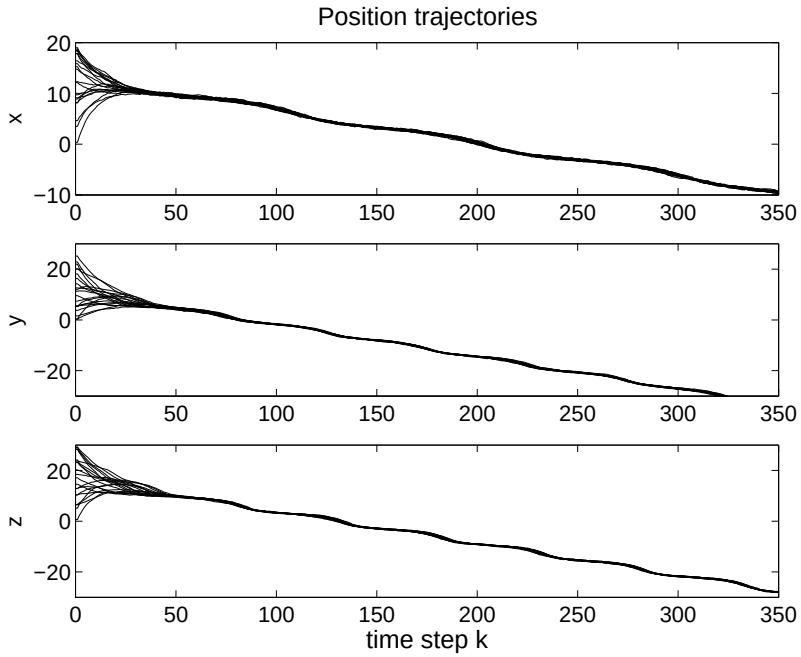

(a) No sensing delay case ($B_s = 0$).

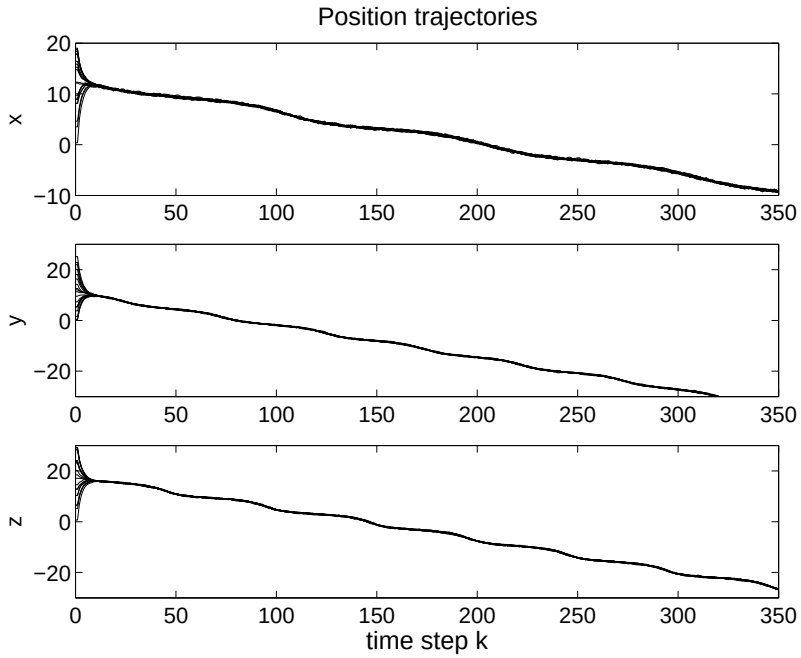

(b) Complete sensing graph ($B_s = 0$ and $P = 1$).

Figure 4.6: Position trajectories with parameter changes.

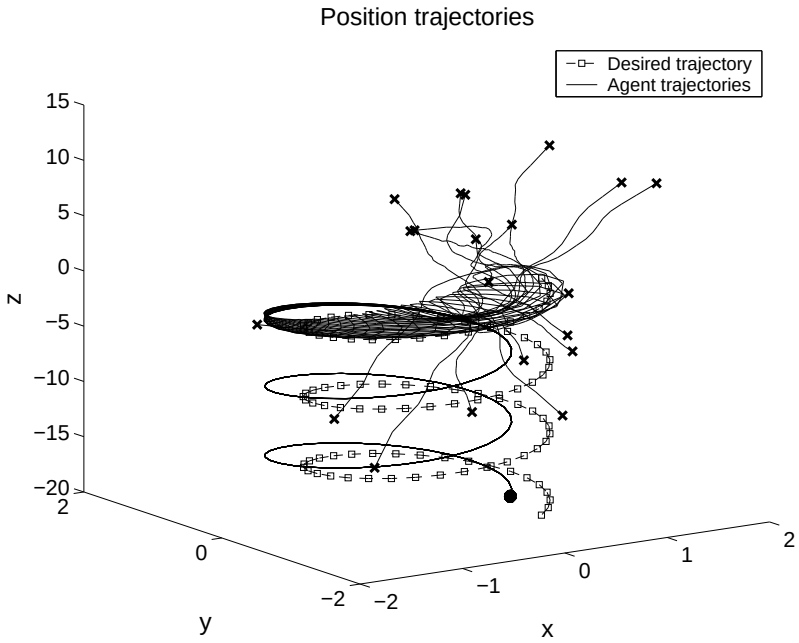

(a) Position trajectories in (x, y, z).

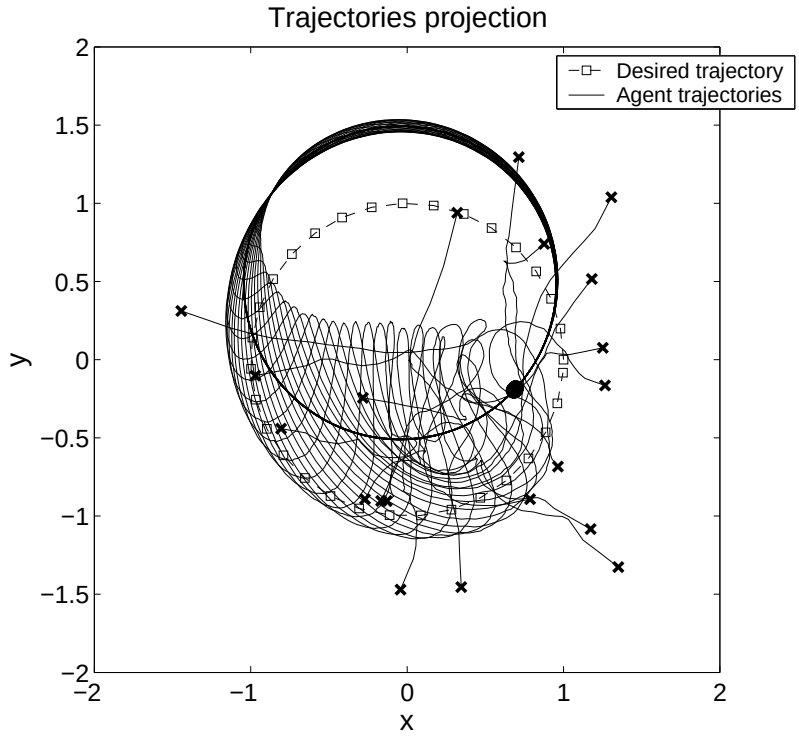

(b) Position trajectories projection to (x, y).

Figure 4.7: Position trajectories with gradient following ((x, y, z) denotes the three dimensions).

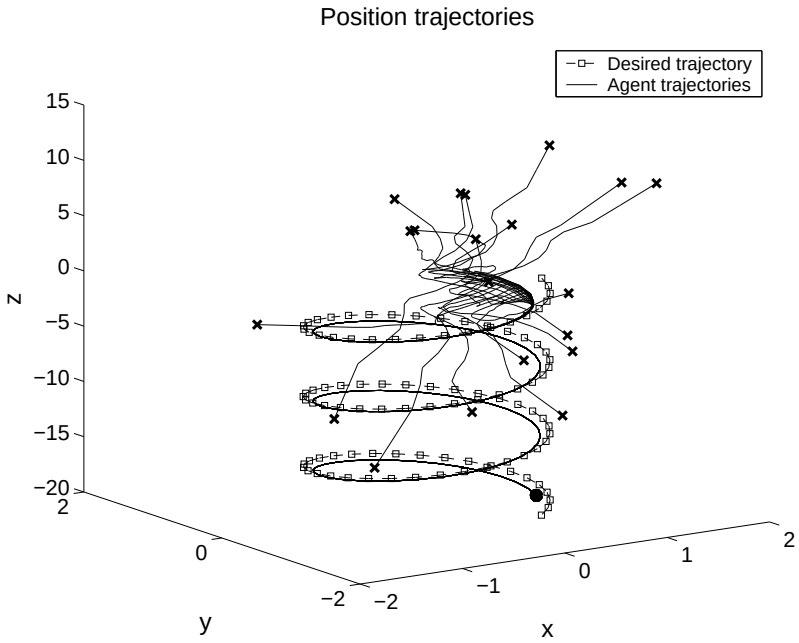

(a) Position trajectories in (x, y, z).

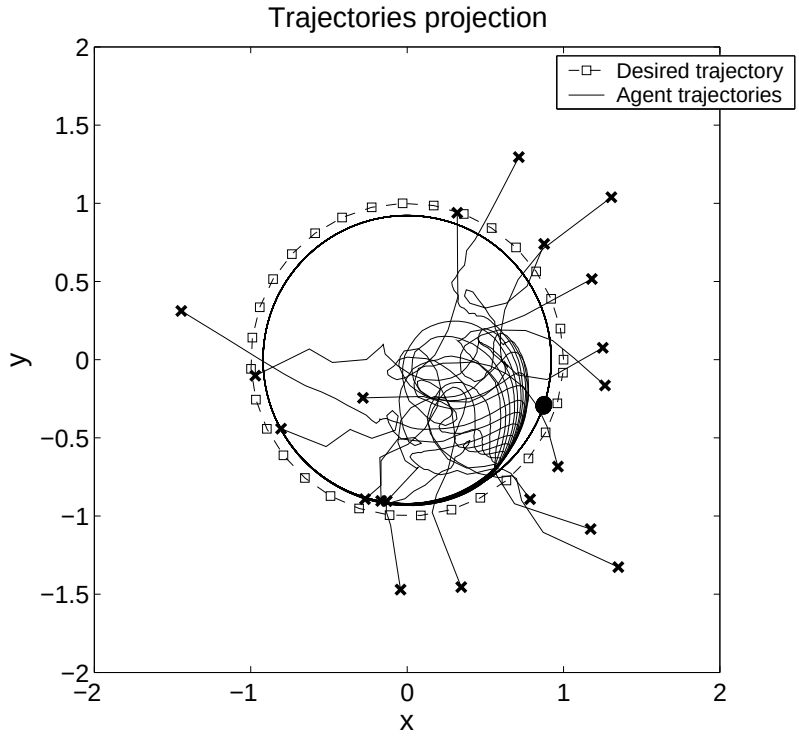

(b) Position trajectories projection to (x, y).

Figure 4.8: Position trajectories with trajectory following ((x, y, z) denotes the three dimensions).

CHAPTER 5

CONCLUSIONS

5.1 Summary of the Dissertation

The topics of this dissertation focus on mathematical modeling and analysis of stability properties of cooperative multiagent systems, which are sometimes called swarms. In particular, we characterize cohesiveness of swarms as a boundedness (or stability) property of the agents' position trajectories (set of fixed position errors, respectively) and use a Lyapunov approach to develop conditions under which local agent actions will lead to cohesive group behaviors.

In this dissertation, the motion of each swarm agent is characterized by a second-order dynamics. We show in both continuous-time and discrete-time frameworks that under certain conditions, local agent actions will lead to cohesive group behaviors in the presence of "noise" characterized by uncertainty on sensing other agent's position and velocity, and in sensing a resource profile that each agent is moving on. In particular, we assume for position and velocity that the sensing errors have a linear relationship with the magnitude of the state of the error system. The results quantify

earlier claims that social foraging is in a certain sense superior to individual foraging when noise is present, and provide clear connections between local agent-agent interactions and emergent group behavior.

Moreover, we are able to show in a discrete-time framework that swarms can stay cohesive even in the presence of (*i*) an interagent "sensing topology" that constrains information flow, where by "information flow," we mean the sensing of positions and velocities of agents of our interest, (*ii*) a random but bounded delay in sensing other agents' positions and velocities, and (*iii*) "noise" with constant bound in sensing other agents' positions and velocities, and in sensing a resource profile.

5.2 Contributions

The main contribution of this dissertation lies in that we have characterized swarm "cohesiveness" as a stability property and provided conditions under which swarms will keep cohesive even with certain information flow constraints.

Starting within the continuous-time framework, we presented a single swarm member (or, agent) model, with the motion of each agent characterized by second-order dynamics. Then, we built an n-dimensional swarm model by putting many single agents together, where the agents can be heterogeneous in that they can have different values on their system parameters, something not found in literature, e.g., [35, 44]. We have derived conditions under which social foraging swarms maintain cohesiveness and follow resource profiles even with information flow constraints, where the constraints are "noise" characterized by uncertainty on sensing other agent's position and velocity, and in sensing resource profile that each agent is moving on [56, 57]. In particular, we studied the case when for position and velocity the sensing errors have

a linear relationship with the magnitude of the state of the error system. No earlier work on swarm systems that deals with such sensing errors seems to exist.

We also investigated special types of noise and the case where all agents are identical [56, 57]. Although we only studied one type of attraction and repulsion function, the results can be extended to other classes using approaches such as the ones in [35, 45]. Moreover, while we only studied the plane profile, extensions to profiles with other shapes such as those studied in [46] are possible. In fact, any profile that is smooth and has a known bounded slope can be fit into the framework without significantly changing our major results. We also briefly analyzed the stability of the swarm error system when each agent is trying to track their respective trajectories. Our simulations illustrated advantages of social foraging in large groups relative to foraging alone since they show that a noisy resource profile can be more accurately tracked by a swarm than an individual, the so-called "Grünbaum Principle" [4, 51]. We also give some explanations on this principle through theoretical analysis, which has not been found in literature.

In this dissertation, we also studied cohesive behaviors of swarms with information flow constraints other than sensing noise. Specifically, we also considered the effects of an interagent "sensing topology," which specifies that some agents may not sense the positions and velocities of some other agents, and random but bounded sensing delays in an asynchronous discrete-time framework. The topology and delays both impose information flow constraints on the multiagent system, which significantly complicate its ability to achieve cohesive and purposeful behavior. We are able to show that under certain conditions, even with noisy measurements and the group

objective of following a resource profile, the swarm can become cohesive in the sense that interagent distances are uniformly ultimately bounded.

By defining such a sensing topology, we remove the requirement (as in [56]) that each agent has to be able to detect all other agents. Thus, the results represent our progress in studying multiagent systems that demonstrate certain global "emergent" behaviors through local interactions. Also, our sensing topology with time-varying sensing delays and sensing errors captures some features observed in a switching (or time-varying) topology. Thus, the results we obtained here represent some progress toward establishment of stability properties of multiagent systems with a switching topology including time delays. This is something, to the best of our knowledge, that has not been done by any other researchers. For instance, the authors in [48, 50] make some progress in switching topology, but no time delay is considered in their work. Moreover, the agents in their framework do not have second order dynamics like in this dissertation.

5.3 Future Directions

There are several problems that remain open in the research in this dissertation. Clearly, it would be useful to consider nonlinear models for the agents. Throughout the dissertation, we assumed the control input for each agent is determined by the system states and thus, there exists no constant bound for it. However, generally this is not the case in reality. So, it would be interesting to investigate how a control input that is saturated will affect the cohesiveness of the swarms. Also, note that the resource profile that we considered in this dissertation is a static one. It will be useful to analyze the cohesion properties of a multiagent system with dynamically

varying resource profiles. This will, for instance, allow us to handle cases of moving or "pop-up" targets and threats for multi-UAV team in the context of military applications. Moreover, we mentioned in Chapter 4 that our framework allows a form of asynchronism with a fixed T that is the same for all agents. We would like to determine whether different agents could have different sampling times, i.e., T^i, for each agent i, without affecting the stability properties of the system. This will be useful for the case when a global clock is not available to all the agents to synchronize the length of their sampling time.

Note that in comparison with the "agreement algorithm" in [58], we were not able to accommodate in Chapter 4 the case of $k \notin \mathcal{K}^i$, with which the control input could have been defined as $u_p^i(k)$ and had the following form.

$$\begin{aligned} u_p^i(k+1) &= u_p^i(k), \text{ if } k \notin \mathcal{K}^i \\ u_p^i(k+1) &= u^i(k), \text{ if } k \in \mathcal{K}^i \end{aligned} \tag{5.1}$$

with $u^i(k)$ given by (4.4). Alternatively, one could redefine (4.2) as

$$\begin{aligned} x^i(k+1) &= x^i(k) + v^i(k)T \\ v^i(k+1) &= v^i(k) + \frac{1}{M_i} u^i(k - \tau^i(k))T \end{aligned} \tag{5.2}$$

where $\tau^i(k) \in [0, B_p] \subset \mathcal{Z}^+$ quantifies some random "processing delay." Obviously, a system with control input (5.1) is a special case of one with control input (5.2). It would be interesting to determine how this "processing delay" would impact the cohesion properties of a multiagent system, as in our work, with sensing errors, sensing delays, and sensing topology. Moreover, it will help study the dynamic behaviors of a multiagent system in the *discrete-event* framework (instead of the *discrete-time* framework in this dissertation).

Our results indicated that when some assumptions are satisfied, convergence can be achieved for arbitrary but *finite* B_s. In fact, this "finiteness" of B_s corresponds to the concept of "partial asynchronism" in [58], which represents an asynchronism that is arbitrary but finite. In contrast, there is the concept of "total asynchronism" in [58], which allows a more general form of asynchronicity where the sensing delays can go to infinity, but with the information updating infinitely often. It would be useful to characterize conditions under which results like those found here would hold for this total asynchronism case.

In the dissertation, our work involving sensing topology, asynchronism and time delays was done in the discrete-time framework, and we used a Lyapunov function quantifying the maximum difference among agents' positions in our proof to obtain the results. It would be interesting to determine whether the work can be extended to a continuous-time swarm model, and with a quadratic Lyapunov function. Also, it would be useful to further extend the work presented here to include a dynamically changing topology, asynchronism, time delays, and sensing noise having linear relationship with the magnitude of the system state in an error coordinate system. To the best of our knowledge, no work, either in the continuous-time framework or in the discrete-time framework, has combined all these information flow constraints together yet.

In summary, this dissertation has presented stability analysis of swarms with information flow constraints. Future research needs to be conducted to broaden the results achieved here so that a solid theoretical foundation could be set up for the application of engineering cooperative multiagent systems.

BIBLIOGRAPHY

[1] C. M. Breder, "Equations descriptive of fish schools and other animal aggregations," *Ecology*, vol. 35, no. 3, pp. 361–370, 1954.

[2] A. Okubo, "Dynamical aspects of animal grouping: swarms, schools, flocks, and herds," *Advances in Biophysics*, vol. 22, pp. 1–94, 1986.

[3] H.-S. Niwa, "Self-organizing dynamic model of fish schooling," *Journal of Theoretical Biology*, vol. 171, pp. 123–136, 1994.

[4] D. Grunbaum, "Schooling as a strategy for taxis in a noisy environment," *Evolutionary Ecology*, vol. 12, pp. 503–522, 1998.

[5] A. Mogilner and L. Edelstein-Keshet, "A non-local model for a swarm," *Journal of Mathematical Biology*, vol. 38, pp. 534–570, 1999.

[6] A. Stevens, "A stochastic cellular automaton, modeling gliding and aggregation of myxobacteria," *SIAM J. Applied Mathematics*, vol. 61, no. 1, pp. 172–182, 2000.

[7] I. D. Couzin, J. Krause, R. James, G. D. Ruxton, and N. R. Franks, "Collective memory and spatial sorting in animal groups," *Journal of Theoretical Biology*, vol. 218, pp. 1–11, 2002.

[8] R. Axelrod, *The Evolution of Cooperation*. New York: Basic Books, 1984.

[9] A. Stevens, "The derivation of chemotaxis equations as limit dynamics of moderately interacting stochastic many-particle systems," *SIAM J. Applied Mathematics*, vol. 61, no. 1, pp. 183–212, 2000.

[10] J. Parrish and W. Hamner, eds., *Animal Groups in Three Dimensions*. Cambridge, England: Cambridge Univ. Press, 1997.

[11] L. Edelstein-Keshet, *Mathematical Models in Biology*. Brikhäuser Mathematics Series, New York: The Random House, 1989.

[12] J. D. Murray, *Mathematical Biology*. New York: Springer-Verlag, 1989.

[13] D. Stephens and J. Krebs, *Foraging Theory*. Princeton, NJ: Princeton Univ. Press, 1986.

[14] E. M. Rauch, M. M. Millonas, and D. R. Chialvo, "Pattern formation and functionality in swarm models," *Physics Letters A*, vol. 207, pp. 185–193, October 1995.

[15] T. Vicsek, A. Czirok, E. Ben-Jacob, I. Cohen, and O. Shochet, "Novel type of phase transition in a system of self-driven particles," *Physical Review Letters*, vol. 75, pp. 1226–1229, August 1995.

[16] N. Shimoyama, K. Sugawa, T. Mizuguchi, Y. Hayakawa, and M. Sano, "Collective motion in a system of motile elements," *Physical Review Letters*, vol. 76, pp. 3870–3873, May 1996.

[17] J. Toner and Y. Tu, "Flocks, herds, and schools: A quantitative theory of flocking," *Physical Review E*, vol. 58, pp. 4828–4858, October 1998.

[18] H. Levine, W.-J. Rappel, and I. Cohen, "Self-organization in systems of self-propelled particles," *Physical Review E*, vol. 63, pp. 017101–1–017101–4, January 2001.

[19] G. Grégoire, H. Chaté, and Y. Tu, "Moving and staying together without a leader," *Physica D*, vol. 181, pp. 157–170, 2003.

[20] A. Czirok, H. E. Stanley, and T. Vicsek, "Spontaneously ordered motion of self-propelled partciles," *Journal of Physics A: Mathematical, Nuclear and General*, vol. 30, pp. 1375–1385, 1997.

[21] C. W. Reynolds, "Flocks, herds, and schools: A distributed behavioral model," *Computer Graphics*, vol. 21, no. 4, pp. 25–34, 1987.

[22] Y. Shi and R. C. Eberhart, "Parameter selection in particle swarm optimization," in *Evolutionary Programming VII: Proc. EP98*, pp. 591–600, Springer-Verlag, 1998.

[23] M. Clerc and J. Kennedy, "The particle swarm—explosion, stability, and convergence in a multidimensional complex space," *IEEE Trans. on Evolutionary Computation*, vol. 6, pp. 58–73, February 2002.

[24] D. Swaroop, J. K. Hedrick, C. C. Chien, and P. Ioannou, "A comparison of spacing and headway control laws for automatically controlled vehicles," *Vehicle System Dynamics*, vol. 23, pp. 597–625, 1994.

[25] D. Swaroop, *String Stability of Interconnected systems: An Application to Platooning in Automated Highway Systems*. PhD thesis, Departnent of Mechanical Engineering, University of California, Berkeley 1995.

[26] D. N. Godbole and J. Lygeros, "Longitudinal control of the lead car of a platoon," *IEEE Transactions on Vehicular Technology*, vol. 43, no. 4, pp. 1125–1135, 1994.

[27] J. T. Spooner and K. M. Passino, "Fault-tolerant control for automated highway systems," *IEEE Transactions on Vehicular Technology*, vol. 46, no. 3, pp. 770–785, 1997.

[28] J. H. Reif and H. Wang, "Social potential fields: A distributed behavioral control for autonomous robots," *Robotics and Autonomous Systems*, vol. 27, pp. 171–194, 1999.

[29] H. Yamaguchi, "A cooperative hunting behavior by mobile-robot troops," *Int. Journal of Robotics Research*, vol. 18, pp. 931–940, Sep. 1999.

[30] A. Fujimori, M. Teramoto, P. N. Nikiforuk, and M. M. Gupta, "Cooperative collision avoidance between multiple mobile robots," *Journal of Robotic Systems*, vol. 17, no. 7, pp. 347–363, 2000.

[31] T. Balch and R. C. Arkin, "Behavior-based formation control for multirobot teams," *IEEE Trans. on Robotics and Automation*, vol. 14, pp. 926–939, December 1998.

[32] I. Suzuki and M. Yamashita, "Distributed anonymous mobile robots: Formation of geometric patterns," *SIAM Journal on Computing*, vol. 28, no. 4, pp. 1347–1363, 1999.

[33] J. P. Desai, J. Ostrowski, and V. Kumar, "Modeling and control of formations of nonholonomic mobile robots," *IEEE Trans. on Robotics and Automation*, vol. 17, pp. 905–908, December 2001.

[34] M. Egerstedt and X. Hu, "Formation constrained multi-agent control," *IEEE Trans. on Robotics and Automation*, vol. 17, pp. 947–951, December 2001.

[35] N. E. Leonard and E. Fiorelli, "Virtual leaders, artificial potentials and coordinated control of groups," in *Proc. of Conf. Decision Control*, (Orlando, FL), pp. 2968–2973, December 2001.

[36] P. Ögren, E. Fiorelli, and N. E. Leonard, "Formations with a mission: Stable coordination of vehicle group maneuvers," *Proc. Symposium on Mathematical Theory of Networks and Systems*, August 2002.

[37] K. Jin, P. Liang, and G. Beni, "Stability of synchronized distributed control of discrete swarm structures," in *Proc. of IEEE International IEEE Conference on Robotics and Automation*, (San Diego, California), pp. 1033–1038, May 1994.

[38] G. Beni and P. Liang, "Pattern reconfiguration in swarms—convergence of a distributed asynchronous and bounded iterative algorithm," *IEEE Trans. on Robotics and Automation*, vol. 12, pp. 485–490, June 1996.

[39] Y. Liu, K. M. Passino, and M. Polycarpou, "Stability analysis of one-dimensional asynchronous swarms," in *Proc. American Control Conf.*, (Arlington, VA), pp. 716–721, June 2001.

[40] Y. Liu, K. M. Passino, and M. M. Polycarpou, "Stability analysis of one-dimensional asynchronous swarms," *IEEE Transactions on Automatic Control*, vol. 48, no. 10, pp. 1848–1854, 2003.

[41] Y. Liu, K. M. Passino, and M. M. Polycarpou, "Stability analysis of M-dimensional asynchronous swarms with a fixed communication topology," *IEEE Transactions on Automatic Control*, vol. 48, no. 1, pp. 76–95, 2003.

[42] V. Gazi and K. M. Passino, "Stability of a one-dimensional discrete-time asynchronous swarm," in *Proc. of the joint IEEE Int. Symp. on Intelligent Control/IEEE Conf. on Control Applications*, (Mexico City, Mexico), pp. 19–24, September 2001.

[43] V. Gazi and K. M. Passino, "Stability analysis of swarms," in *Proc. American Control Conf.*, (Anchorage, Alaska), pp. 1813–1818, May 2002.

[44] V. Gazi and K. M. Passino, "Stability analysis of swarms," *IEEE Trans. on Automatic Control*, vol. 48, no. 4, pp. 692–697, 2003.

[45] V. Gazi and K. M. Passino, "A class of attraction/repulsion functions for stable swarm aggregations," in *Proc. of Conf. Decision Control*, (Las Vegas, Nevada), pp. 2842–2847, December 2002.

[46] V. Gazi and K. M. Passino, "Stability analysis of social foraging swarms," *IEEE Trans. on Systems, Man, and Cybernetics, Part B: Cybernetics*, vol. 34, no. 1, pp. 539–557, 2004.

[47] R. Bachmayer and N. E. Leonard, "Vehicle networks for gradient descent in a sampled environment," in *Proc. of Conf. Decision Control*, (Las Vegas, Nevada), pp. 113–117, December 2002.

[48] A. Jadbabaie, J. Lin, and A. S. Morse, "Coordination of groups of mobile autonomous agents using nearest neighbor rules," *IEEE Trans. on Automatic Control*, vol. 48, no. 6, pp. 988–1001, 2003.

[49] H. Tanner, A. Jadbabaie, and G. J. Pappas, "Flocking in fixed and switching networks," *Preprint*, 2003.

[50] R. O. Saber and R. M. Murray, "Agreement problems in networks with directed graphs and switching topology," in *Proc. of Conf. Decision Control*, (Maui, Hawaii), pp. 4126–4132, December 2003.

[51] Y. Liu and K. M. Passino, "Biomimicry of social foraging behavior for distributed optimization: Models, principles, and emergent behaviors," *Journal of Optimization Theory and Applications*, vol. 115, pp. 603–628, Dec. 2002.

[52] H. K. Khalil, *Nonlinear Systems*. Englewood Cliffs, NJ: Prentice-Hall, 3rd ed., 1999.

[53] A. N. Michel and R. K. Miller, *Qualitative Analysis of Large Scale Dynamical Systems*. New York: Academic Press, 1977.

[54] Y. Liu, K. M. Passino, and M. Polycarpou, "Stability analysis of one-dimensional asynchronous mobile swarms," in *Proc. of Conf. Decision Control*, (Orlando, FL), pp. 1077–1082, December 2001.

[55] Y. Liu, K. M. Passino, and M. M. Polycarpou, "Stability analysis of m-dimensional asynchronous swarms with a fixed communication topology," in *Proc. American Control Conf.*, (Anchorage, Alaska), pp. 1278–1283, May 2002.

[56] Y. Liu and K. M. Passino, "Stable social foraging swarms in a noisy environment," *IEEE Transactions on Automatic Control*, vol. 49, no. 1, pp. 30–44, 2004.

[57] Y. Liu and K. M. Passino, "Stability analysis of swarms in a noisy environment," in *Proc. of Conf. Decision Control*, (Maui, Hawaii), pp. 3573–3578, December 2003.

[58] D. Bertsekas and J. Tsitsiklis, *Parallel and Distributed Computation: Numerical Methods*. Engelwood Cliffs, NJ: Prentice-Hall, Inc., 1989.

[59] K. Passino and K. Burgess, *Stability Analysis of Discrete Event Systems*. New York: John Wiley and Sons Pub., 1998.

[60] K. Passino, "Biomimicry of bacterial foraging for distributed optimization and control," *IEEE Control Systems Magazine*, vol. 22, no. 3, pp. 52–67, 2002.

[61] C. Godsil and G. Royle, *Algebraic Graph Theory*. New York: Springer, 2001.

[62] H. Tanner, A. Jadbabaie, and G. J. Pappas, "Stable flocking of mobile agents part i: Fixed topology," in *Proc. of Conf. Decision Control*, (Maui, Hawaii), pp. 2016–2021, December 2003.

[63] Y. Liu and K. M. Passino, "Cohesive behaviors of multiple cooperative mobile discrete-time agents in a noisy environment," in *the 4th International Conference on Cooperative Control and Optimization*, (Fort Walton Beach, Florida), November 2003.

[64] S. H. Strogatz, R. E. Mirollo, and P. C. Matthews, "Coupled nonlinear oscillators below the synchronization threshold: Relaxation be gneralized landau damping," *Physical Review Letters*, vol. 68, pp. 2730–2733, May 1992.

[65] Y. Kuramoto and D. Battogtokh, "Coexistence of coherence and incoherence in nonlocally coupled phase oscillators," *Nonlinear Phenomena in Complex Systems*, vol. 5, no. 4, pp. 380–385, 2002.

[66] S. Strogatz, *SYNC: The Emerging Science of Spontaneous Order*. New York: Hyperion Press, 2003.

[67] A. Jadbabaie, N. Motee, and M. Barahona, "On the stability of the kuramoto model of coupled nonlinear oscillators," in *Proceedings of the American Control Conference*, (Boston, MA), 2004.